N O T I C E

8.1 - 1 0.1 5.1

CR - 164323

AgRISTARS

Supporting Research

Final Report

Vol. I
Field Research on the Spectral Properties of Crops and Soils

by M.E. Bauer, L.L. Biehl, B.F. Robinson

Purdue University
Laboratory for Applications of Remote Sensing
West Lafayette, Indiana 47907

Final Report

FIELD RESEARCH ON THE SPECTRAL PROPERTIES
OF CROPS AND SOILS

M.E. Bauer, L.L. Biehl and B.F. Robinson

Purdue University
Laboratory for Applications of Remote Sensing
West Lafayette, Indiana 47907

November 1980

Star Information Form

1. Report No. SR-PO-04022	2. Government Accession No.	3. Recipient's Catalog No

4. Title and Subtitle	5. Report Date November 1980
Field Research on the Spectral Properties of Crops and Soils	6. Performing Organization Code

7. Author(s) M.E. Bauer, L.L. Biehl and B.F. Robinson	8. Performing Organization Report No. 112680

9. Performing Organization Name and Address Purdue University Laboratory for Applications of Remote Sensing West Lafayette, Indiana 47907	10. Work Unit No.
	11. Contract or Grant No NAS9-15466

12. Sponsoring Agency Name and Address NASA Johnson Space Center Earth Observations Division Houston, Texas 77058	13. Type of Report and Period Covered Final 12-1-79 to 11-30-80
	14. Sponsoring Agency Code

15. Supplementary Notes
J.D. Erickson, Technical Monitor
M.E. Bauer, Principal Investigator

16. Abstract

   This report describes the experiment design, data acquisition and preprocessing, data base management, analysis results and development of instrumentation for the AgRISTARS Supporting Research Project, Field Research task. It reports results of several investigations on the spectral reflectance of corn and soybean canopies as influenced by cultural practices, development stage and nitrogen nutrition. Results of analyses of the spectral properties of crop canopies as a function of canopy geometry, row orientation, sensor view angle and solar illumination angle are presented. The objectives, experiment designs and data acquired in 1980 for field research experiments are described. The development and performance characteristics of a prototype multiband radiometer, data logger, and aerial tower for field research are described.

17. Key Words (Suggested by Author(s)) Remote Sensing, field research, crop spectra, crop reflectance	18. Distribution Statement

19. Security Classif. (of this report)	20. Security Classif. (of this page)	21. No. of Pages 158	22. Price*

*For sale by the National Technical Information Service, Springfield, Virginia 22161

NASA - JSC

TABLE OF CONTENTS   Page

    1. Introduction 136

    2. Description and Features of the Prototype Multi-
        band Radiometer 138

        2.1 Calibration 138
        2.2 Features 138

    3. Performance of Prototype Radiometer 140

        3.1 Accuracy 140
        3.2 Field of View 144
        3.3 Filters and Spectral Response 147
        3.4 Dynamic Range 147
        3.5 Field Test 151

    4. General Features of the Data Recording Module 153

        4.1 Specifications for Developed Prototype
            Data Recording Module Data Acquisition: 154
        4.2 Results of Laboratory and Chamber Tests of the Data
            Logger 155

    5. Development of Prototype Intervalometer and
        Databack Camera 156

        5.1 Specifications for Intervalometer/Databack
             Camera System 156

    6. Testing of the Truck-Mounted Boom 157

        6.1 Operation Characteristics 157
        6.2 Modifications 158
        6.3 Fatigue Test 158

    7. Interface Hardware and Software 158

    8. System and User Manuals 158

    9. References 158

LIST OF FIGURES

LIST OF TABLES

A. FIELD RESEARCH EXPERIMENT DESIGN AND DATA ANALYSIS

1. Introduction

Mankind is becoming increasingly aware of the need to better manage the resources of the earth--atmosphere, water, soils, vegetation and minerals. As the world's population increases and a higher standard of living is sought for all, more careful planning and effective use of these resources, particularly soils, vegetation and water, is required to produce adequate food supplies. Agricultural crop production is highly dynamic in nature and dependent on complex interactions of weather, soils, technology and socio-economics.

Accurate and timely information on crops and soils on a global basis is required to successfully plan for and manage food production. The repetitive, synoptic view of earth provided by satellite-borne sensors such as Landsat MSS provide the opportunity to obtain the necessary information on soil productivity and crop acreage and condition. For example, the recently completed Large Area Crop Inventory Experiment established the feasibility of multispectral remote sensing to inventory and monitor global wheat production.

But, to fully develop the potential of multispectral measurements acquired from satellite or aircraft sensors to monitor, inventory and map agricultural resources, increased knowledge and understanding of the spectral properties of crops and soils in relation to their physical, biological and agronomic characteristics is needed.

Quantitative understanding of the relationships between the spectral characteristics and important biological-physical parameters of crops and soils can best be obtained by carefully controlled studies of fields and plots where complete data describing the condition of targets are attainable and where frequent, timely spectral measurements can be obtained. It is these attributes which distinguish field research from other remote sensing research activities.

The activities and results described in this report are part of the AgRISTARS Supporting Field Research task. Its overall objectives are to:

- Conduct analyses and develop physical models of the spectral properties of crops and soils in relation to agronomic and physical properties of the scene.

- Provide candidate models, analysis techniques, and analyst aids as inputs to Supporting Research Project experiments.

- Assess the capability of current, planned, and possible future satellite sensors to capture available information for identification and assessment of crops and soils.

Specific objectives currently being pursued in experiment design, data acquisition, and data analysis include:

- To determine the reflectance and radiant temperature characteristics of corn, soybeans, spring wheat, and barley as functions of development stage and amount of vegetation present.

- To determine the effects of stresses including moisture deficits, nutrient deficiencies and disease on the reflectance and radiant temperature properties of corn, soybeans, and wheat.

- To determine the effect of important agronomic practices (e.g., planting date, plant population, fertilization) and environmental factors on the spectral characteristics of corn, soybeans, and small grains.

- To support the development of corn, soybean and small grain development stage and yield models which use as an input spectral response as a function of crop development stage.

- To determine the spectral separability of crops as a function of date, maturity stage, soil background conditions, and other agronomic and measurement variables using Landsat MSS and TM spectral bands. Separation of corn and soybeans from other typical Corn Belt crops is first priority; separation of spring wheat and barley is a secondary objective.

Results of several analysis topics are presented in section A of this report. They include: (1) estimation of corn and soybean development stages from spectral and meteorological measurements, (2) soybean canopy reflectance as influenced by cultural practices, (3) influence of nitrogen nutrition on the spectral reflectance of corn, (4) modeling the reflectance of soybean canopies as a function of row direction and solar illumination angles, (5) simulated response of a multispectral scanner as a function of view angle and solar illumination angles, and (6) polarization properties of crop canopies.

These and future studies are supported by acquisition and preprocessing of agronomic, spectral and meteorological measurements at test sites in Indiana (corn, soybeans, and winter wheat), Iowa (corn and soybeans), North Dakota (spring wheat, barley, and sunflowers), and Texas (rice and cotton). The sensor systems used include truck-mounted radiometers and spectrometers, a helicopter-borne spectrometer, aircraft multispectral scanner and Landsat MSS. Key agronomic observations and measurements include: development stage, percent soil cover, and leaf

area index. Experiment designs, data acquisition, and preprocessing during 1980 are described in Section B.

To enhance the capability to economically acquire large numbers of accurate, calibrated spectral measurements the prototypes of an 8-band multiband radiometer and data recorder have been developed this year. These instruments, which will be made available to a number of additional investigators in 1981, are described in Section C.

2. Estimation of Corn and Soybean Development Stages from Spectral Measurements

K.J. Ranson, M.M. Hixson, V.C. Vanderbilt, and M.E. Bauer

2.1 Introduction

Crop development stage is an important variable to two AgRISTARS activities: Landsat image analysis and development of crop yield models which utilize spectral inputs. Knowledge of the temporal-spectral response of crops is probably the single most important item of information required for accurate image interpretation. Crop development stage is a key input to crop yield models; it is needed to relate weather events and history to specific development stages.

To accurately identify crop species, the image analyst must be able to determine the development patterns throughout the growing season for each crop type (temporal characteristics), as well as the spectral response in specific time periods corresponding to given crop type biostages (spectral characteristics). There appears, however, to be only very general information available relating development stage to spectral response of corn and soybeans.

Review of the literature (Seeley et al., 1978) indicates there are three approaches for estimating crop development stages: (1) normal or average phenology based on accumulation of days between stages, (2) meteorological methods based on accumulation of thermal or photo-thermal units between stages, and (3) spectral methods based on changes in spectral resonse as a function of development stage. The goal of this analysis task is to investigate the use of spectral measurements to determine crop development stage.

Presently crop growth rates and development stages for yield prediction models are estimated from meteorological data, particularly temperature and daylength, using empirically derived relationships. However, a number of other factors, including planting date, soil moisture, nutrient supply and varietal response, are also important determinants of crop growth and development. The interaction of these factors is complex and attempts to model them using statistical, as well as physiological models are not available for large areas. Both approaches are limited by the relatively low density of weather stations.

The spectral response of the crop represents the integrated effect of all cultural, soil, and meteorological factors affecting crop growth and development. The possible use of satellite-acquired spectral data to determine crop development stages offers the advantage of making

estimates at the segment, field, or even pixel level. Satellite estimates of development stage can be used to check and adjust statistical or physiological models of development stage periodically during the growing season.

There is a growing body of evidence and experience, particularly for wheat, indicating that crop phenology can be related to spectral parameters. Badhwar (1980) has proposed an analytic method of estimating the spring green-up of wheat and barley from multitemporal Landsat MSS data. The method assumes that a given crop, after emergence, has a unique spectral profile in time which is shifted by differences in planting date. A similar approach has been developed by Holmes et al. (1979) and applied to soybeans by Rice, Crist, and Malila (1980).

There are a number of spectral variables available from Landsat type data that are potentially useful for characterization of crop development stage. Landsat bands 2 (0.6-0.7 μm) and 4 (0.8-1.1 μm) are generally considered most useful for vegetation assessment. A ratio of band 4 and band 2 has been shown to be strongly correlated to biomass and vigor. The well-known tasseled cap transformation of Kauth and Thomas (1976) provides spectral variables sensitive to the temporal changes of crops in terms of greenness, brightness, and yellowness. The greenness parameter in particular has been shown to have strong correlations with agronomic variables such as biomass and leaf area index (Daughtry et al., 1980) and thus was emphasized in this initial analysis.

2.2 Objectives

The overall objective of this analysis task is to determine and model the relationship between spectral characteristics of corn and soybean canopies and development stage. For this reporting period, we examined the relationships of several spectral variables and development stage. These included individual wavelength bands and various transformed spectral variables. We were, however, primarily interested in evaluating the usefulness of greenness for development stage prediction. Specifically, our immediate goals were:

1. Examine the relationships of spectral variables and development stage for corn and soybeans.

2. Given a response value for the spectral variable greenness, determine the distribution of possible development stages and the most likely development stage.

3. Given a development stage, determine the expected range of values for greenness.

2.3 Data Acquisition and Reduction

The data for this study were collected at the Purdue Agronomy Farm during the 1979 growing season (Bauer et al., 1979). Spectral data included reflectance factors in the four Landsat MSS bands and development stages for plots of corn and soybeans with varying planting date, plant population, row width, and soil color (lighter, darker). Development stages were determined according to the Hanway scale for corn and the Fehr-Caviness scale for soybeans (Table A-2.1). To fully monitor the growth history of the crops, development stages were measured from pre-planting to post harvest.

Since spectral data are collected only on clear days the distribution of the data may tend to have more observations at development stages which occur over the longest time intervals. To account for this, a sampling distribution was devised that weights the observation frequency by the duration of development stages. This is a first step towards normalizing the data by the probability of observing a given development stage.

The reflectance factors were transformed into additional spectral variables of near infrared/red ratio, brightness and greenness. The ratio variable is simply the ratio of band 4 to band 2. Brightness and greenness were calculated by a linear transformation of the four spectral bands. The transformations developed specifically for reflectance factor data, as discussed by Rice et al. (1980), are:

$$Brightness = .3236 (R1) + .4852 (R2) + .5663 (R3) + .6095 (R4)$$

$$Greenness = -.4894 (R1) - .6125 (R2) + .1729 (R3) + .5954 (R4)$$

where R(i) = reflectance factor in wavelength band i, i = 1, 4.

2.4 Modeling Approach

The modeling approach involved the use of the theory of random variables (Papoulis, 1975). Mathematically, the approach assumes that the spectral response of a crop is a random variable. Using greenness as an example a probability density function relating development stage to a particular greenness value can be defined as:

$$f_{ds, gr} (DS,GR) = \frac{\partial^2}{\partial ds\, \partial gr} (Prob(DS < ds, GS < gr))$$

Where DS = development stage
GR = greenness value
ds, gr, = probabilistic limits for development stage and greenness, respectively.

Table A-2.1 Description of corn and soybean development stages.

Corn*		Soybean**		
Develop-ment Stage	Description	Develop-ment Stage	Description	Coded as
0	planting to emergence	V0	planting to emergence	1
0.5	2 leaves fully emerged	VE	emergence	2
1.0	4 leaves fully emerged	VC	cotyledon	3
1.5	6 leaves fully emerged	V1	1 node	4
2.0	8 leaves fully emerged	V2	2 nodes	5
2.5	10 leaves fully emerged	V3	3 nodes	6
3.0	12 leaves fully emerged	V4	4 nodes	7
3.5	14 leaves fully emerged	V5	5 nodes	8
4.0	16 leaves fully emerged	V6	6 nodes	9
4.5	18 leaves fully emerged (tasselling) silking	V7	7 nodes	10
5.0	silking	V8	8 nodes	11
6.0	blister stage	V9	9 nodes	12
7.0	dough stage	R1	beginning bloom	13
8.0	beginning dent stage	R2	fully bloom	14
9.0	full dent	R3	beginning pod	15
10.0	physiologic maturity	R4	full pod	16
10.5	harvest maturity	R5	beginning seed	17
11.0	post-harvest	R6	full seed	18
			beginning maturity	19
			full maturity	20

* Adapted from Hanway (1966)
** Adapted from Fehr and Caviness (1977)

This density function is used to determine the probability density function of development stages with GR = gr1 (a specific value of measured greenness). Due to the discrete nature of development stage measurements, discrete statistical distributions were used in the initial analysis. Figure A-2.1 illustrates a hypothetical distribution of greenness values plotted over development stage. A horizontal slice through the data at a particular greenness level (gr1) results in a distribution of probable development stages. Slicing horizontally through the data would, conversely, give a range of greenness values for a particular development stage.
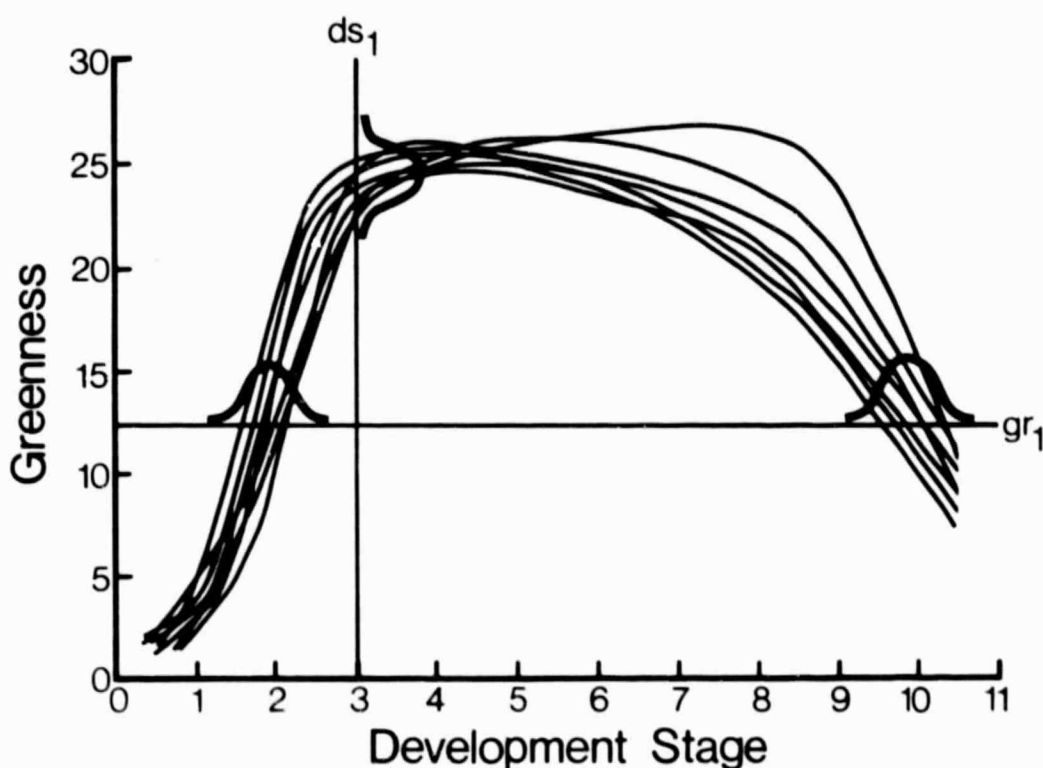
Figure A-2.1. Idealized distribution of greenness response and development stage showing distributions of development stage with a horizontal slicing at greenness level gr_1 and greenness response with a vertical slicing at development stage ds_1. Curves illustrate hypothetical development trajectories for individual plots or fields through time.

2.5 Relationships of Spectral Variables and Development Stage

The relationship of reflectance factor and development stage in Landsat MSS band 2 is illustrated in Figure A-2.2 for corn and soybeans. For both crops reflectance decreases from early in the season and then increases as the crops approach maturity. The effects of different soil type are evident early in the season when the plots containing lighter colored soils have higher reflectance. These differences diminish as the ground cover increases until the soil in the field of view of the radiometer is predominately shaded. In the highly reflective near infrared band 4 (Figure A-2.3), reflectance of corn increases early in the season, remains constant between development stage three (twelve leaves emerged) and eight (beginning dent), and then decreases as the corn matures. For the soybean canopies, the reflectance has a more gradual increase with development stage. The influence of soil type is again apparent for both crops.

Ratioing the red and infrared reflectance factors eliminated the early season differences due to soil type as seen in Figure A-2.4. Ratio values for corn increased rapidly to a maximum near tasseling at development stage 4.5 followed by a decrease near maturity. Soybean ratio values increased up to development stage 17 (beginning seed) then rapidly decreased.

Applying the greenness transformation to the data (Figure A-2.5) minimized the differences due to soil type and showed a general increase through early development stages for corn. The greenness response then leveled off for most of the growing season and then decreased approaching maturity. Soybean greenness response increased until development stage 17 then decreased rapidly to maturity.

The midseason variability of spectral response apparent in Figures A-2.1 through A-2.5 indicated that an effect possibly due to population density, planting date or soil type was present in the data. Figure A-2.6 illustrates the effect of population density on greenness response for the two crops. For corn it appears that for a given development stage greenness increases as population density increases. A similar trend is apparent in the soybean data with greenness increasing as row widths decrease.

Slicing vertically through the distribution of greenness versus development stage as discussed in section 2.4 provides a histogram of greenness values at a specified development stage. In Figure A-2.7 it can be seen that the lowest population density corresponds to the lowest greenness values. For corn at development stage 4.5 (tasseling) there was an overlap of low (25,000 plants/ha) and medium (50,000 plants/ha) densities while the highest population density (75,000 plants/ha) showed a distinct range of greenness values. The soybean histogram shows a distinct separation of population densities due to different row spacings at the V5 stage (fifth node).
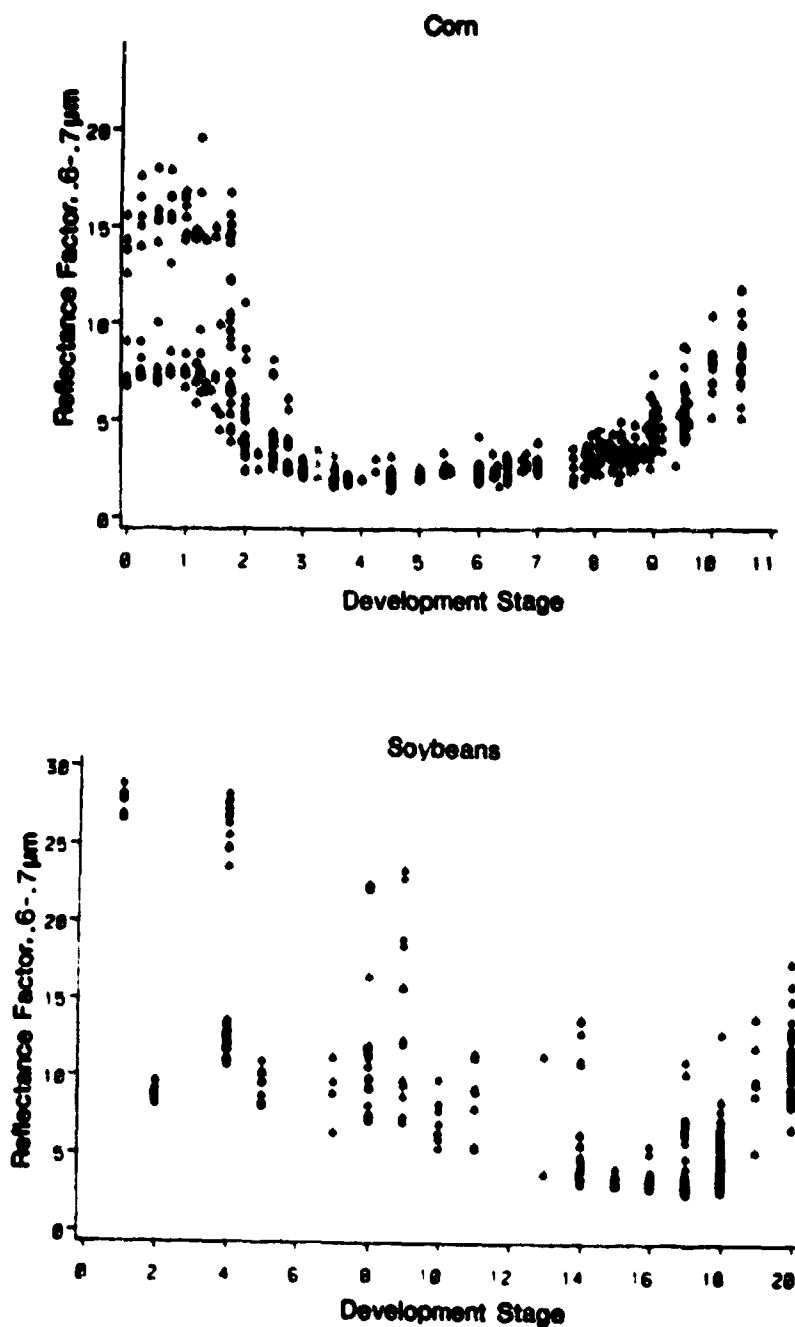
Figure A-2.2. Relationships of red (.6-.7 μm) reflectance and development
stage of corn and soybeans.
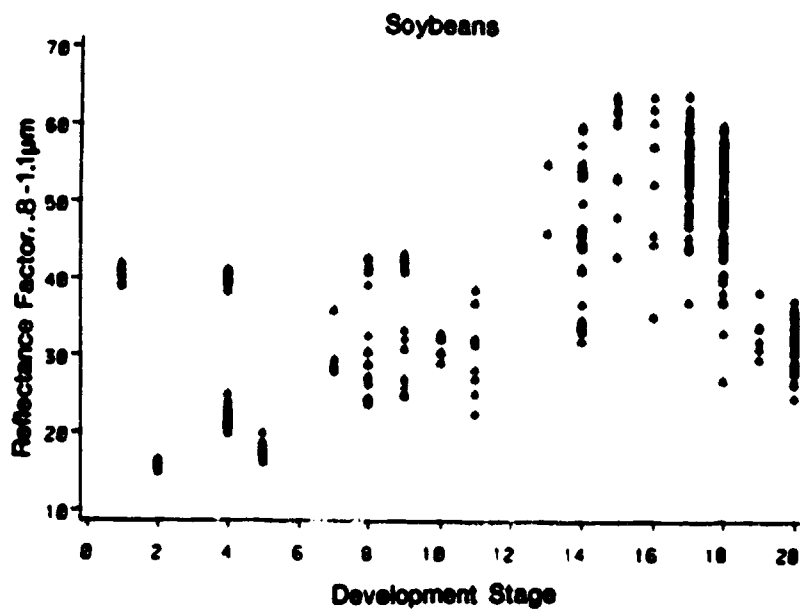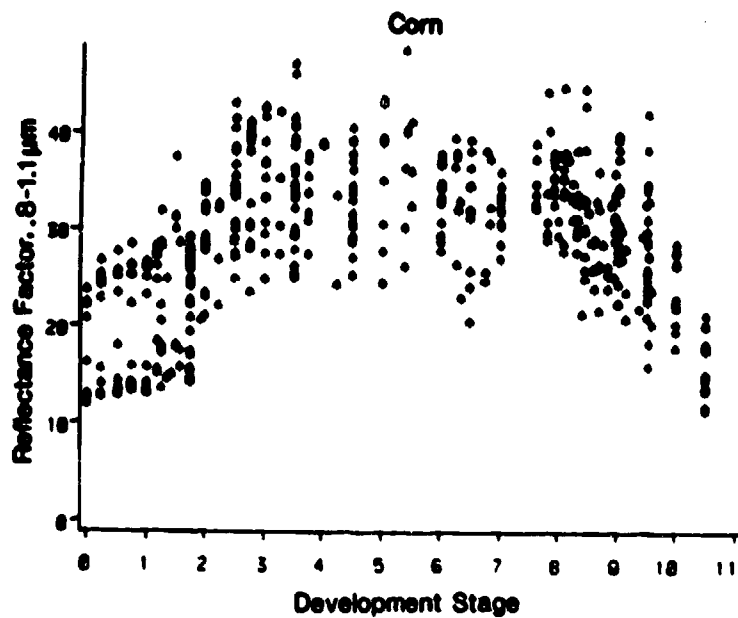
Figure A-2.3. Relationships of near infrared (.8-1.1 μm) reflectance and
development stage of corn and soybeans.
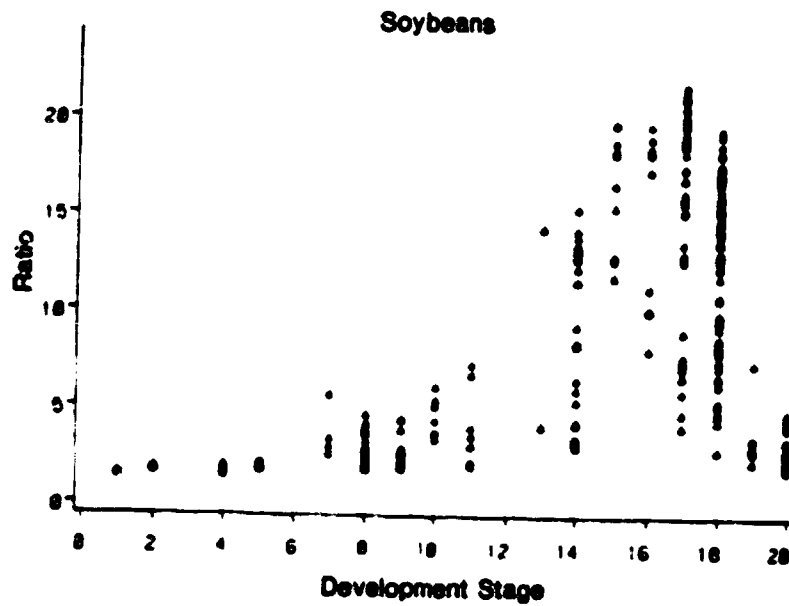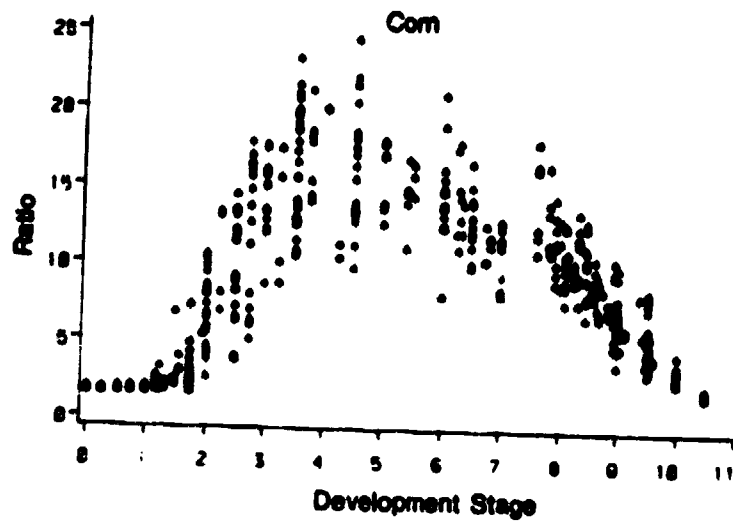
Figure A-2.4. Relationships of near infrared and red ratio and development
stage of corn and soybeans.

Corn
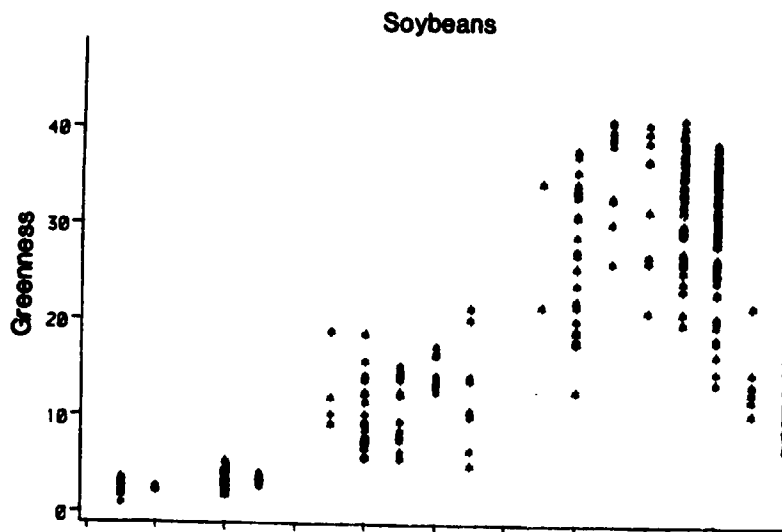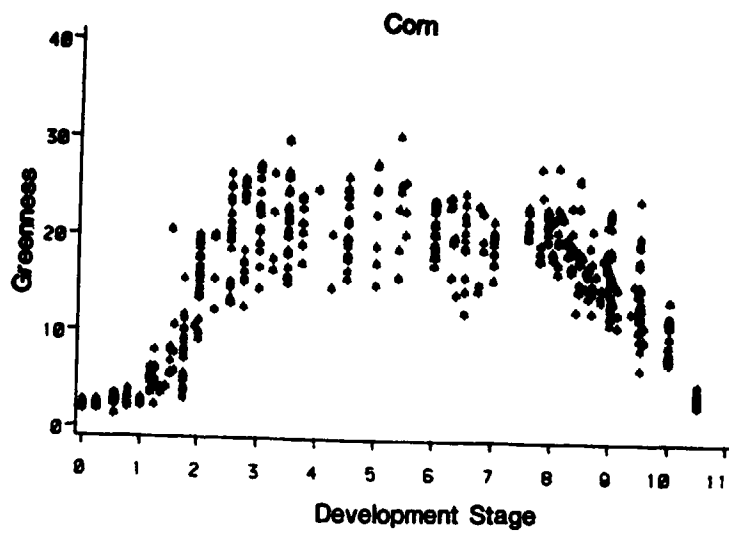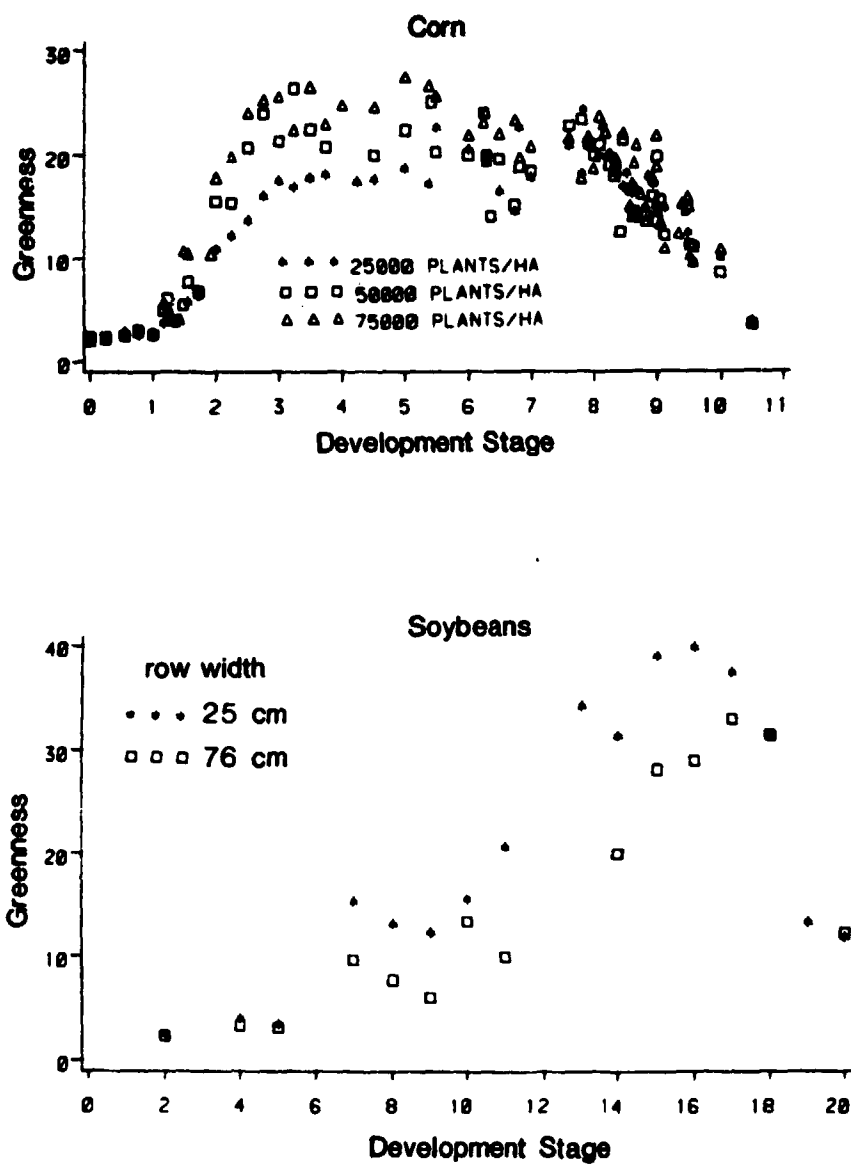
Soybeans

Figure A-2.6. Effects of planting pattern on green response throughout the growing season. Soybean data includes only plots on darker soils.
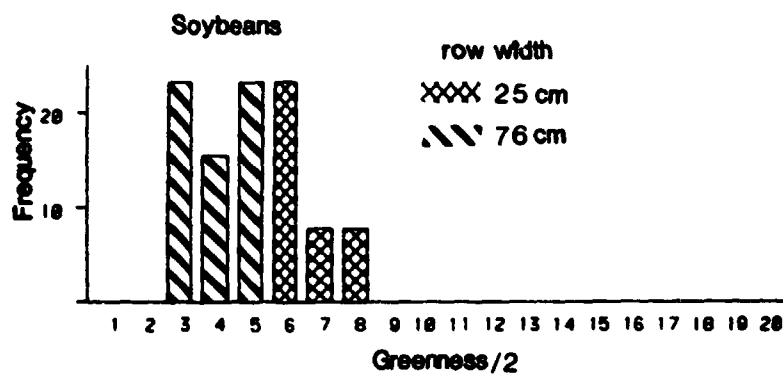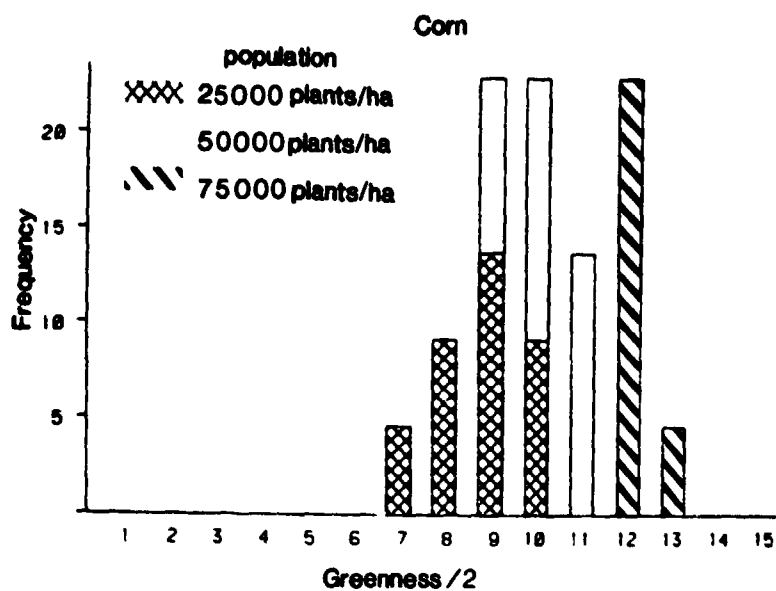
Figure A-2.7. Histograms of greenness response levels for given development stages illustrating the effect planting pattern. Development stages shown are 4.5 (tasseling) for corn and 8 (fifth node) for soybeans.
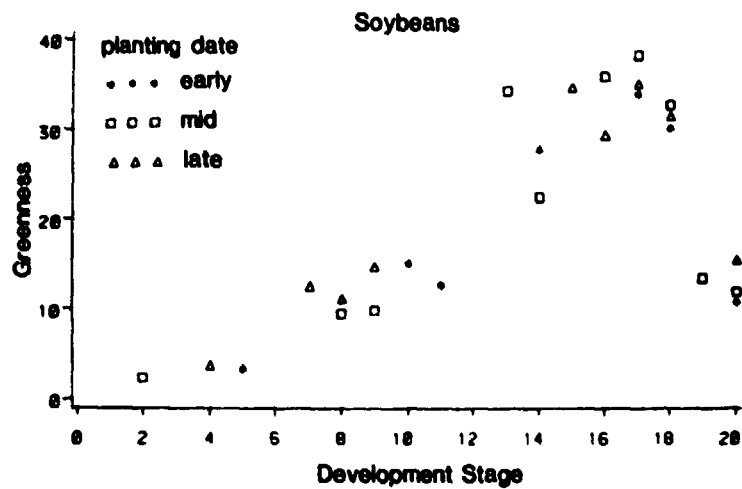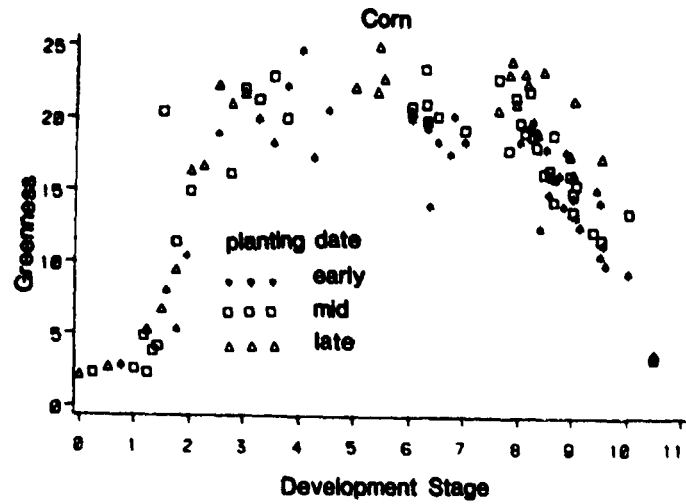
Figure A-2.8. Relationship of mean greenness response and development stage
showing minimal effect due to planting date. Corn data includes only a
planting pattern of 50,000 plants/ha. Soybean data includes only row width
of 76 cm and darker colored soils.
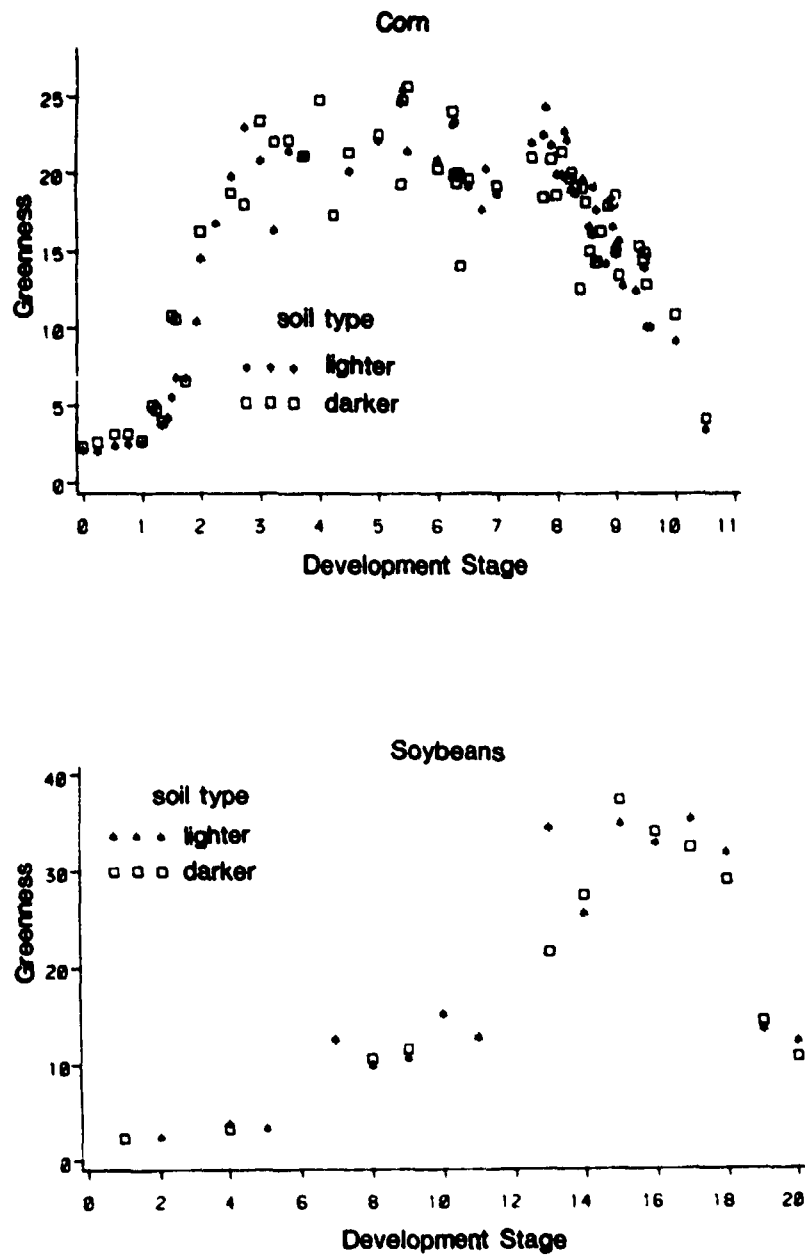
Figure A-2.9. Mean greenness response as a function of development stage
showing minimal effect due to soil type.

These results further support the findings of various authors
(e.g., Daughtry et al., 1980) that greenness is highly sensitive to the
amount of vegetative matter present. Table A-2.2 presents the leaf area
index (LAI) and percent ground cover, both indicators of amount of
vegetation present, which increase with increasing population density.
These results indicate that greenness response alone may not be
sufficient to predict development stage.

The effects of planting date and soil type on greenness response as
a function of development stage appeared to be less than that of pop-
ulation density. Figures A-2.8 and A-2.9 show greenness response
plotted over development stage for planting date and soil type,
respectively. In neither case is there an evident trend.

2.6 Modeling Results

The distribution of greenness response versus development stage as
depicted in Figure A-2.5 shows an increase early in the season and
decrease late in the season. Figure A-2.10 illustrates how this affects
our efforts to predict development stage given a greenness value for
corn (goal 1). For a greenness value of 4 there is a bimodal
distribution of development stage with values early and late in the
season. A greenness response of 8 occurs both early and late in the
season and results in a range of development stages from two through
nine. Another bimodal distribution exists for greenness level 12. It
would be difficult to assign meaningful selection probabilities for
development stage based on these distributions.

Figure A-2.11 illustrates our second goal: given development
stage, predict an expected range of greenness values. In this example,
we would expect that if the development stage is eight then greenness
response would be between 6 and 12. If not, then the development stage
would be something different. Based on the distribution the expected
value of greenness for development stage eight would fall within a
greenness level of 9 or 17-19 units.

To further evaluate the relationship of greenness to development
stage regression, models were developed for the corn data distribution
shown earlier in Figure A-2.5. Our first attempt was to apply to the
data a tenth degree polynomial in development stage and greenness with
no interaction terms. The resulting regression function did not appear
to fit the data very well and gave a coefficient of determination of
only 0.25.

The next step was to try to reduce the number of dimensions in the
distribution by modeling the data adjusted by the mean greenness
response at each development stage. This technique resulted in an
improved r-square value of 0.78. Figure A-2.12 shows the distribution
of mean adjusted greenness values with development stage. Differences
from the mean are small early in the growing season, and diverge from
the mean throughout the remainder of the growing season.

Table A-2.2. Mean corn canopy characteristics and greenness response
ranges at tasseling for three population densities. Standard
deviations are in parenthesis.

	Population Density (plants/ha)		
	25,000	50,000	75,000
Leaf Area Index	1.9 (.34)	3.5 (.90)	5.7 (.94)
Percent Ground Cover	60.0 (10.0)	68.0 (9.0)	76 (6.0)
Greenness Response Range	14.0-20.0	18.0-22.0	24.-26.
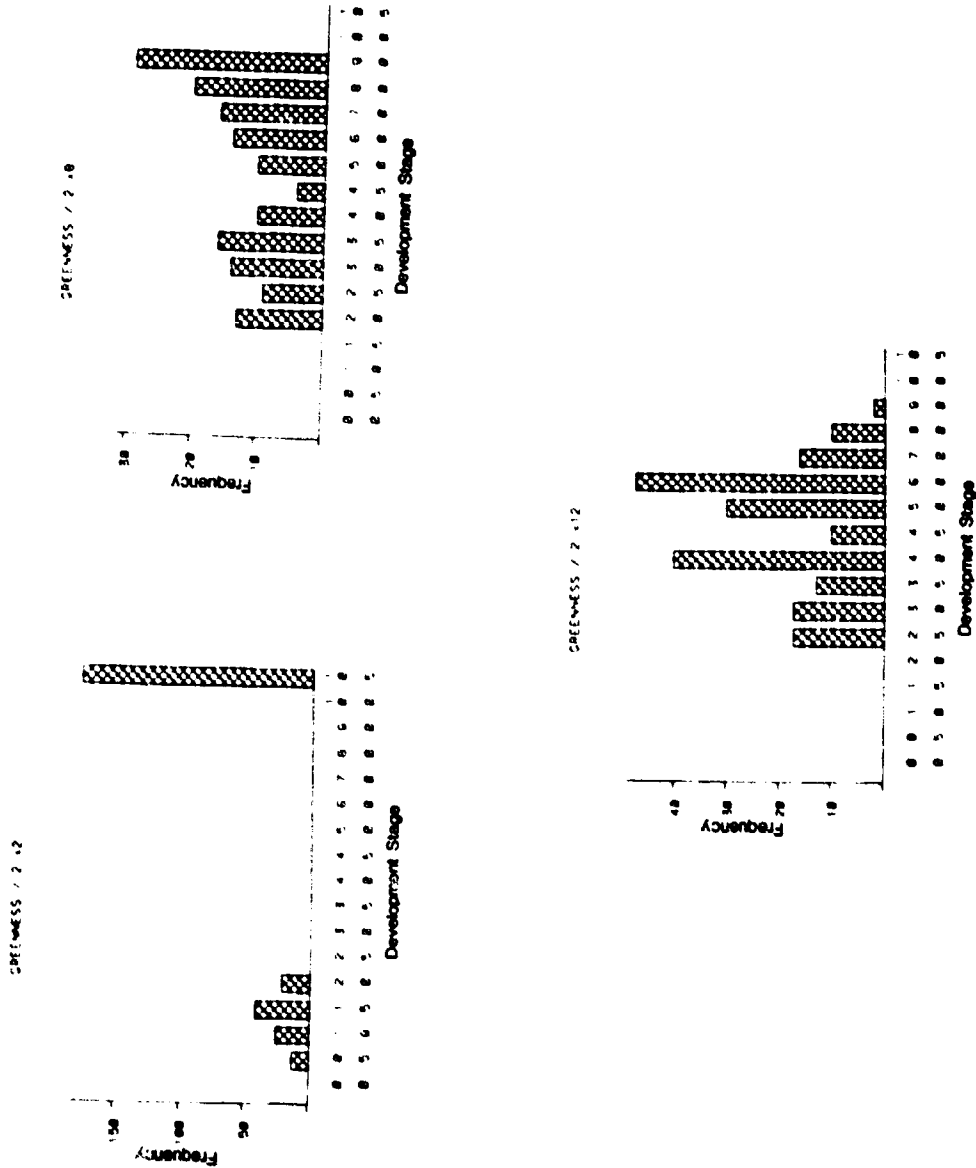
Figure A-2.10. Histograms of development stage for greenness levels of 2, 8, and 12 representing greenest response ranges of 3-5, 15-17, and 23-25 units respectively. These examples for corn illustrate multi-modal and widely dispersed distributions.
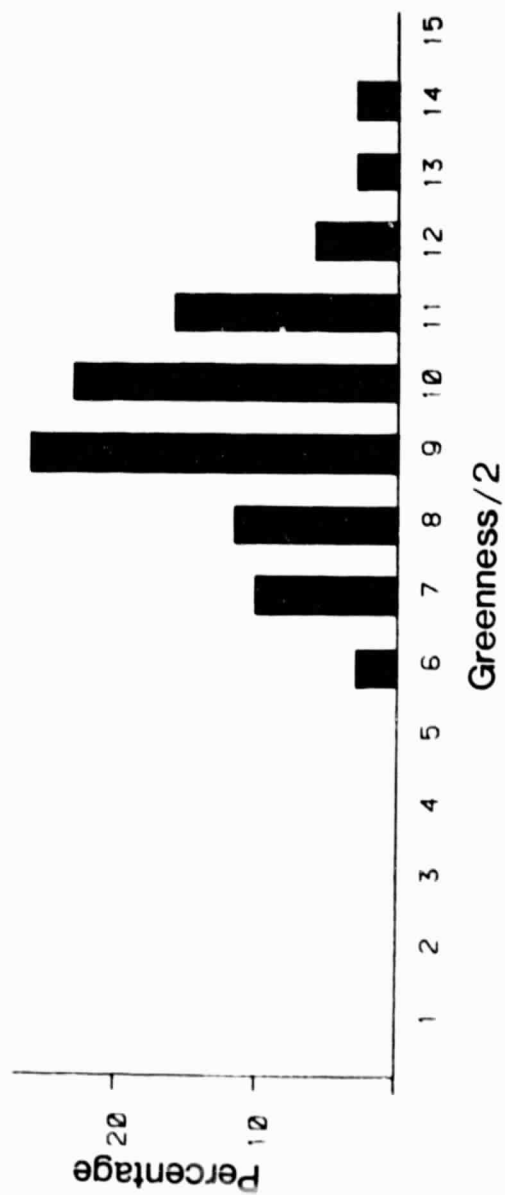
Figure A-2.11. Percent frequency histogram of greenness response of soybeans at development stage 8 (fifth node).
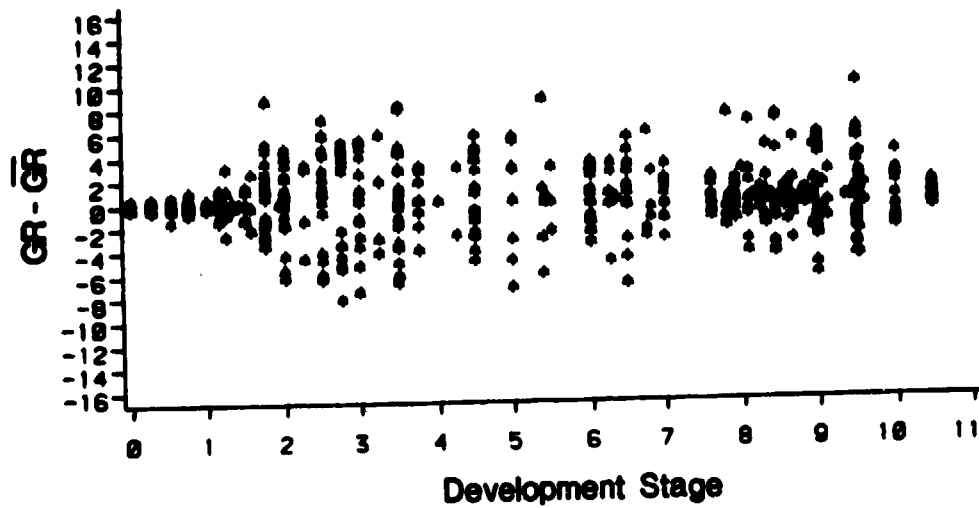
Figure A-2.12. Relationship of mean adjusted greenness responses
and development stage for corn.
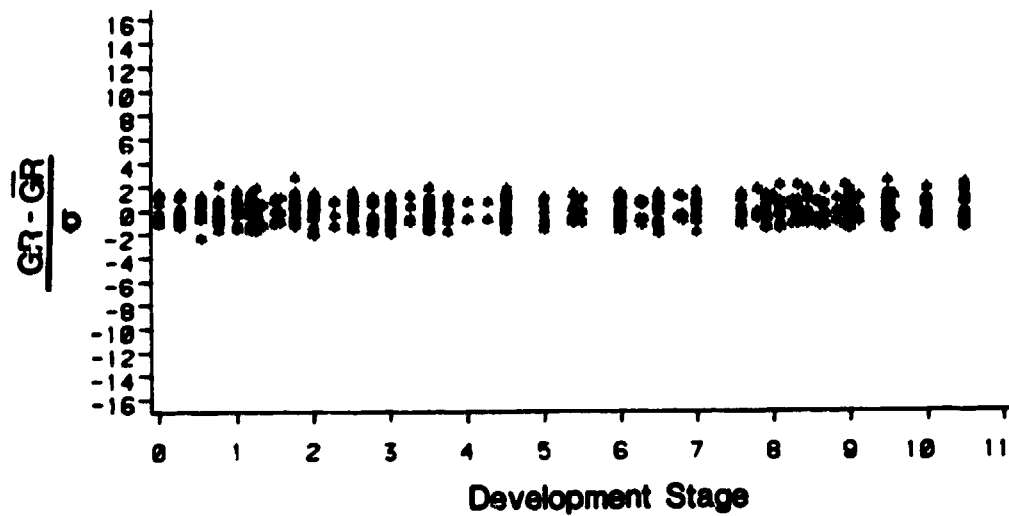
Figure A-2.13. Relationship of normalized N (μ,σ^2) greenness and
development stage for corn..
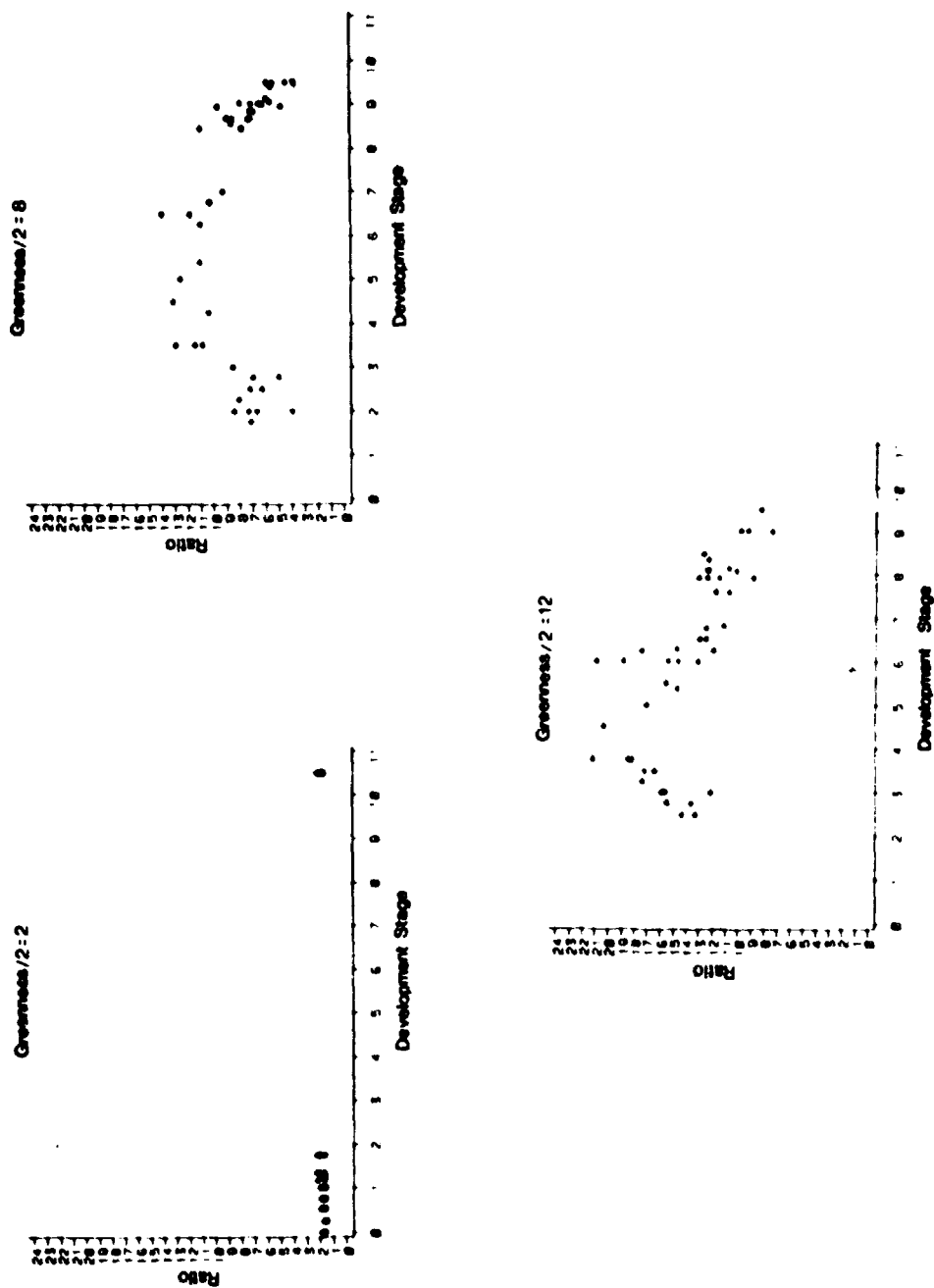
Figure A-2.14. Example relationships of red and near infrared ratio values and development stage for corn greenness response levels of 2, 8, and 12 showing potential increase in information over using greenness alone.
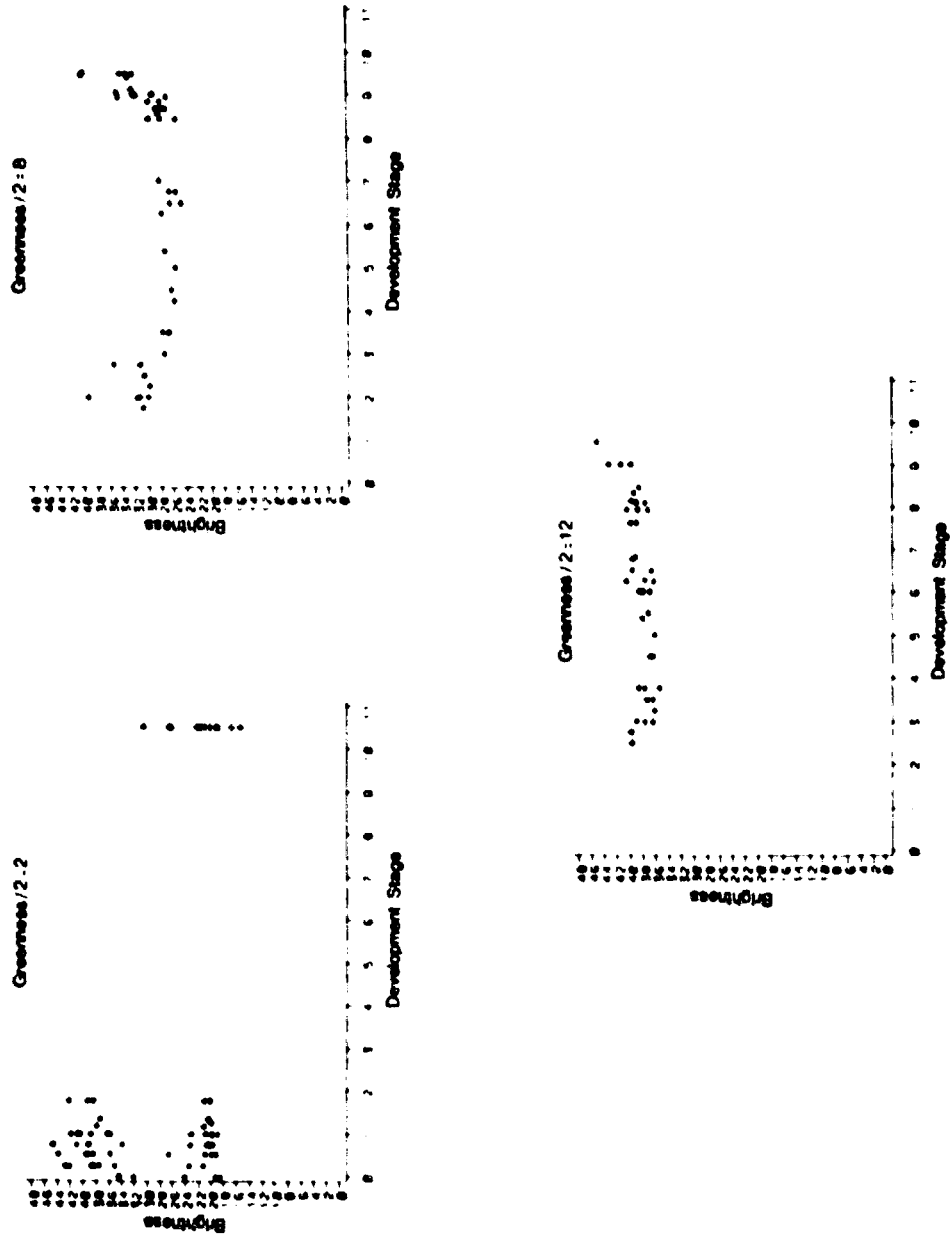
Figure A-2.15. Example relationships of transformed brightness values and development stage for corn greenness response levels of 2, 8, and 12. The increase in information is not as apparent as in Figure A-2.14.

Normalizing the mean adjusted data by the standard deviation
provides a narrower distribution of the data as seen in Figure A-2.13.
This should have provided an ideal situation for modeling the frequency
response surface (the third dimension of the data represented in Figure
A-2.13). The r-square value for this regression analysis, however, was
only 0.22. This result was caused in part by assigning missing values
in the data the value of 0.0. Applying the regression analysis to data
where missing values were ignored increased the r-square value to 0.66.

These initial results indicate that the modeling approach has
potential, but greenness alone does not appear to result in a definitive
distribution from which development stage can be predicted. Our next
step was to evaluate the addition of the ratio and brightness spectral
variables to the model.

The approach was to develop the probability density function for
greenness and development stage and use an additional spectral variable
to enhance the prediction. Plots of ratio values over corn development
stage at greenness levels 2, 8 and 12 illustrate this concept (Figure
A-2.14). At greenness level 2 a ratio value of between 1 and 2 narrows
the choices of probable development stages to between 0 and 2 and 10.5.
For this greenness level there is no enhancement over using greenness
alone as shown in Figure A-2.10. Ratio values of between 3 and 9 at
greenness level 8 narrow the probable development stages to between two
and three, and eight and ten while ratio values between 13 and 15
correspond to development stages 3.5 to 6.5. Addition of ratio values
also provides enhanced prediction for greenness level 12. The
distributions combined with ratios would provide better predictions when
used with an additional temporal variable such as Julian date or
possibly growing degree days.

A similar analysis was performed using brightness as the added
variable as shown in Figure A-2.15 for greenness levels 2, 8 and 12.
For greenness level 2, which occurs most frequently early in the season,
the effects of soil type are evident as noted earlier with no
substantial increase in information. For greenness levels 8 and 12 the
distribution of brightness values is probably too broad and level to
provide much more information than using greenness alone. Analysis of
other greenness levels for both ratio and brightness produced mixed
results.

2.7 Summary and Conclusions

The relationships of a number of spectral variables to development
stages of corn and soybeans were examined. A model was proposed that
uses a spectral variable to specify prediction probabilities for a
development stage. Evaluating the model with the spectral variable
greenness showed that the technique has promise. However, use of the
greenness variable alone did not provide a suitable distribution for
predicting development stage. Additions of ratio and brightness
variables to the model appeared to enhance the prediction capability.

The next step in this continuing study will be to examine the usefulness of other spectral variables including the tasseled cap feature of yellowness. In addition to spectral variables we plan to evaluate meteorological variables for our development stage model. This includes implementing a predictor variable derived from meteorological data such as growing degree days. This approach has the advantage that it would enable refinement of development stage prediction on the basis of both meteorological and spectral variables.

2.8 References

1. Badhwar, G.D. 1980. Crop emergence date determination from spectral data. Photogram. Eng. Rem. Sens. 46(3): 369-377.

2. Bauer, M.E., L.L. Biehl, C.S.T. Daughtry, B.F. Robinson and E.R. Stoner. 1979. Agricultural scene understanding and supporting field research. Final Report, Vol. I. Contract NAS9-15466. Laboratory for Applications of Remote Sensing, Purdue University, W. Lafayette, IN. (SR-P9-00410).

3. Daughtry, C.S.T., M.E. Bauer, D.W. Crecelius and M.M. Hixson. 1980. Effects of management practices on reflectance of spring wheat canopies. Agron. J. (In press).

4. Fehr, W.R. and C.E. Caviness. 1977. Stages of soybean development. Iowa State University, Special Report No. 80. Cooperative Extension Service, Ames, Iowa.

5. Hanway, J.J. 1966. How a corn plant develops. Iowa State University, Special Report No. 48. Cooperative Extension Service, Ames, Iowa.

6. Holmes, Q.A., R. Horvath, R.C. Cicone, R.J. Kauth and W.A. Malila. 1979. Development of Landsat based technology for crop inventories. Final Report, Contract NAS9-15476, (SR-E9004041). Environmental Reseach Institute of Michigan, Ann Arbor, MI.

7. Papoulis, A. 1965. Probability, Random Variables and Stochastic Processes. McGraw-Hill Book Co., New York.

8. Rice, D.P., E.P. Crist and W.A. Malila. 1980. Applicability of selected wheat remote sensing technology to corn and soybeans. Final Report, Contract NAS9-15082, (NASA CR-9-F, ERIM 124000). Environmental Research Institute of Michigan, Ann Arbor, MI.

9. Seely, M.W., M.H. Trechard, D.E. Phinney, J.R. Baker, and R.G. Stuff. 1978. Prediction of wheat phenological development: State-of-the-art review. Proc. LACIE Symp., JSC-16015. NASA Johnson Space Center, Houston, TX. pp. 981-990.

3. Soybean Canopy Reflectance as Influenced by Cultural Practices

J. C. Kollenkark, C. S. T. Daughtry, and M. E. Bauer

3.1 Introduction

As world demand for food continues to expand, increased pressures are being placed on our agricultural systems to supply timely and accurate crop production information. In recent years considerable progress has been made toward the operational use of remote sensing technology to inventory crop acreages, assess crop stresses, and predict yields (Bauer et al., 1978). Understanding the relationship between the reflectance measured and the various cultural practices used in today's soybean production is one of the keys for further development and use of remote sensing as a tool for crop inventory.

Spectral reflectance values have been related to leaf area index, fresh and dry biomass, plant water content, chlorophyll content, percent soil cover and crop yield (Bauer, 1975; Bauer et al., 1978; Ahlrichs, 1978; Tucker et al., 1977). Colwell (1974) observed that at high soil cover levels, the reflectance factor in the red wavelength region was less sensitive to changes in percent soil cover as solar elevation decreased. The reflectance factor in the near infrared wavelength region is best for estimating leaf area index and biomass in dense canopy situations (Ahlrichs, 1978; Colwell, 1974). Holben et al. (1980) observed a high correlation of radiance in the red wavelength region to changes in percent soil cover in soybeans, but a poor correlation between crop cover and leaf area index because the leaf area index continued to increase beyond the point of 100 percent soil cover. Field data acquired by Tucker (1977) and laboratory work by Gausman et al. (1971) show that the spectral response in the visible region levels off at low leaf area indicies (approximately 2.0), compared to the near infrared region where the spectral response levels off at much higher leaf area indicies (approximately 8.0).

The importance of the soil background, especially under low soil cover, to spectral reflectance has been recognized by many. Colwell (1974) examined two differently colored soils with similar soil covers (approximately 37 percent) and reported a spectral response nearly three times higher on the light-colored soil than on the dark-colored soil in the red wavelength region. Increasing soil moisture decreases the reflectance in all wavelengths (Stoner, 1979) and may increase or decrease the contrast between the soil and vegetative reflectance (Colwell, 1974; Tucker, 1977).

The appearance of crops are greatly influenced by many cultural and environmental factors which may be sources of variation or error in remotely-sensed observations of crops.

In the search for maximum soybean yields, cultural practices including row spacing, population, and planting date are being modified. The trend has been to move from wide rows to narrower rows, to higher plant populations, and to earlier planting dates. All of these changes result in greater light interception early in the growing season and higher yields.

The objectives of this research were to study the reflectance characteristics of soybean canopies throughout the growing season as affected by several current cultural practices and to relate changes in reflectance factor to changes in agronomic characteristics of soybean canopies.

3.2 Materials and Methods

Experimental Conditions. Experiments were conducted on the Purdue Agronomy Farm northwest of West Lafayette, Indiana. The 1978 experiment was a randomized, complete block design which included three blocks, three cultivars (Amsoy 71, Wells, and Elf), three populations (111,000, 185,000, and 259,000 plants/ha), and three row widths (15, 45, and 90 cm) for a total of 81 plots. The plot size was 2.3 x 14.5 meters and all rows were in a north-south orientation. The plots were hand thinned to obtain the desired populations.

The 1979 soybean cultural practices experiment was a randomized, complete block design with two soil types (Chalmers silty clay loam, typic Argiaquoll, and Russell silt loam, typic Hapludalf), two blocks within each soil type, two row widths (25 and 75 cm), two cultivars (Amsoy 71, Williams), and three planting dates. Planting dates for the Chalmers silty clay loam were May 10, May 24, and June 15. Poor drainage on the Russell silt loam delayed the planting dates on it to May 24, June 15, and July 3. The plot size was 3.4 x 15 meters and all rows were planted in the north-south orientation.

Spectral Measurements. Reflectance factor data were acquired with a Landsat-band radiometer (Exotech Model 100) several times throughout the growing season each year. The Exotech Model 100 is a four-band radiometer with a 15 degree field of view that acquires data in the following wavelength regions 0.5-0.6, 0.6-0.7, 0.7-0.8, and 0.8-1.1 μm. Data were taken only under near cloud-free conditions (especially in the vicinity of the sun) when the solar elevation angle was at least 45 degrees above the horizon.

The radiometer and motor driven camera were attached to a boom mounted on a pickup truck for quick and efficient data collection in the field (Figure A-3.1). The instruments were elevated 3.4 meters above the soil surface in 1978 and 5.2 meters in 1979. Instruments were leveled for a nadir look angle and measurements were taken over two locations in each plot. Observations were taken on-row and off-row to obtain a better estimate of the overall canopy response for the plot and to reduce any bias. Measurements in all four bands were recorded concurrently by a printing data logger. A vertical photograph was taken of each plot for later crop assessment and soil cover determination.
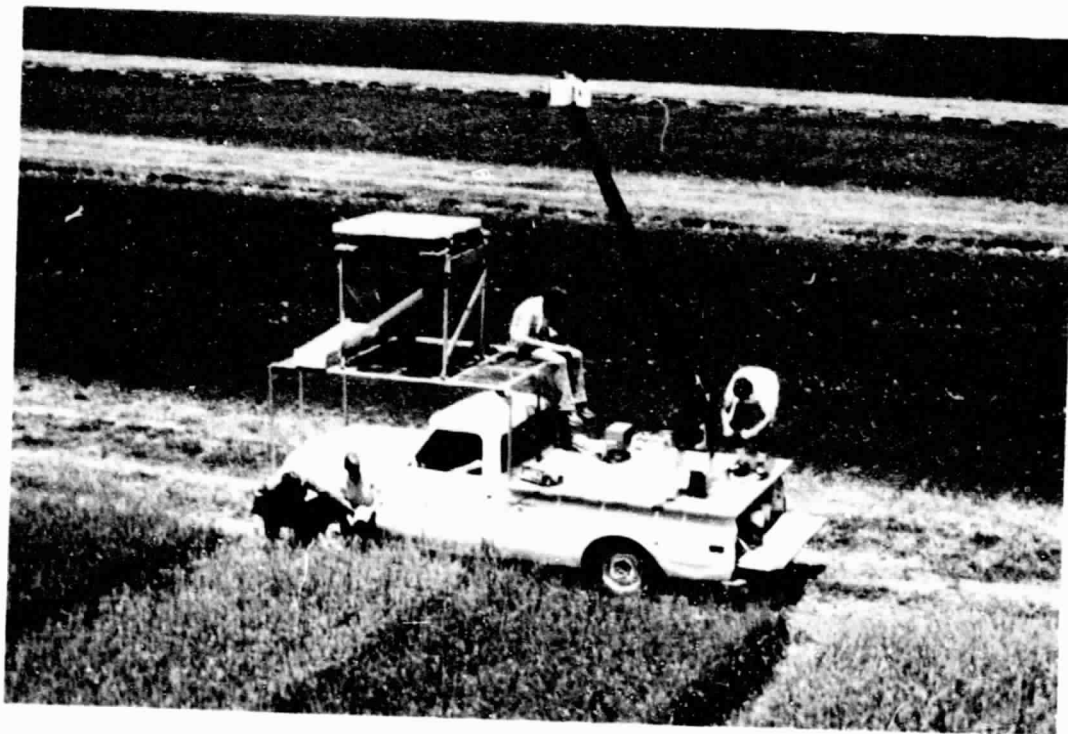
Figure A-3.1 Field radiometer system including Exotech Model 100
radiometer, camera, and $BaSO_4$ calibration standard.

Agronomic measurements, which were collected coincidentally with the reflectance factor data in 1979 and weekly in 1978, included height, leaf area index, development stage, total fresh and dry biomass, and dry stem (including petioles), pod, and green leaf blade weights, and soil moisture. Percent soil cover was determined by placing a grid over the vertical photograph and counting the intersections occupied by green vegetation. Leaf area index (LAI) was calculated by multiplying the leaf area/dry leaf weight ratio of a random subsample of green leaves by the total dry green leaf weight and dividing by the soil area represented. Visual assessment of the soil moisture and crop condition were made during the spectral data collection. Crop condition assessment included evaluation of lodging, hail, insect, and herbicide damage.

Data Analysis. The reflectance factor data were analyzed as band means and as transformations. The reflectance factor data were transformed into greenness as described by Kauth and Thomas (1976) for Landsat MSS data and modified for spectrometer data (Malila and Gleason, 1977). The greenness funtion used was as follows: Greenness = ((Band3 * 0.17289) + (Band4 * 0.59538)) - ((Band1 * 0.48935) + (Band2 * 0.61249)). Band1 to Band4 refer to the reflectance factors in each band. A near infrared/red reflectance ratio, 0.8-1.1 μm/0.6-0.7 μm, was also considered in the analysis. Regression and correlation analyses were used to quantify the relationship between spectral values and agronomic characteristics. Analysis of variance and Duncan's Multiple Range Test were used to determine which of the experimental treatments accounted for the variability in spectral responses.

3.3 Results and Discussion

Relationships Between Reflectance Factor and Agronomic Variables. Previous research has indicated that the reflectance of crop canopies is related to the amount of vegetation present and in particular to the amount of photosynthetically active vegetation present in the canopy (Aase and Siddaway, 1980; Bauer et al., 1979; Leamer et al., 1978). The senescing plant canopy causes an increased spectral response in the visible wavelength region due to a decrease in the pigment concentration and thus absorption. A decreased response in the near infrared region may be due to a deterioration of the cell constituents (Knipling, 1970). Ahlrichs (1978) and Leamer et al. (1978) observed substantial decreases in the correlation of canopy variables and reflectance factor as the canopy began to senesce or ripen. Plots with senescing canopies still have a high soil cover, but have a reflectance factor value approaching that of a low soil cover plot. The remainder of the analyses of reflectance factor with canopy variables do not include dates with senescent vegetation.

Reflectance factors in both the visible and near infrared bands were greatly affected by changes in soil background, especially under low soil covers, whereas the near infrared/red and greenness functions were not greatly influenced by changes in soil moisture. The

relationship of canopy variables and reflectance factors are not clear if wet, moist, and dry soils are treated together. Therefore, data from those dates with wet or moist soil were removed for those analyses involving the two single bands as they were strongly affected by the changes in soil moisture.

Soil color was a new factor introduced into the 1979 soybean cultural practices experiment. The effects of soil color background differences were quite similar to those observed with the wet versus dry soils. Figure A-3.2 is a plot of the mean response of the band or transformation by the percent soil cover. The two single bands (Figures A-3.2a and A-3.2b) show significant differences in reflectance factor to soil type when equal soil cover percentages are compared. This was especially noted for lower soil covers. In both the red and near-infrared bands, the dark soil response was significantly lower until the canopy reached 80-90 percent cover. The effect of soil background on response was less in the near-infrared/red ratio and greenness plots (Figures A-3.2c and A3.2d). The greennes) transformation is essentially a difference of the near infrared and red bands, respectively. Since the reflectance factor response to soil background changes were similar in all bands, a normalizing effect occurs in both transformations.

Table A-3.1 shows the results of fitting a quadratic equation $y = b_0 + bx_1 + bx_2$ to the data where y is the agronomic variable, x is the spectral band or transformation, and b is the regression coefficient. Percent soil cover and leaf area index were highly correlated with the different bands and transformations. The near infrared/red and greenness transformations had stronger relationships to the canopy characteristics than either single band. More spectral information is contained in these transformations and more data, including moist soil data, can be utilized in the analysis. In 1978, the coefficient of determination values (r-square) for percent soil cover were 0.90, 0.93, 0.97, and 0.97 to the red and near infrared bands, and the near infrared/red and greenness transformations, respectively.

Figure A-3.3 illustrates the relationship between four different agronomically important crop variables with greenness on the dark soil plots. A near linear relationship with little scatter is evident between the percent soil cover and the greenness function (Figure A-3.3a). The function reaches an asymptote as the maximum value for soil cover is reached. The curvilinear shape for the other factors were the result of a non-linear relationship between soil cover and leaf area index and biomass. Complete canopy cover was reached before the maximum values were reached for leaf area index or biomass.

A fairly strong relationship between increases in greenness to increases in leaf area index is shown in Figure A-3.3b. The moderately high amount of scatter at higher greenness levels was probably due to sampling errors. This could include irregular plant distribution and size within a plot, or poor estimates of plant populations from the counts taken in late June.

A question that may be asked is why are the coefficients of determination between greenness and fresh and dry biomass so much lower than those between greenness and soil cover or leaf area index? The
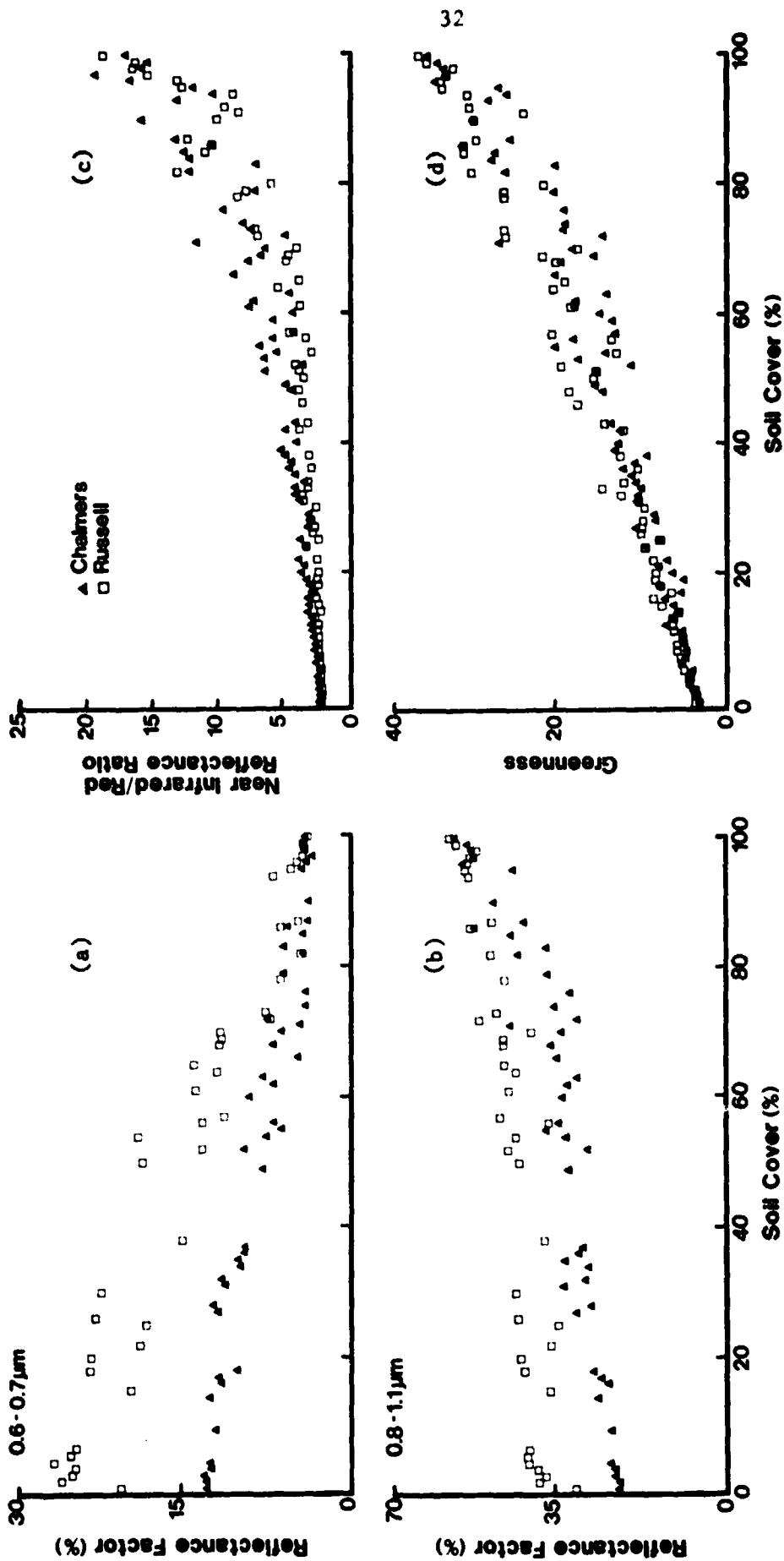
Figure A-3.2. Effect of soil background on the relationship of percent soil cover to four different spectral variables (a) RF in red wavelength region (0.6-0.7 μm) (b) RF in near infrared wavelength region (0.8-1.1 μm) (c) near infrared/red reflectance ratio (d) greenness.

Table A-3.1. Coefficient of determination values (R^2) from fitting both the linear and quadratic values of four spectral variables for two soil types to explain the variation in percent soil cover, leaf area index, fresh biomass, and dry biomass in 1979.

Soil Type	Agronomic Variable	Spectral Variable				Range of Data
		Red	NIR	NIR/Red	Greenness	
Chalmers	Soil Cover	.94	.93	.95	.98	0-100 %
	Leaf Area Index	.65	.80	.85	.86	0-8.9
	Fresh Biomass	.61	.71	.81	.81	0-9120 (g/m^2)
	Dry Biomass	.53	.64	.73	.74	0-2489 (g/m^2)
Russell	Soil Cover	.98	.93	.92	.98	0-100 %
	Leaf Area Index	.73	.69	.83	.84	0-8.8
	Fresh Biomass	.59	.49	.71	.66	0-9633 (g/m^2)
	Dry Biomass	.47	.36	.57	.52	0-3027 (g/m^2)
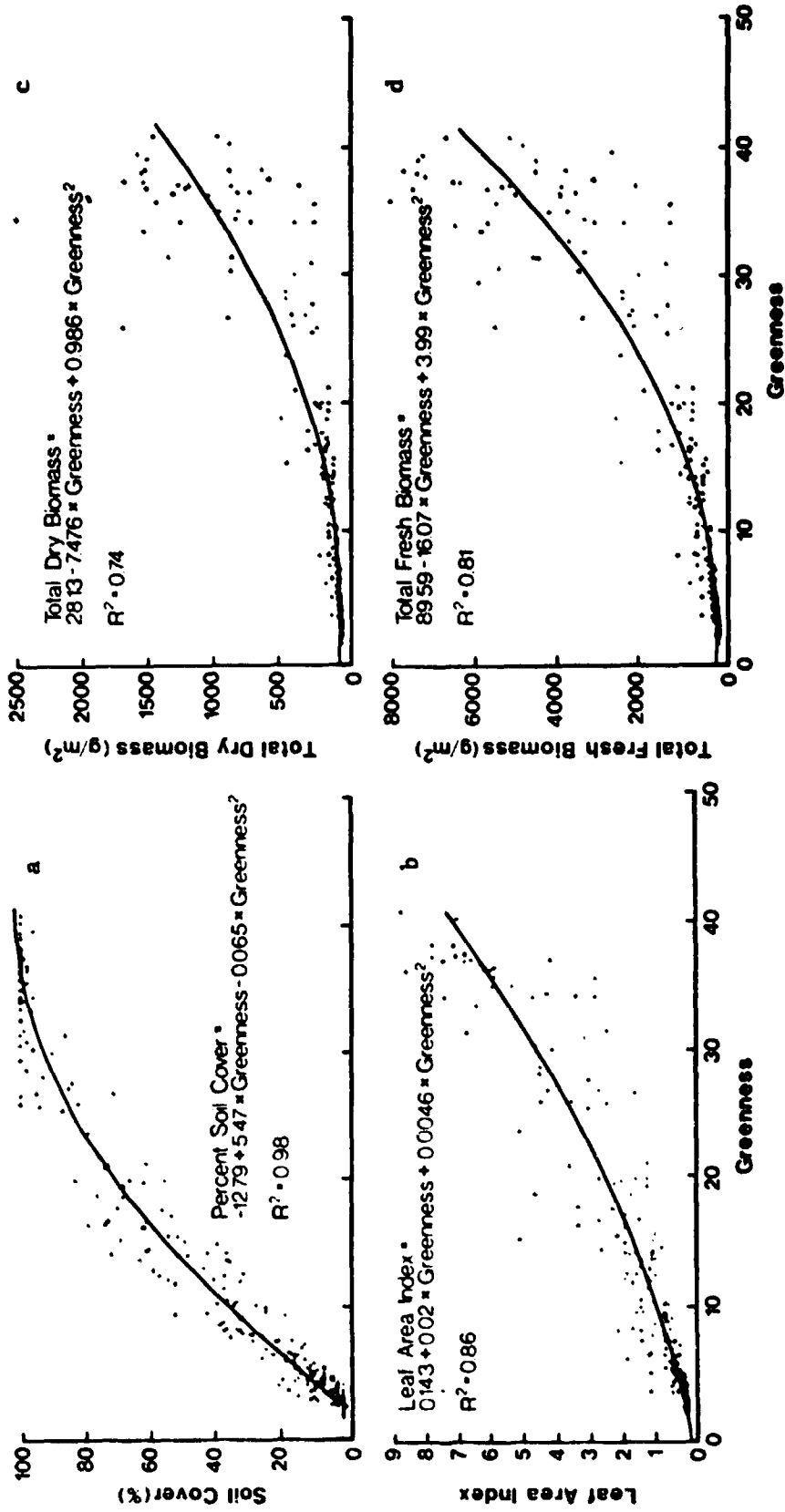
Figure A-3.3. Plots of four agronomic variables versus greenness (a) percent soil cover (b) leaf area index (c) total dry biomass (d) total fresh biomass. (Chalmers silty clay loam)

35
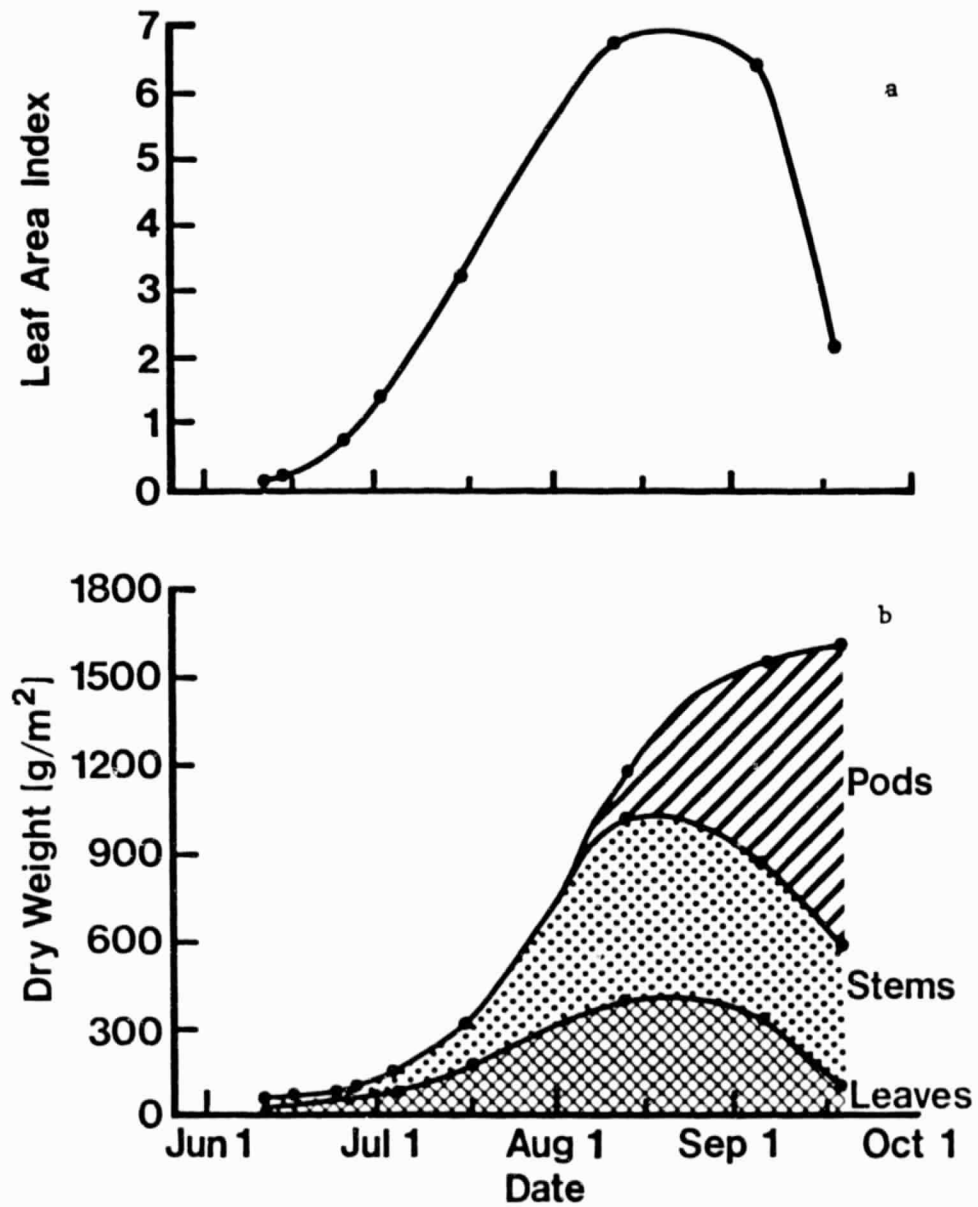
Figure A-3.4. Seasonal changes in (a) leaf area index and (b) soybean canopy components for the May 24 planting date on Chalmers silty clay loam.

upper periphery of a soybean canopy, the primary radiation reflecting portion of the canopy, is largely comprised of leaves. Percent soil cover and leaf area index are mainly functions of the green leaves throughout most of the growing season. The green leaf area index, as illustrated in Figure A-3.4a, reaches a maximum value in late August, and then falls off. It is about this same time when maximum values of greenness are noted, that the dry leaf weight becomes a smaller proportion of the total dry weight. Other components, including stems and pods that are not observed from the nadir view angle prior to the onset of senescence, have a faster growth rate late in the season and thus make up a larger portion of the total dry weight. Similar results were observed by Hanway and Thompson (1967). Therefore, later in the season after near-full canopies are obtained, the canopy may still be accumulating biomass that, perhaps, is not spectrally detectable.

Effects of Cultural Practices on Reflectance Factor. In the 1978 experiment, row width and cultivar were the primary factors affecting the measured spectral response (Figures A-3.5 and A-3.6). Row width significantly affected the measured soil cover and reflectance through the first part of the season when canopies were filling in at different rates (Figure A-3.5). The canopies with the two narrow row widths developed quite similarly, but the canopy with the 90 cm row width developed slowly. Very little difference was seen after August 20, when all three canopies reached nearly 100 percent cover.

Differences in spectral response among cultivars early in the season were attributed to differences in soil cover. Elf, a compact and determinate semi-dwarf, filled in faster than the other two taller indeterminate cultivars. By September 1, differences were due to the three cultivars senescing at different times and rates (Figure A-3.6). Elf (maturity group III) had considerably more green leaf area later in the season than Amsoy 71 or Wells (maturity group II). Leamer et al. (1978) also showed spectral differences in wheat cultivars having different maturity dates. Plant population in the 1978 experiment did not show any significant effect on either soil cover or reflectance measurements.

In the 1979 experiments, row width and cultivar showed trends similar to those seen in the 1978 experiment. Again, the response seemed related to the amount of photosynthetically active (green) vegetation present. The effect of row width on percent soil cover and reflectance are shown in Figure A-3.7. The differences were greatest in the first part of the season. Amsoy 71 (maturity group II) and Williams (maturity group III), had similar soil covers and spectral responses except for late in the season when differences in plant senescense occurred, with Amsoy 71 showing signs of senescence first. Amsoy 71 was also the taller of the two indeterminate cultivars and was somewhat more susceptible to lodging.

The effect due to the three planting dates was a result of differing amounts of green vegetation present and thus the measured reflectance factor and transformations. Figure A-3.8 shows an example of the seasonal changes in soil cover and spectral response of soybeans in the 75 cm wide rows on the light-colored soil as a function of planting date. Early planting dates had higher percent soil covers
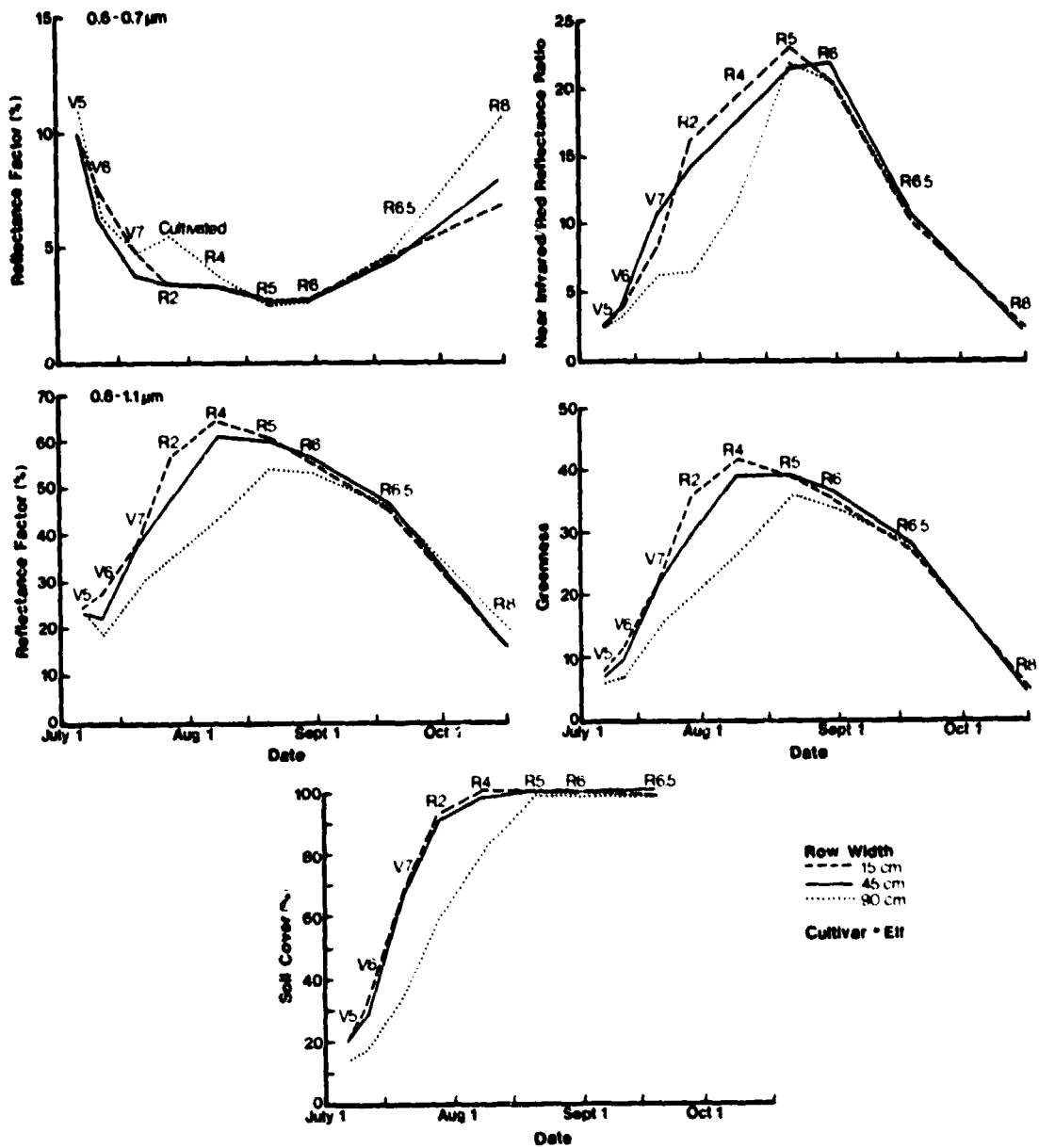
Figure A-3.5. Seasonal changes in four spectral variables and percent
soil cover for three row widths in 1978 for the cultivar Elf. Dev-
elopment stages (Fehr and Caviness, 1977) are indicated for each
observation date.
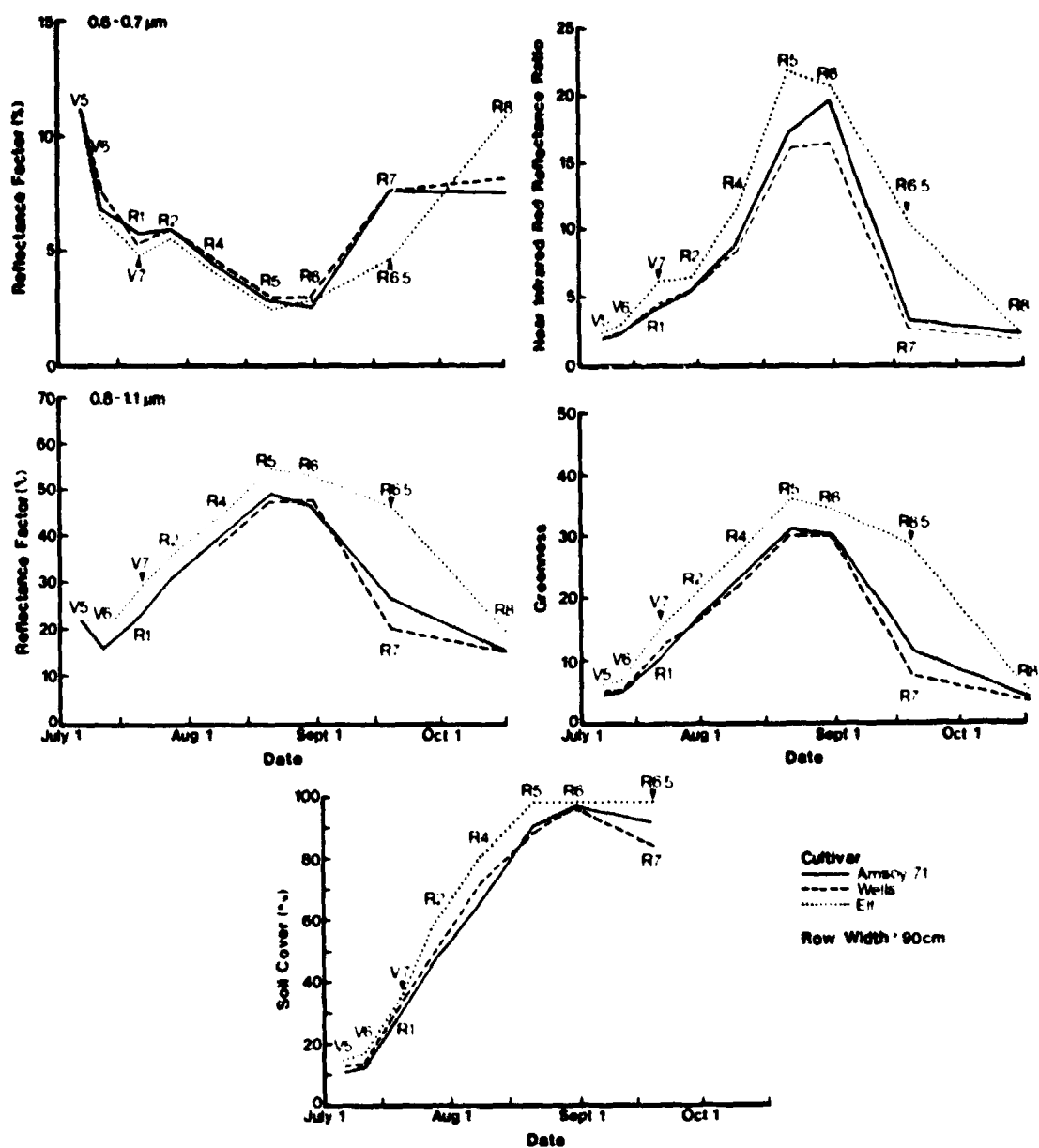
Figure A-3.6. Seasonal changes in four spectral variables and percent
soil cover for three cultivars in 1978 on 90 cm wide rows. Development
stages (Fehr and Caviness, 1977) are identified for each observation
date. Arrows indicate development stages that are unique for that cul-
tivar.
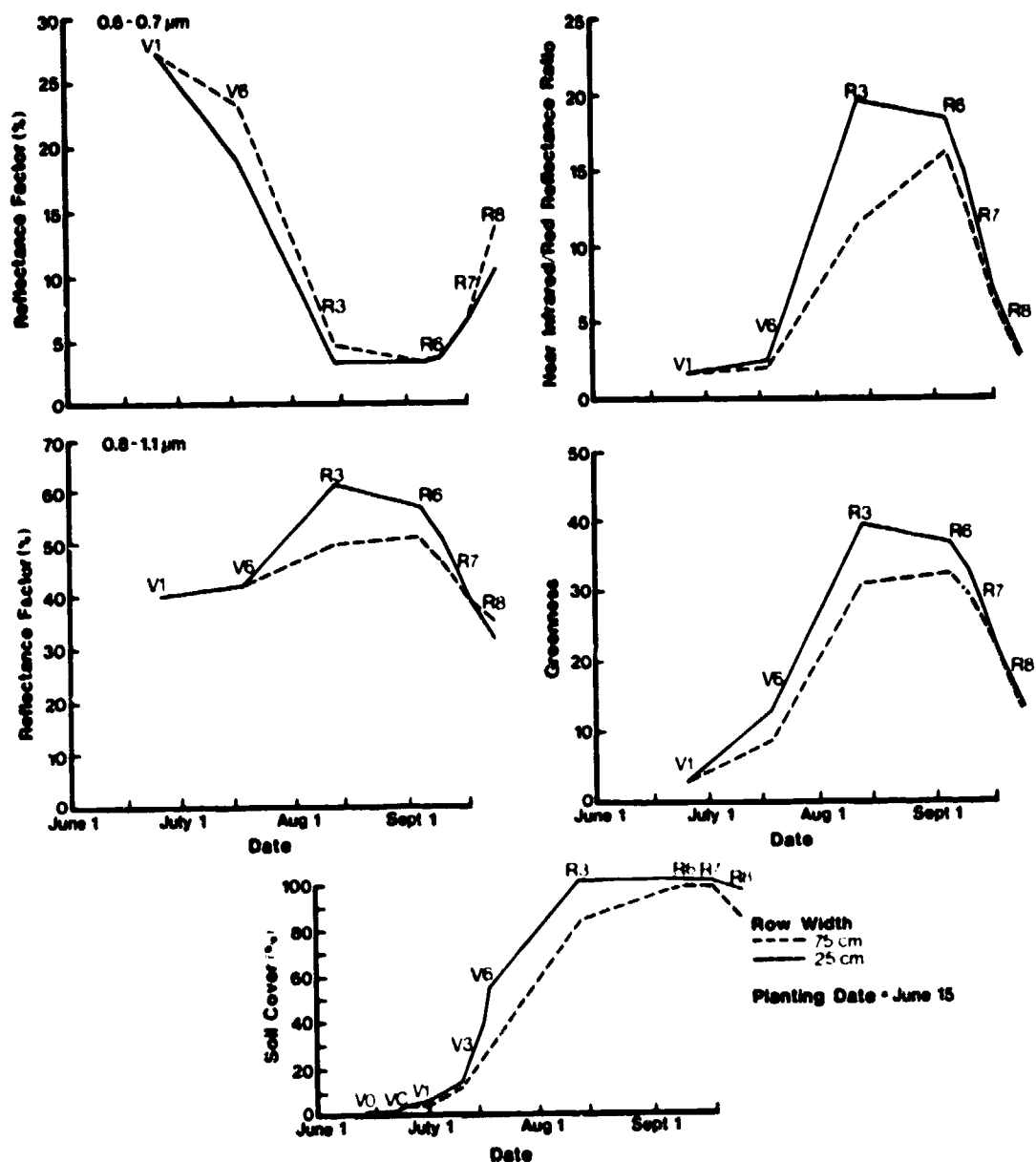
Figure A-3.7. Seasonal changes in four spectral variables and percent soil cover for two row widths in 1979 for the June 15 planting date. Development stages are indicated for each observation date (Russell silt loam).
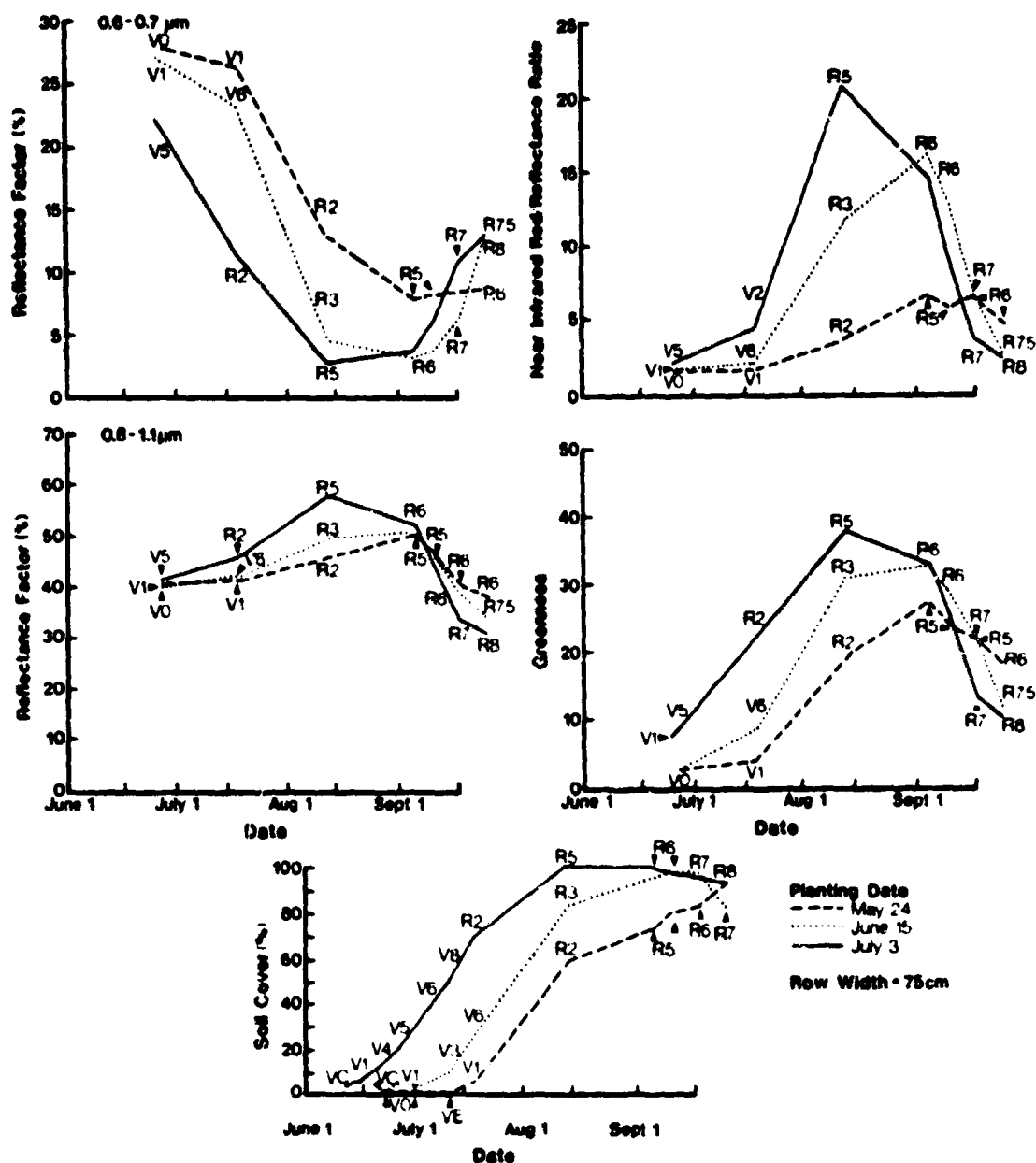
Figure A-3.8. Seasonal changes in four spectral variables and percent
soil cover for three planting dates in 1979 for 75 cm wide rows. Dev-
elopment stages (Fehr and Caviness, 1977) are indicated for each
observation date. Arrows indicate development stages that are unique
for that planting date (Russell silt loam).

early in the season and therefore a dramatic effect on the four spectral
variables was noted. The largest differences due to planting date were
usually observed in the spectral functions involving the red wavelength
band. The maximum soil cover and infrared spectral response to green
vegetation was observed for all planting dates at approximately the time
the plants were at development stage R5 (beginning seed).

3.4 Conclusions

The results of these experiments indicate that several cultural
practices cause differences in percent soil cover, leaf area index, and
biomass which in turn are manifested in the spectral reflectance
characteristics of soybean canopies. Soil color and moisture were found
to be important factors to consider when measuring reflectance in single
bands within the visible and infrared wavelength regions.   Spectral
response was found to be very sensitive to plant senescense.   For
predicting agronomically important crop canopy variables with
reflectance data, dates which include senscing plant vegetation should
be deleted from the analysis.   The near infrared/red reflectance ratio
and the greenness transformation were useful in predicting percent soil
cover and leaf area index, and were found to be less sensitive than
single bands to the soil background present.

Understanding both the agronomic and spectral changes in the
soybean crop canopy is a key to further development and use of remote
sensing technology. This study has evaluated several cultural practices
in soybeans that affect the percent soil cover, leaf area index, and
biomass and which in turn are closely related to the canopy reflectance.
This information will be useful in future applications on a large scale
for crop identification and for estimation of agronomic variables
related to crop growth, development, and yield.

3.5 References

1. Aase, J.K. and F.H. Siddaway. 1980. Determining winter wheat
    stand densities using spectral reflectance measurements. Agronomy
    Journal 72: 149-152.

2. Ahlrichs, J.S. 1978. Relation of crop canopy variables to the
    multispectral reflectance of spring wheat. M.S. Thesis, Purdue
    University, West Lafayette, IN.

3. Bauer, M.E. 1975. The role of remote sensing in determining the
    distribution and yield of crops. Advances in Agronomy 27:
    271-304.

4. Bauer, M.E., M.C. McEwen, W.A. Malila, and J.C. Harlan. 1978.
    Implementation and results of LACIE field research. Proc. Design,
    LACIE Symposium. NASA/Johnson Space Center, Houston, TX.
    JSC-16015, pp. 1037-1066.

5. Colwell, J.E. 1974. Vegetation canopy reflectance. Remote
    Sensing of Environment 3: 175-183.

6. Duggin, M.J. 1977. Likely effects of solar elevation on the quantification of changes in vegetation with maturity using sequential Landsat imagery. Applied Optics 16: 521-523.

7. Gausman, H.W., W.A. Allen, R. Cardenas, and A.J. Richardson. 1971. Effects of leaf nodal position on absorption and scattering coefficients and infinite reflectance of cotton leaves, *Gossypium hirsutum* L. Agronomy Journal 63: 87-91.

8. Hanway, J.J. and H.E. Thompson. 1967. How a soybean plant develops. Special Report 53. Iowa State University, Ames, Iowa pp. 1-18.

9. Holben, B.N., C.J. Tucker, and C. Fan. 1980. Assessing soybean leaf area and leaf biomass. Photogrammetric Engineering and Remote Sensing 46: 651-656.

10. Malila, W.A. and J.M. Gleason. 1977. Investigations of spectral separability of small grains, early season wheat detection, and multicrop inventory planning. ERIM Report 122700-34-F. Environmental Research Institute of Michigan, Ann Arbor, MI.

11. Stoner, E.R. 1979. Physiochemical, site, and bidirectional reflectance characteristics of uniformly moist soils. Ph.D. Thesis. Purdue University, West Lafayette, IN.

12. Tucker, C.J. and L.D. Miller. 1977. Soil spectra contributions to grass remote sensing. Photogrammetric Engineering and Remote Sensing 43:721-726.

4. Maize Canopy Reflectance as Influenced by Nitrogen Nutrition

G. Walburg, C.S.T. Daughtry, and M.E. Bauer

4.1 Introduction

Satellite measurements of radiation reflected from crop canopies have been used to identify crop type and estimate crop areas (MacDonald and Hall, 1980); spectral measurements also have potential for use in monitoring crop condition and predicting yields (Bauer, 1975). Accurate assessments of growth and condition from spectral measurements will require further understanding of the relationship between canopy development and spectral response. Aspects of this relationship have been described for several crop species (Leamer et al., 1978; Daughtry et al., 1980; Tucker et al., 1979). Yet, greater knowledge of how canopy spectral response is affected by the many environmental and cultural factors which alter crop development is needed. In particular, relatively little research has been conducted on the effects of plant stresses on canopy reflectance.

Several laboratory studies of stress effects on single leaves have been performed. Al-Abbas et al. (1974) found that several mineral deficiencies increased the reflectance of radiation in the visible wavelength region of maize leaves, while effects on near and middle infrared reflectance varied with the specific mineral deficiency. Nitrogen deficiency increased visible (0.4 to 0.7 μm) and near infrared (0.7 to 1.4 μm) reflectance while decreasing middle infrared (1.4 to 2.5 μm) reflectance from sweet pepper leaves (Thomas and Oerther, 1972). The sensitivity of chlorophyll to metabolic disruption accounted for the response of leaf reflectance in the visible wavelengths to stress conditions (Knipling, 1970). Stress-induced leaf reflectance variations in the near and middle infrared wavelengths have been attributed to altered leaf mesophyll structure (Gausman, et al., 1969) and water content (Carlson et al., 1971), respectively.

While changes in leaf reflectance are important stress indicators, frequently the most important factor for spectrally separating healthy from stressed plant canopies is differences in leaf area index (LAI) (Knipling, 1970). A decrease in LAI causes canopy reflectance to decrease in the near infrared and increase in the red without any change in the reflectance properties of individual leaves (Colwell, 1974). Stanhill et al. (1972) concluded that the major factor causing the altered spectral response of nitrogen deficient wheat canopies was changes in total biomass, while altered leaf optical properties or changed canopy configuration were only secondarily important.

The objectives of this research were: (1) to determine the seasonal spectral responses of maize canopies under varying levels of applied nitrogen, (2) to relate measurements of canopy spectral response to canopy agronomic characteristics, and (3) to determine the spectral separability of maize canopies under different treatments.

4.2 Materials and Methods

Experimental Conditions. The experiment was conducted at the Purdue Agronomy Farm, West Lafayette, Indiana, during the 1978 and 1979 growing seasons. The soil was a Raub silt loam (Aquic Argiudoll). June through September rainfall was 34 cm in 1978 and 39 cm in 1979, both near the 27-year average of 39 cm.

A randomized, complete block design was used, with three replications of each treatment. Each plot consisted of six rows of maize planted 71 cm apart in an east-west orientation. Maize hybrid Beck (Zea mays L.) 65X was planted on May 31, 1978 at a population of 54,000 plants/ha and Pioneer 3183 hybrid was planted on May 10, 1979 at 66,000 plants/ha. Nitrogen treatments were four levels of urea, 0, 67, 134, and 202 kg N/ha, applied in the spring. Identical rates have been applied to the same plots continuously since 1965. In the fall, prior to planting, 49 kg/ha P and 93 kg/ha K were added to each plot. Atrazine was applied after planting for weed control.

Spectral Data Collection. Spectral reflectance measurements over the 0.4 to 2.4 μm wavelength region were collected with an Exotech 20 spectroradiometer (Leamer et al., 1973) mounted on the boom of a mobile aerial tower. Spectral data were acquired on 11 dates during 1978 and 12 dates during 1979. Measurements were made centered on the plot, looking straight down from an altitude of 9.1 m. With a 15 degree field of view the sensor viewed a 2.3 m diameter ground area from this altitude. All spectral measurements were made on cloudless or near cloudless days when the sun angle was greater than 45° above the horizon and prior to solar noon. Each spectral data set was collected within a 1.5 hour time period. A 1.2 m square panel painted with barium sulfate was used as a reference surface for determining the reflectance factor (Robinson and Biehl, 1979). The response of the reference panel was measured approximately every 20 minutes throughout the data acquisition period.

Canopy Characterization. Agronomic measurements and observations were acquired throughout each season corresponding to the dates of spectral measurements. These data included: development stage, leaf area index, percent soil cover, fresh and dry biomass, leaf chlorophyll concentration, leaf nitrogen content, and grain yield.

Data Analysis. Spectral data were analyzed as band means corresponding to the Landsat multispectral scanner (MSS) bands and to
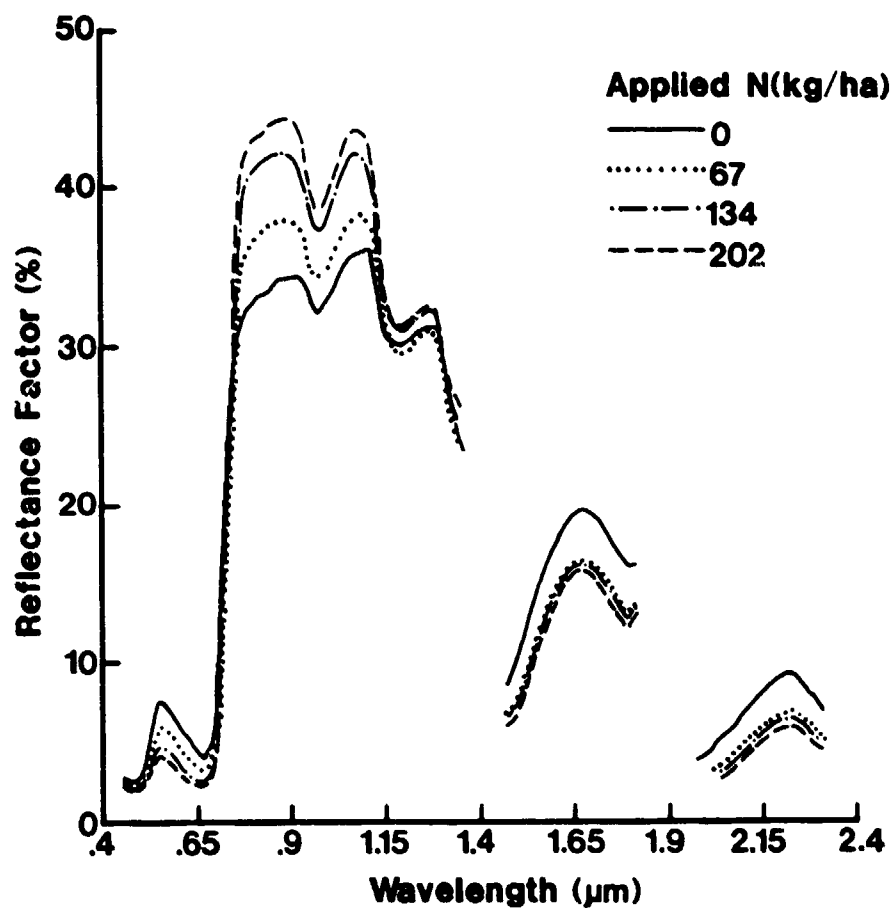
Figure A-4.1. Reflectance factor as a function of wavelength for maize canopies under four N treatment levels on 4 August 1979. Each curve is the mean of three replications.

the thematic mapper bands. The thematic mapper is an updated multispectral scanner scheduled for launching aboard the Landsat-D satellite (Blanchard and Weinstein, 1979). The thematic mapper bands are narrower and are more optimally placed for spectral characterization of vegetation than the Landsat MSS bands. The Landsat MSS spectral bands are: 0.5-0.6, 0.6-0.7, 0.7-0.8, and 0.8-1.1 μm. The reflective thematic mapper bands are: 0.45-0.52, 0.52-0.60, 0.63-0.69, 0.76-0.90, 1.55-1.75, and 2.08-2.35 μm. In addition to these single bands, the data were analyzed as ratios and transformations of the band means. Greenness, a transformation of the Landsat MSS bands (Kauth and Thomas, 1976), was computed using coefficients derived for spectrometer data (Rice et al., 1980). Greenness = (-0.48935) (R, 0.5-0.6 μm) + (-0.61249) (R, 0.6-0.7 μm) + (0.17289) (R, 0.7-0.8 μm) + (0.59538) (R, 0.8-1.1 μm). The ratio of near infrared/red reflectance was computed using the 0.76-0.90 and 0.63-0.69 μm bands. Correlation and regression analyses of spectral response and the various agronomic measurements were performed and scatter plots made of their relationships. Duncan's multiple range test with P = 0.05 was used to perform mean separation tests on both the spectral and agronomic data.

4.3 Results and Discussion

Reflectance spectra of corn canopies grown with varying rates of nitrogen (N) fertilization for a selected date (4 August 1979) are shown in Figure A-4.1. Similar responses were observed on other dates in July and August during both years. The effects of varying nutrition were exhibited across the entire wavelength interval measured. Reflectance decreased in the visible and middle infrared wavelength regions with increasing N fertilizer application, while in the near infrared wavelength region reflectance was increased. Similar changes in visible and near infrared reflectance have previously been attributed to differences in LAI, percent soil cover, and plant biomass (Colwell, 1974; Knipling, 1970). It is likely that variation in spectral reflectance among N treatments also resulted from charges in leaf structure and composition including pigment concentration, cell size, and cell wall composition and structure, all of which are altered by N treatment (Vesk et al., 1966).

Seasonal patterns of spectral response and canopy characteristics Figure A-4.2 and A-4.3) were closely related and the effects of varying N fertilization both on crop growth and spectral response are seen throughout both seasons. As LAI, biomass and soil cover increased, the red (0.63 to 0.69 μm) reflectance decreased, while the near infrared (0.76 to 0.90 μm) reflectance increased. The middle infrared showed seasonal trends similar to the visible wavelengths. The middle infrared differs from the visible in that absorption in the middle infrared region is due to plant water content while absorption in the visible region is due to plant pigments (Gates et al, 1965). Near infrared reflectance increases with increasing vegetative cover due to increased light scattering and reflectance by multiple leaf layers (Gausman et al., 1976).
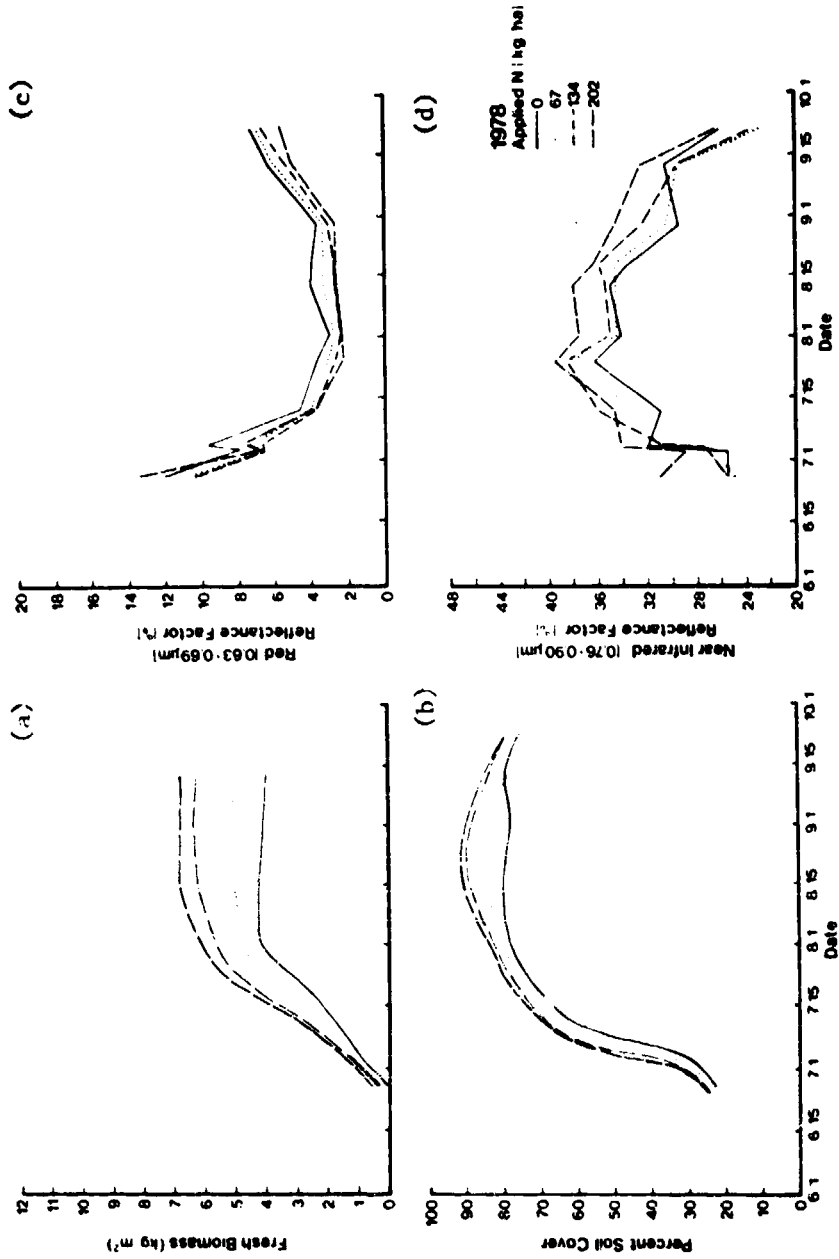
Figure A-4.2. Temporal changes in (a) fresh biomass, (b) percent soil cover, (c) red (0.63-0.69 μm) and (d) near infrared (0.76-0.90 μm) reflectance factor for maize canopies under four N treatment levels in 1978.
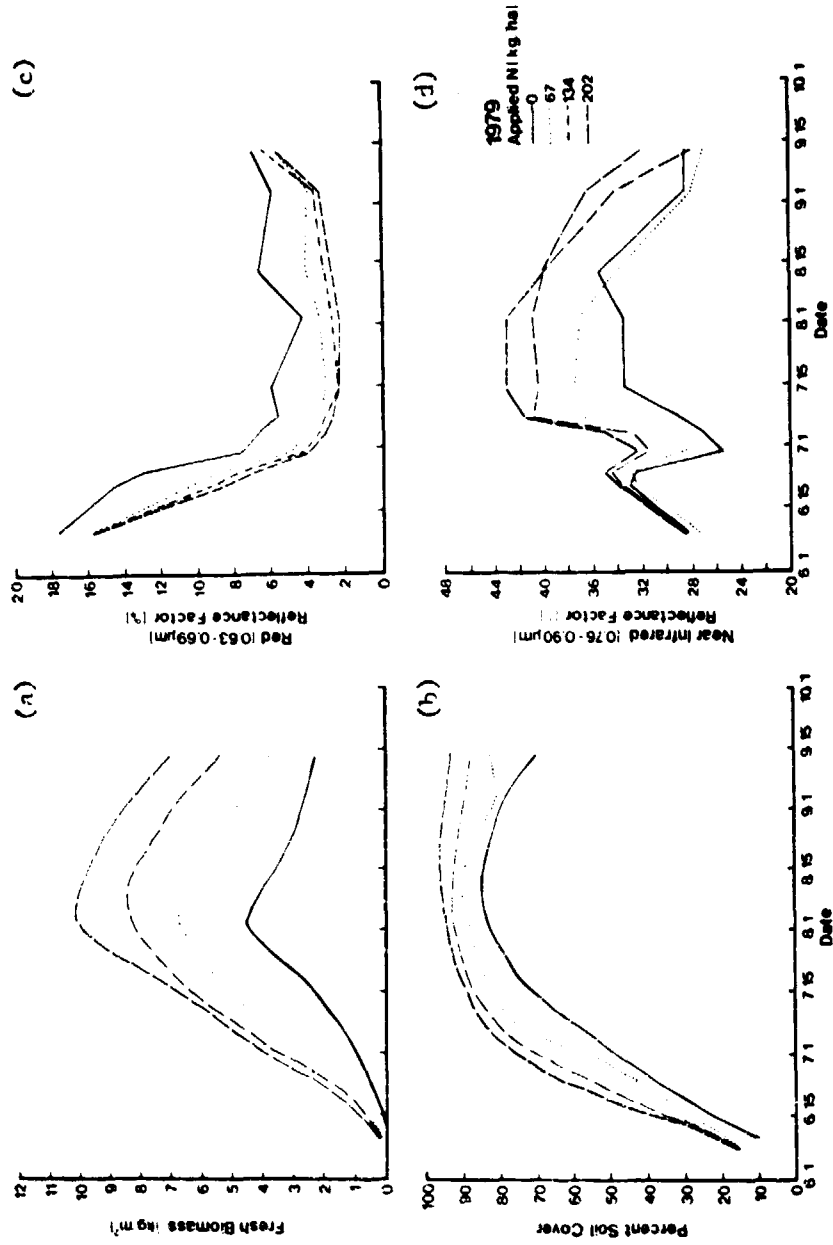
Figure A-4.3. Temporal changes in (a) fresh biomass, (b) percent soil cover, (c) red (0.63-0.69 μm) and (d) near infrared (0.76-0.90 μm) reflectance factor for maize canopies under four N treatment levels in 1979.

The large reflectance decrease measured on June 30, 1979, was due to 4.8 cm rainfall earlier that day which caused a large decrease in the soil reflectance at a time when the canopy cover was relatively low.

The larger treatment effects observed in both red and near infrared reflectance in 1979 compared to 1978 were attributed to the greater differences in biomass and LAI between treatments in 1979. These were in turn attributed mainly to planting date. Date of planting is known to have major effects on crop development and yields (Genter and Jones, 1970). Wet soils delayed planting in 1978 until May 31, while in 1979 planting was nearer the mean for the 15-year history of these plots. The 1979 results are more typical of mean treatment differences in grain yield.

A frequently applied method of multispectral data analysis is based on ratios between different spectral bands. The near infrared/red reflectance ratio has been shown analytically by Bunnik (1978) to be strongly related to variations in LAI of vegetative canopies, while being relatively insensitive to variations in soil background reflectance. The advantages of this ratio are indicated in Figure A-4.4 which relates the near infrared/red reflectance ratio and red reflectance to LAI. A strong positive relation of LAI to the near infrared/red ratio is found even when data from two growing seasons are included, while there is a considerable degree of scatter, particularly at low LAI values, for the red reflectance to LAI relationship. The latter is attributed to variations in soil reflectance due primarily to changes in soil moisture and roughness. The near infrared/red ratio was a more sensitive indicator of LAI changes throughout the range of values encountered for this data set, than either the near infrared band or the red band which approached an asymptote at LAI values above three. Figure A-4.5 shows the accentuation of treatment differences throughout the growing season by use of the near infrared/red ratio over that exhibited by single bands (Figure A-4.2 and A-4.3).

Six spectral variables, the near infrared/red ratio, greenness transformation, and the reflectances in four thematic mapper bands in different parts of the spectrum, were chosen for further analysis. Greenness has shown strong correlations with agronomic characteristics of crop canopies (Daughtry et al., 1980). The thematic mapper bands were selected for analysis since reflectances in these bands have shown higher correlations with crop canopy characteristics than the Landsat MSS bands (Ahlrichs and Bauer, 1978; Tucker and Maxwell, 1976).

Spectral discriminability of the N treatments varied over the season (Tables A-4.1 and A-4.2). For all spectral variables treatment separation was maximum on the August dates. This period corresponds to the stage of maximum vegetative development. At early dates, when the percent soil cover was low, treatment differences were less recognizable due to the spectral response of the soil overweighing the canopy response (Colwell, 1974). Late in the season, as senescence caused treatment differences to erode, treatments were again less separable.
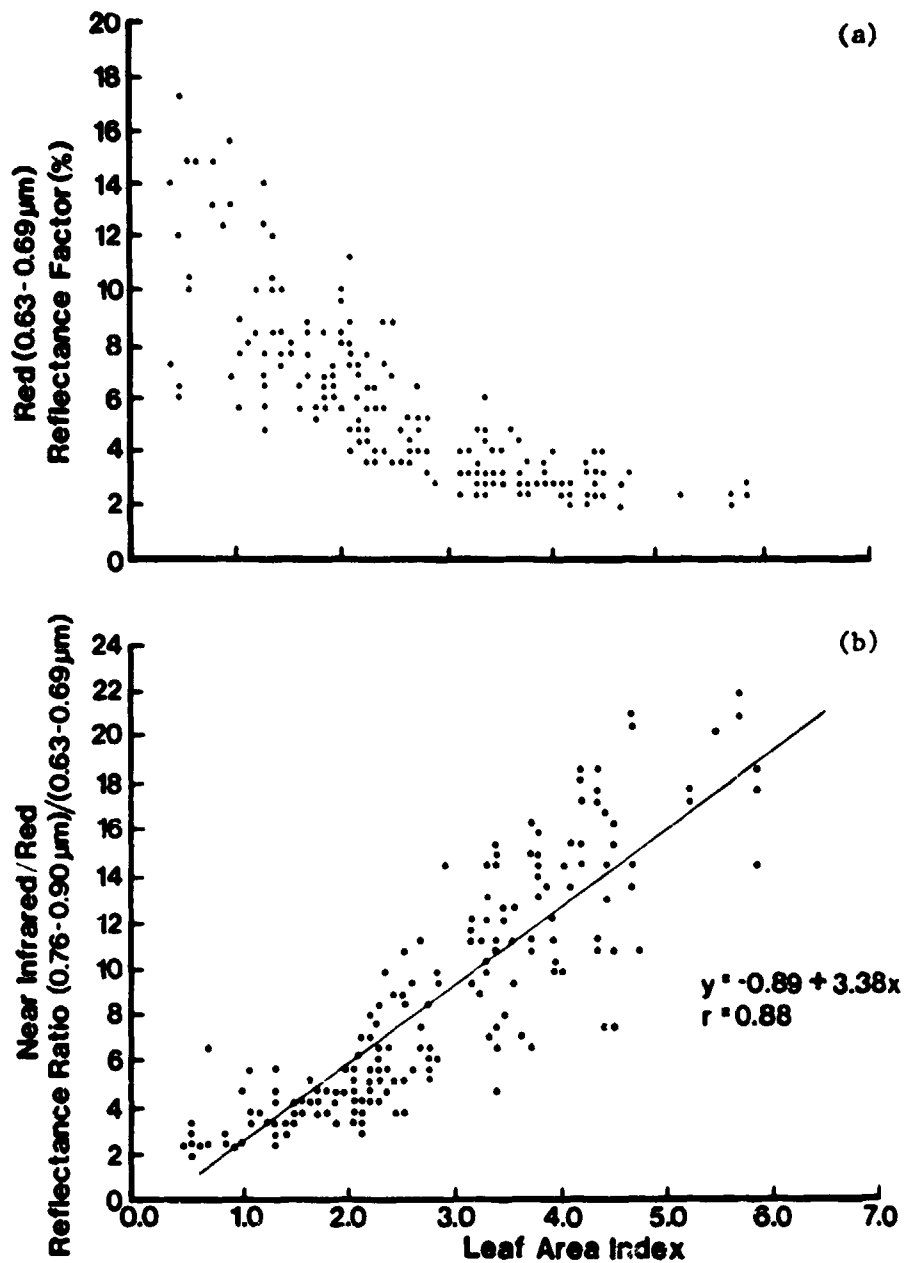
Figure A-4.4. The relationship of (a) the red (0.63-0.69 μm) reflectance factor and (b) the near infrared/red reflectance ratio, (0.76-0.90 μm)/ (0.63-0.69 μm), to leaf area index. Both 1978 and 1979 data are included.
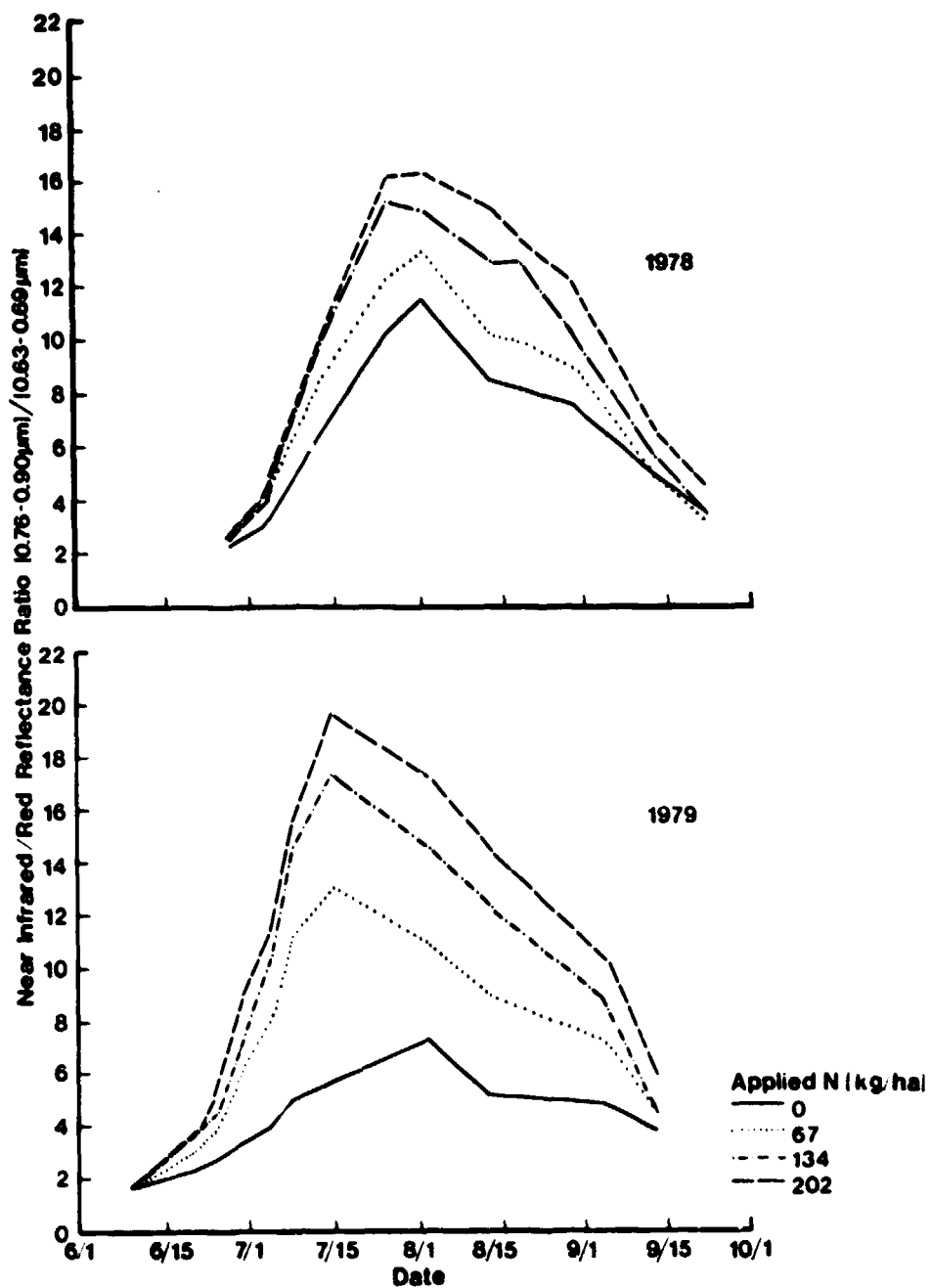
Figure A-4.5. Temporal changes in the near infrared/red reflectance ratio, (0.76-0.90 μm)/(0.63-0.69 μm), for maize canopies under four N treatment levels in 1978 (top) and 1979 (bottom).

Table A-4.1. Spectral responses of corn canopies under four nitrogen treatment levels for selected dates in 1978.

Measurement Date	Applied Nitrogen kg/ha	MIR/red	Greenness	Spectral Variable				
				0.52-0.60µm	0.63-0.69µm	0.76-0.90µm	2.08-2.35µm	
				Bidirectional Reflectance Factor (%)				
July 6	0	3.1a*	15.1a	8.8a	9.7a	32.0ab	22.4a	
	67	4.4a	16.3b	7.1b	7.2b	31.0ab	15.6a	
	134	4.6b	16.4b	6.7b	6.8b	30.6b	16.1b	
	202	4.5b	18.0c	7.3b	7.6b	33.8a	18.1b	
July 13	0	6.4a	17.4a	5.9a	4.8a	30.9a	10.0a	
	67	8.2b	19.6b	5.2b	4.0b	33.0ab	8.7b	
	134	9.6c	21.9c	4.6c	3.7c	36.0b	8.3c	
	202	9.5d	21.2d	4.7d	3.7d	34.7b	9.0d	
July 28	0	10.4a	22.1a	5.1a	3.6a	36.6a	8.1a	
	67	12.5b	23.6ab	4.6b	3.1b	37.9a	7.4ab	
	134	15.3c	24.5ab	3.6c	2.3x	38.6a	6.1c	
	202	16.1c	25.1b	3.6c	2.5c	39.4a	6.3bc	
August 3	0	11.3a	20.6a	4.6a	3.0a	34.2a	5.8a	
	67	13.5ab	21.6a	3.8a	2.8a	34.7a	5.2a	
	134	13.2bc	21.7a	3.3x	2.3a	34.9a	4.9b	
	202	16.4c	23.4a	3.6c	2.3b	37.4a	4.7b	
August 20	0	8.4a	19.9a	5.1a	4.0a	33.4a	8.2a	
	67	10.2b	21.2ab	4.6b	3.4b	34.6ab	7.0b	
	134	12.9c	22.6bc	3.7c	2.8c	35.8b	5.6c	
	202	13.9d	23.3c	3.6c	2.6c	36.7b	5.8c	
August 31	0	7.6a	17.1a	5.0a	3.8a	29.5a	7.2a	
	67	9.1b	18.3ab	4.4b	3.4b	30.5ab	6.6a	
	134	10.4c	19.5bc	3.9bc	3.1bc	32.5bc	6.1b	
	200	12.3d	21.7c	3.3x	2.6c	34.5c	5.9b	
September 13	0	4.9a	16.5a	6.4a	6.2a	30.5ab	10.8a	
	67	4.9a	16.3a	5.9ab	6.1b	29.6b	10.2a	
	134	5.8ab	17.6a	5.2bc	5.3b	30.5ab	9.0a	
	202	6.7b	19.4b	4.5c	4.6b	32.1a	9.3a	

*Means followed by the same letter within each date are not significantly different at P=0.05 level by Duncan's Multiple Range test.

Table A-4.2. Spectral responses of corn canopies under four nitrogen treatment levels for selected dates in 1979.

Measurement Date	Applied Nitrogen kg/ha	NIR/red	Greenness	Spectral Variable				
				0.52-0.60µm	0.63-0.69µm	0.76-0.90µm	2.08-2.35µm	
				Bidirectional Reflectance Factor (%)				
June 26	0	2.5a[†]	12.7a	11.5a	13.0a	32.4a	28.2a
	67	3.6a	16.6b	8.5b	8.8a	33.2b	20.2b
	134	4.5b	18.3c	7.7b	7.8a	34.7b	17.8c
	202	5.0b	19.8c	7.3b	7.7b	35.0b	16.4c
July 10	0	5.6a	15.3a	7.0a	5.0a	29.0a	11.8a
	67	10.9b	22.1b	5.3b	3.4b	37.1b	7.3b
	134	16.2c	25.2c	4.6c	2.9c	41.2c	6.4b
	202	15.2c	25.3c	4.2c	2.7c	41.3c	6.1c
July 18	0	5.6a	18.3a	7.6a	5.2a	33.6a	11.6a
	67	12.9b	22.7b	4.8b	2.8b	37.6b	6.0b
	134	17.6c	25.3c	3.6c	2.3c	40.9c	5.7b
	202	18.6c	27.1c	3.6c	2.2c	43.2c	5.3b
August 6	0	7.6a	18.6a	6.5a	4.5a	33.2a	8.8a
	67	11.1b	22.8b	5.1b	3.2b	37.1b	5.8b
	134	14.8c	25.3c	4.1c	2.6c	41.2c	5.3b
	202	17.4d	26.6c	3.6d	2.3c	43.1c	5.0b
August 16	0	5.3a	19.1a	7.7a	6.4a	35.3a	12.2a
	67	8.8b	20.1b	5.3b	3.9b	38.6b	6.8b
	134	12.7c	24.7c	4.6c	3.2c	39.8b	6.0c
	202	16.6d	25.2c	3.6c	2.6c	40.1b	5.4c
September 6	0	4.9a	15.2a	6.7a	5.9a	28.3a	12.6a
	67	7.2b	16.2a	5.1b	3.8b	28.6a	7.3b
	134	9.1c	20.5b	4.9bc	3.3b	34.1b	7.8b
	202	10.6d	22.4b	4.4c	3.3b	34.3b	6.4b
September 13	0	4.1a	14.7a	7.3a	7.1a	28.7a	13.4a
	67	4.5a	14.4a	6.2b	5.0b	28.5a	9.2b
	134	6.6b	15.1a	6.0bc	6.3b	27.9a	10.0b
	202	5.9b	18.7b	5.3c	5.6b	32.2b	9.0b

[†] Means followed by the same letter within each date are not significantly different at P=0.05 level by Duncan's Multiple Range Test.

Table A-4.3. Mean agronomic characteristics of corn canopies under four nitrogen fertilization levels in 1978.

Measurement Date	Development Stage‡	Applied Nitrogen	Plant Height	Leaf Area Index	Soil Cover	Fresh Biomass	Dry Biomass	Leaf Nitrogen
		kg/ha	m		%	g/m^2	g/m^2	%
July 6	Eight leaf	0	1.0a†	1.2a	30a	1031a	96a	2.7a
		67	1.1b	1.6a	36a	1301a	113a	2.6a
		134	1.2b	1.7a	38a	1430a	118a	3.2a
		202	1.3b	1.7a	37a	1449a	124a	3.3a
July 13	Ten leaf	0	1.2a	2.1a	64a	1827a	167a	2.4a
		67	1.5b	2.3ab	64a	2171ab	192ab	2.5a
		134	1.6c	2.6bc	75a	2783bc	234b	3.0b
		202	1.7d	2.8c	75a	3031c	250b	3.4c
August 3	Tasseling	0	2.8a	3.3a	79a	4260a	644a	1.5a
		67	2.9a	3.2a	80a	4518a	740ab	1.7a
		134	3.1b	3.7ab	79a	4973ab	905bc	2.2b
		202	3.1b	4.1b	83a	6200b	996c	2.6b
August 20	Blister	0	2.9a	2.6a	82a	4167a	701a	1.3a
		67	3.0ab	3.0ab	88a	5072ab	933a	1.6a
		134	3.1b	3.5ab	95bc	6141b	1037a	1.6a
		202	3.1b	3.8b	91bc	6787b	1168a	2.6b
September 13	Early dent	0	3.0a	2.0a	80ab	3985a	1075a	1.2a
		67	3.0a	2.3b	78a	5132ab	1529ab	1.0a
		134	3.2a	2.6c	85b	5401b	1562ab	1.6a
		202	3.2a	3.1d	84ab	6881c	1995b	1.7a

†Means followed by the same letter within each date are not significantly different at P=0.05 level by Duncan's Multiple Range test.
‡Haanway Scale

Table A-4.4. Mean agronomic characteristics of corn canopies under four nitrogen fertilization levels in 1979.

Measurement Date	Development Stage†	Applied Nitrogen	Plant Height	Leaf Area Index	Soil Cover	Fresh Biomass	Dry Biomass	Leaf Nitrogen	Leaf Chlorophyll
		kg/ha	m		%	g/m²	g/m²	%	µg/cm²
June 26	Eight leaf	0	--	1.0a†	45a	689a	83a	3.0a	25.1a
	Eight leaf	67	--	1.7b	61b	1188b	135b	3.0a	34.9b
	Eight leaf	134	--	2.0b	57ab	1669bc	183bc	3.2a	38.5bc
	Eight leaf	202	--	2.3b	66b	1905c	198c	3.2a	42.8c
July 10	Ten leaf	0	1.2a	2.1a	56a	1567a	199a	1.7a	14.2a
	Eleven leaf	67	1.7b	3.6b	76b	3757b	411b	2.4b	26.8b
	Eleven leaf	134	1.9c	3.9b	87c	4788c	476c	2.7b	36.8c
	Twelve leaf	202	2.0c	5.8c	85c	5182c	511c	2.7b	41.1c
July 18	Eleven leaf	0	1.4a	2.3a	71a	2281a	271a	1.2a	11.1a
	Thirteen leaf	67	2.0b	3.9b	85b	5101b	623b	2.1b	21.9b
	Thirteen leaf	134	2.3c	5.1b	88b	6415b	601b	2.3b	40.7c
	Fourteen leaf	202	2.3c	4.8b	84b	6565b	669b	2.4b	47.5c
August 4	Tasseling	0	2.3a	--	83a	4677a	--	1.5a	--
	Blister	67	2.7b	--	89ab	6894ab	--	1.8ab	--
	Blister	134	2.7b	--	93ab	8097bc	--	2.1ab	--
	Blister	202	2.8b	--	94b	10211c	--	2.3b	--
August 16	Silking	0	2.2a	--	85a	2884a	--	1.2a	25.1a
	Late blister	67	2.9b	--	91a	5707b	--	1.4a	34.9a
	Dough	134	3.0bc	--	93a	8134c	--	2.0b	51.0b
	Dough	202	3.2c	--	93a	8360c	--	1.9b	67.9c
September 4	Dough	0	2.1a	1.5a	78a	2581a	678a	1.2a	--
	Early dent	67	2.8b	2.2b	80a	4839b	1261b	1.1a	--
	Early dent	134	3.0bc	3.2c	88b	6504c	1822c	1.3a	--
	Middle dent	202	3.2c	4.2d	96c	8392d	2296d	1.2a	--

†Means followed by the same letter within each date are not significantly different at P=0.05 level by Duncan's Multiple Range test.
†Hanway Scale

The discriminability of treatments also varied by the spectral variable used (Tables A-4.1 and A-4.2). The near infrared/red ratio separated the treatments into the most classes on the largest number of dates of all spectral variables; the near infrared band formed the fewest classes. On August dates the near infrared/red ratio separated all four treatments into discrete groups for two dates in 1978 and three in 1979. In contrast the near infrared band formed a maximum of three groups for one 1978 date and three 1979 dates. Early in the season greenness separated the treatments into more classes than the near infrared/red ratio; the green band (0.52 to 0.60 μm) formed more classes than the near infrared.

For most spectral variables, the 0 kg/ha N canopies were separable from the other three treatments during nearly all of the season for both years. Spectral separation of 67 kg/ha N canopies from 134 and 202 kg/ha N canopies was possible for most dates during both seasons, while the 134 and 202 kg/ha N canopies were separable on only a few dates.

Comparison of spectral treatment separation between years (Tables A-4.1 and A-4.2) shows that despite the larger treatment differences in 1979, the spectral separation was very similar for seven of the 11 or 12 dates considered each year. This result indicates the robustness of the near infrared/red reflectance ratio. Further, the time after planting at which the treatments became separable was also similar between years.

Differences observed between the spectral responses of canopies under different N treatments can be related to agronomic measurement of treatment differences (Tables A-4.3 and A-4.4). Leaf nitrogen concentrations document the effects of varying the level of applied N. The varying leaf chlorophyll concentrations contributed to visible reflectance variations between treatments. Decreased plant height, leaf area index, and biomass values, all associated with reduced levels of applied N, were evident.

Grain yield represents the integration of all the metabolic activities of crop plants over the growing season and is sensitive to N nutrition. Figure A-4.6 shows a linear relationship between the grain yield and near infrared/red reflectance ratios integrated over the season, i.e., the area under the seasonal reflectance curves from Figure A-4.4. A similar relationship for the two years of data was found, although the hybrid and plant population were different each year.

In summary, analyses of agronomic characterizations and spectral measurements of maize canopies varying in applied N fertilizer level showed that agronomic changes in canopies caused by N treatment resulted in detectable reflectance variations. Reduced leaf area, biomass, and soil cover, lowered chlorophyll content, and decreased plant height were among the effects seen in N-deprived canopies. These changes were in turn related to canopy reflectance changes. The near infrared/red reflectance ratio was shown to enhance treatment differences in canopy reflectance and reduce reflectance variability caused by extraneous factors. The spectral separability of the treatments throughout the
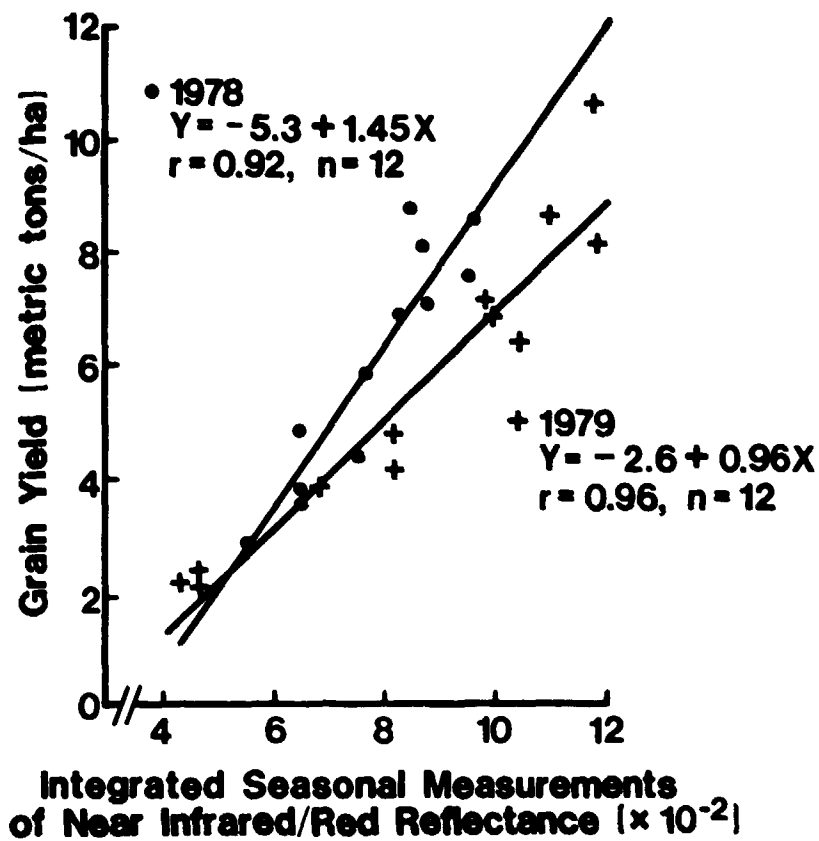
Figure A-4.6. The relationship of grain yield to measurements integrated over the growing season of near infrared/red reflectance.

growing season demonstrates the potential for detecting crop stress by use of multispectral remote sensing methods.

4.4 Acknowledgements

4.5 References

1. Al-Abbas, A.H., R. Barr, J.D. Hall, F.L. Crane, and M.F. Baumgardner. 1974. Spectra of normal and nutrient deficient maize leaves. Agron. J. 66:16-20.

2. Ahlrichs, J.S. and M.E. Bauer. 1978. Relation of crop canopy variables to the multispectral reflectance of spring wheat. Tech. Report 072479, Laboratory for Applications of Remote Sensing, Purdue University, W. Lafayette, IN.

3. Bauer, M.E. 1975. The role of remote sensing in determining the distribution and yield of crops. Adv. Agron. 27:271-304.

4. Blanchard, L.E. and O. Weinstein. 1979. Design challenges of the thematic mapper. Proc. Symp. Machine Proc. Remote Sensing Data, Purdue University, W. Lafayette, IN, pp. 1-16.

5. Bunnik, N.J.J. 1978. The multispectral reflectance of shortwave radiation by agricultural crops in relation with their morphological and optical properties. H.V. Veenman and Zonen B.V., Wageningen. pp. 98-114.

6. Carlson, R.E., D.N. Yarger, and R.H. Shaw. 1971. Factors affecting the spectral properties of leaves with special emphasis on leaf water status. Agron. J. 63:486-489.

7. Colwell, J.E. 1974. Vegetation canopy reflectance. Remote Sensing Environ. 3:175-183.

8. Daughtry, C.S.T., M.E. Bauer, D.W. Crecelius, and M.M. Hixson. 1980. Effects of management practices on reflectance of spring wheat canopies. Agron. J. (In Press).

9. Gates, D.M., H.J. Keegan, J.C. Schleter, and V.R. Weidner. 1965. Spectral properties of plants. Appl. Optics 9:545-552.

10. Gausman, H.W., W.A. Allen, V.I. Myers, and R. Cardenas. 1969. Reflectance and internal structure of cotton leaves, Gossypium hirsutum (L.) Agron. J. 61:374-376.

11. Gausman, H.W., R.R. Rodriguez, and A.J. Richardson. 1976. Infinite reflectance of dead compared with live vegetation. Agron. J. 68:295-296.

12. Genter, C.F. and G.D. Jones. 1970. Planting date and growing season effects and interactions on growth and yield of maize. Agron. J. 62:760-761.

13. Hanway, J.J. 1963. Growth stages of corn. Agron. J. 55:487-492.

14. Kauth, R.J. and G.S. Thomas. 1976. The tasselled cap -a graphic description of spectral-temporal development of agricultural crops as seen by Landsat. Proc. Symp. Machine Proc. Remote Sensing Data. Purdue University, W. Lafayette, IN. pp. 4b-41-51.

15. Knipling, E.B. 1970. Physical and physiological bases for the reflection of visible and near-infrared radiation from vegetation. Remote Sensing Environ. 1:155-159.

16. Leamer, R.W., V.I. Myers and L.F. Silva. 1973. A spectroradiometer for field use. Rev. Sci. Instrum. 44:611-614.

17. Longstreth, D.J. and P.S. Nobel. 1980. Nutrient influences on Leaf Photosynthesis. Pl. Physiol. 65: 541-543.

18. MacDonald, R.B. and F.G. Hall. 1980. Global crop forecasting. Science 208:670-679.

19. Nicodemus, F.E., J.C. Richmond, J.J. Hsia, I.W. Ginsberg, and T. Limperis. 1977. Geometrical considerations and nomenclature for reflectance. NBS Monograph 160, U.S. Govt. Printing Office, Washington, D.C., pp.3-9.

20. Rice, D.P., E.P. Crist, and W. A. Malila. 1980. Applicability of selected wheat remote sensing technology to corn and soybeans. ERIM Final Report 124000-9-F, Environmental Research Institute of Michigan, Ann Arbor, MI, pp. 3-7.

21. Robinson, B.F. and L.L. Biehl. 1979. Calibration procedures for measurement of reflectance factor in remote sensing field research. Proc. Soc. Photo-optical Instrumentation Engr. 196-04:16-26.

22. Stanhill, G., V. Kalkofi, M. Fuchs, and Y. Kagan. 1972. The effects of fertilizer applications on solar reflectance from a wheat crop. Israel J. Agr. Res. 22:109-118.

22. Thomas, J.R. and G.F. Oerther. 1972. Estimating nitrogen content of sweet pepper leaves by reflectance measurements. Agron. J. 64:11-13.

24. Tucker, C.J. 1979. Red and photographic infrared linear combinations for monitoring vegetation. Remote Sensing Environ. 8:127-150.

25. Tucker, C.J., J.H. Elgin, and J.E. McMurtrey. 1979. Temporal spectral measurements of corn and soybean crops. Photogram. Engr. and Remote Sensing 45:643-653.

26. Tucker, C.J. and E.L. Maxwell. 1976. Sensor design for monitoring vegetation canopies. Photogram. Eng. and Remote Sensing 42:1399-1410.

5. Canopy Reflectance as Influenced by Solar Illumination Angle

J. C. Kollenkark, V. C. Vanderbilt, C. S. T. Daughtry, and M. E. Bauer

5.1 Introduction

Understanding the effect of the interactions between solar illumination and crop canopy geometry on the spectral response is necessary to effectively utilize reflectance factor data. Numerous models have been proposed to explain and predict the measured reflectance factor of plant canopies as a function of plant geometry, sun angle, and view angle (Suits, 1972; Smith et al., 1975; Richardson et al., 1975). The models by Suits and Smith deal with a canopy with no horizontal spatial variations.

Richardson et al. (1975) modeled the reflectance of a row crop, with distinct horizontal spatial variations, as a function of plant, soil, and shadow components. By illuminating a surface covered with various shaped objects, Egbert (1977) was able to explain 80 to 85 percent of the variance in the reflectance measurements due to shadows. A model suggested by Jackson et al. (1979) assumes an incomplete canopy of rectangular-shaped rows. The fractions of sunlit and shaded soil and vegetation viewed are calculated as a function of view angle for a particular canopy condition, described by plant cover, height/width ratio, row spacing and direction, time of day, day of year, latitude, and size of the radiometer resolution element.

Studies of sun zenith angle effects on reflectance generally have supported the predictions of the Suit's canopy reflectance model that the reflectance factor should increase as the solar elevation increases (Colwell, 1974; Chance and LeMaster, 1977). Colwell (1974) attributes this to changes in the amount of shadow within the canopy. Field data have shown minor to significant increases in the infrared response with decreasing sun elevations (Duggin, 1977; Chance and LeMasters, 1977; Jackson et al., 1979). Crecelius (1978) noted symmetric and non-symmetric components about solar noon that influenced the observed variation in reflectance throughout the day. The symmetric component, solar angle, explained the majority of the observed variation. Other effects, such as drying of the soil surface and plant wilting will be asymmetric about solar noon and may be significant factors to consider.

Further investigation of reflectance factor data taken in 1978 over incomplete soybean canopies revealed possible time of day effects in the Landsat band regions as illustrated in the red, 0.6-0.7 μm, and the near infrared, 0.8-1.1 μm, in Figure A-5.1. Plots were planted in a north-south row direction.
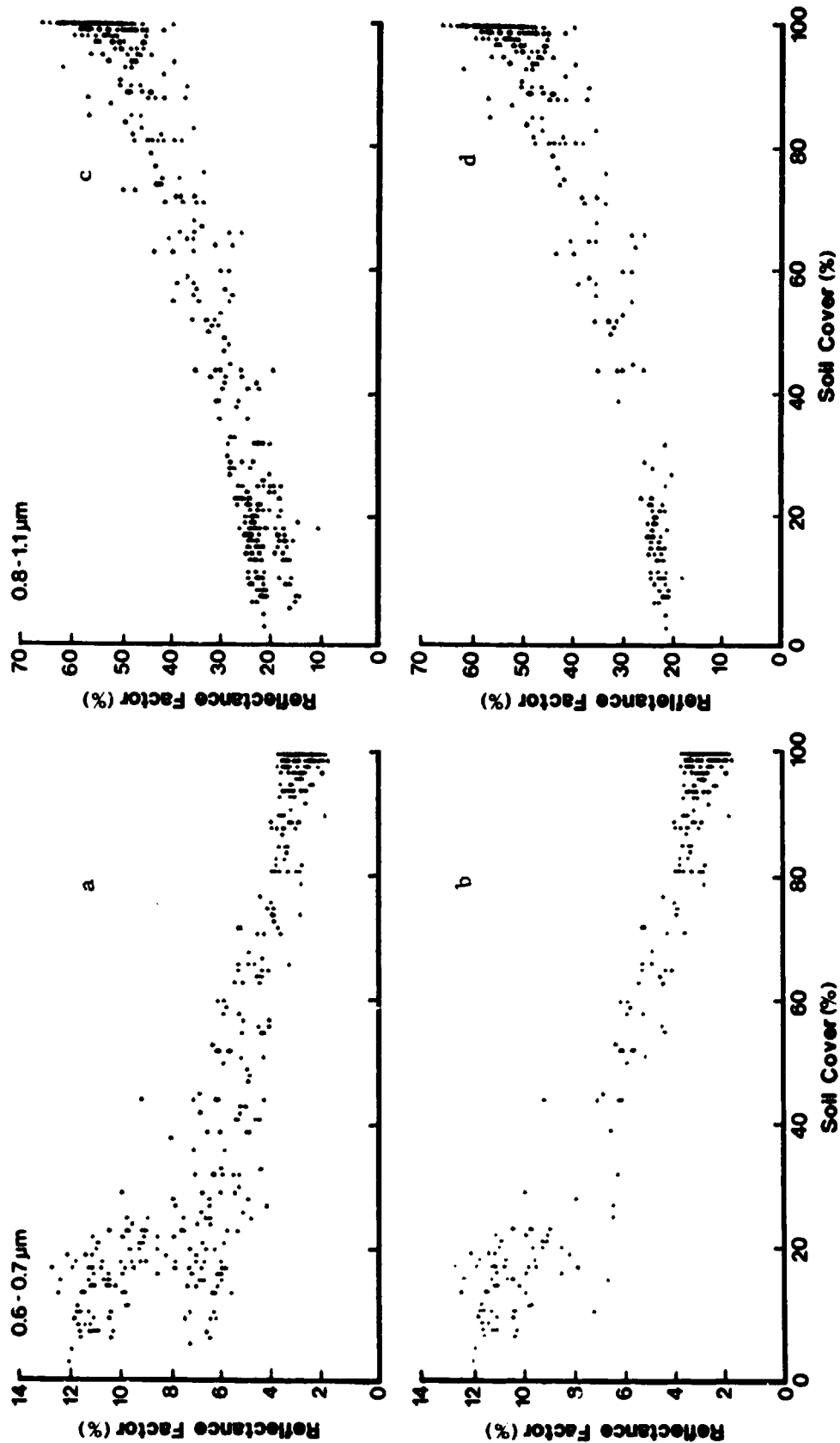
Figure A-5.1. Time of day effect on the RF seen in the 1978 data for the red (0.6-0.7 μm) and the near infrared (0.8-1.1 μm) wavelength regions. (a,c) All 1978 data minus dates which include wet soil and/or senescing vegetation. (b,d) Same as a and c above, but only includes data in the three hour time period centered about solar noon.

Both bands were plotted with and without a 1.5 hour time restriction about solar noon. Low responses were noted over those plots that were measured more than 1.5 hours from solar noon. This resulted in shadows between the rows and a lower response from the soil component.

The objective of this research was to model the effects of rows and row direction on the reflectance of a soybean canopy as a function of solar azimuth and zenith angles. By varying only the row direction, the variation in reflectance could be explained entirely by changes in sun zenith and azimuth angle with respect to row direction.

5.2 Materials and Methods

Experimental Conditions. An experiment to evaluate the effects due to sun angle-row azimuth changes was conducted in 1979 on the Purdue Agronomy Farm. Soybeans (Glycine max (L.) Merr. "Amsoy 71") were planted into a Chalmers silty clay loam (typic Argiaquoll) soil on June 25, 1979. Soybeans were used as an initial crop to study as they have dense foliage with distinct row patterns through much of the season. This is in contrast to many of the other major crops such as wheat and corn that have a much more complex canopy geometry and shadow pattern. Extended periods of cloudy days early in the season limited spectral data acquisition to development stages after full bloom.

The experiment consisted of 11 randomly arranged plots which were 3.5 m wide and 5.2 m long (Figure A-5.2). Nine plots were planted in 71 cm wide rows with the following azimuthal directions: 30-210, 60-240, 90-270, 105-285, 120-300, 135-315, 150-330, 165-345, and 180-360 degrees from north. Another plot was planted in east-west and north-south rows 25 cm wide to obtain a canopy with negligible row effects. A bare soil plot also was included to monitor the sunlit soil background reflectance of the soybean plots. Row directions were selected to favor data collection during the morning hours when cloud-free conditions were more likely.

Three development stages with 65, 78, and 94 percent soil cover on the 71 cm wide rows were represented with the three measurement dates. The canopy with 78 percent soil cover was obtained by trimming a near full canopy just prior to the start of senescence. The cross sectional shape of the canopy was determined by placing a large piece of poster board into the canopy, perpendicular to the row azimuth, at several locations and drawing the perimeter of the canopy onto the board. The canopy shapes for each date are illustrated in Figure A-5.3.

Spectral Measurements. Radiance measurements, used to determine reflectance factor (RF), were taken over all the plots with a Landsat band radiometer (Exotech Model 100) at 15 minute intervals throughout the day on three clear days (August 12, August 31, and September 19). The Exotech 100 is a four band radiometer with a 15 degree field of view that acquires data in the following wavelength regions: 0.5-0.6, 0.6-0.7, 0.7-0.8, and 0.8-1.1 μm. Data were taken only under near cloud-free conditions (especially in the vicinity of the sun).
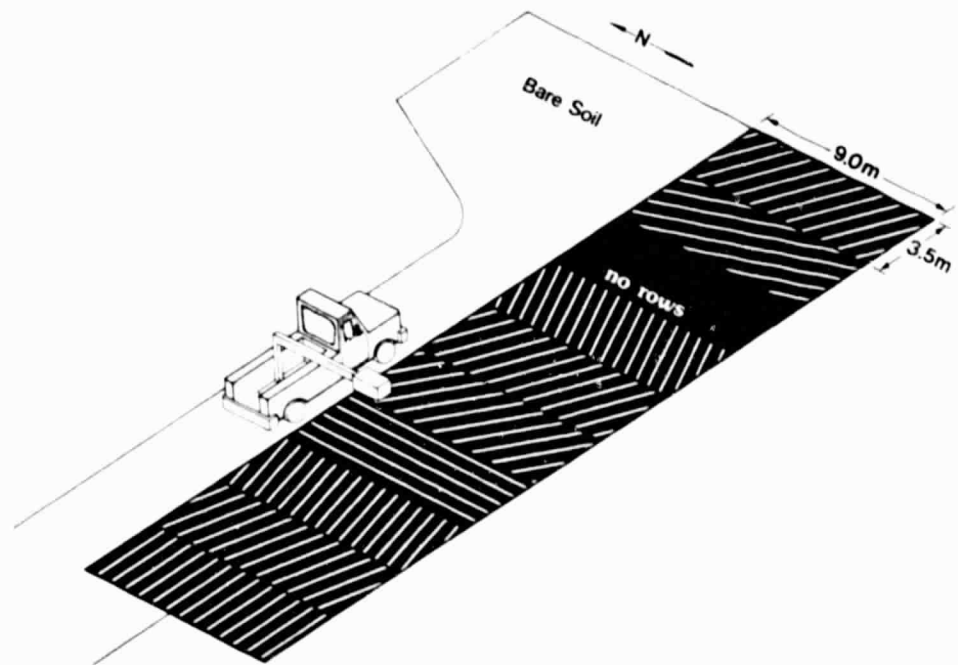
Figure A-5.2. Illustration of field spectral data acquisition over the row direction plots in 1979.
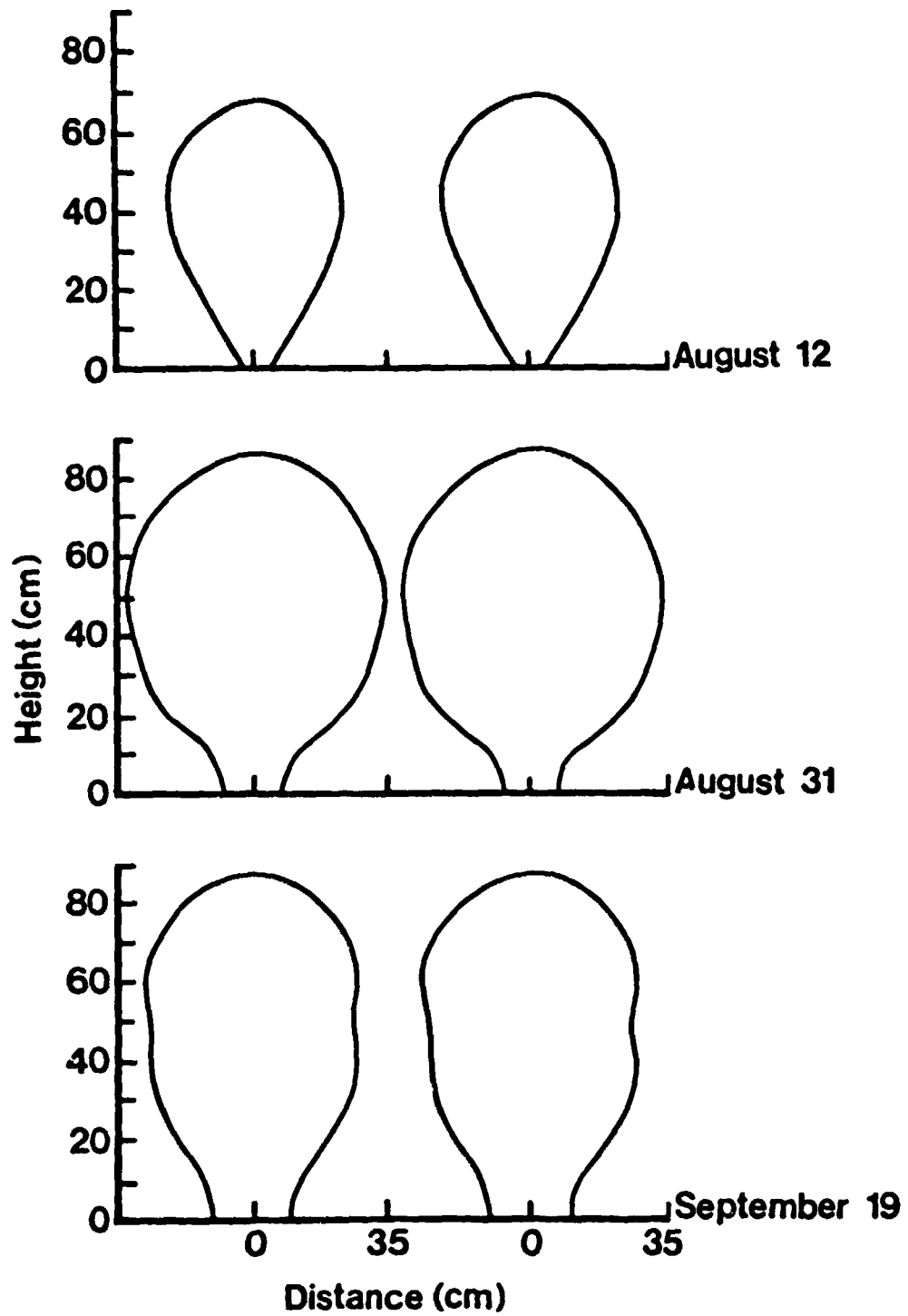
Figure A-5.3. Soybean canopy shapes and dimensions for three dates of data collection.

A mobile truck-mounted radiometer system was used for quick and efficient data collection in the field. A boom mounted on the back of the truck elevated the radiometer and a motor-driven camera 5.2 m above the crop canopy and 3.5 m from the truck. Spectral data were acquired over two locations in each plot on August 12 and over four locations in each plot on August 31 and September 19. The instruments were carefully leveled to obtain all spectral data at a nadir look angle. Several measurements were taken over each plot to insure a representative sampling of the plot and to avoid biased values for on-row or off-row measurements. Measurements in all bands were taken concurrently and recorded by a printing data logger. During data collection, photographs were taken periodically over each plot for soil cover determination and shadow assessment.

Agronomic Measurements collected within two days of the RF data, included plant height, leaf area index, maturity stage (Fehr and Caviness, 1977), surface soil moisture, total fresh and dry biomass, and stem, pod, and green leaf dry biomass. Percent soil cover was determined by placing a grid over the vertical photograph and counting the intersections occupied by green vegetation.

Data Analysis. The reflectance factor data were analyzed as band means. The reflectance data were transformed into greenness as described by Kauth and Thomas (1976) for Landsat MSS data and modified for spectrometer data (Malila and Gleason, 1977). The data transformation was: Greenness = ((Band3 * 0.17289) + (Band4 * 0.59538)) - ((Band1 * 0.48935) + (Band2 * 0.61249)). Band1 to Band4 refer to the four Landsat bands measured. The near infrared/red reflectance ratio ((0.8-1.1 μm)/(0.6-0.7 μm)) was also considered in the analysis. Analysis of variance and Newman-Keuls tests were performed to determine significant effects of row-solar angle interaction and RF.

5.3 Results and Discussion

Examination of the data indicated that definite sun angle effects were present (Figure A-5.4a). The maximum response levels occurred when the sun azimuth angle was equal to the row azimuth angle. Diurnal changes in RF of nearly 140 percent were observed in the red wavelength region, 0.6-0.7 μm, on August 12. The highest reflectance values were obtained when the soil was sunlit and the lowest, when the soil was shaded. Diurnal variations in the RF in the near infrared wavelength region, 0.8-1.1 μm, were minor and apparently unrelated to sun-row interactions (Figure A-5.4b). The shadows of the near infrared region may not be as dark as those observed in the visible region due to low pigment absorption and multiple scattering in the canopy (Colwell, 1974).

Figure A-5.5 further illustrates the effect of sun-row azimuth interactions. The reflectance was plotted over time for three plots of different row directions. The peak response in the red wavelength region for the three plots was not only at different times, but also in
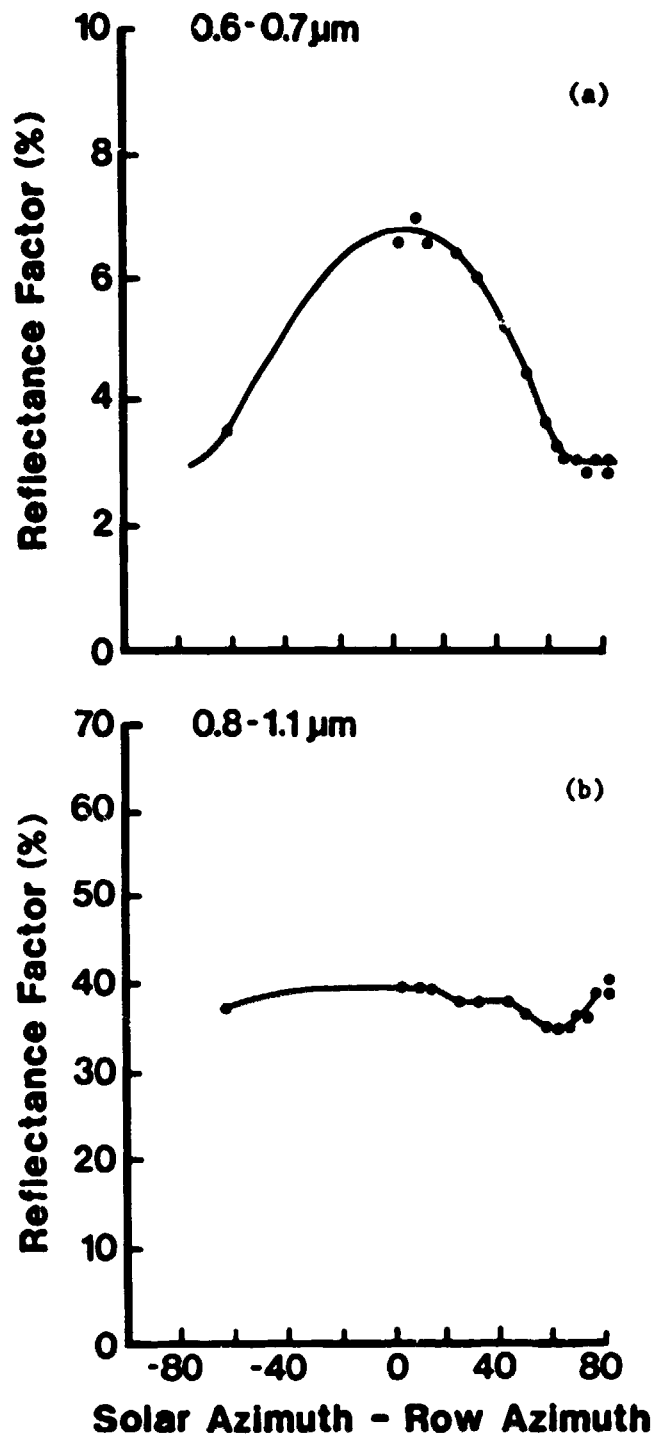
Figure A-5.4. Changes in the RF in (a) the red wavelength band (0.6-0.7 μm) and (b) the near infrared wavelength band (0.8-1.1 μm) plotted against the difference between solar and row azimuth on August 12. Row azimuth = 180°.
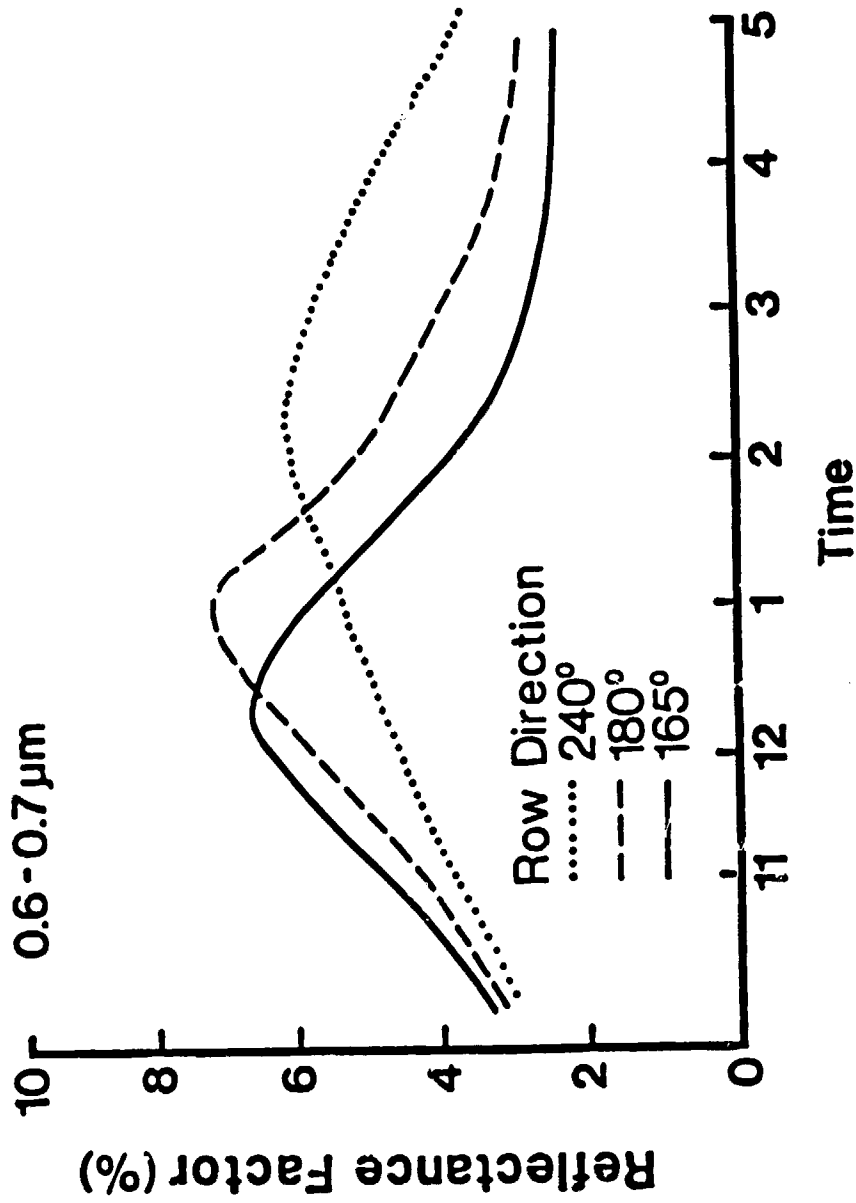
Figure A-5.5. RF in the red wavelength region (0.6-0.7 μm) for three row directions over time on August 12, 1979.

Date	Time	Solar Angle Zenith	Azimuth	θ_{sp}
Aug. 15	12:00	26.3	180.0	26.3
Aug. 21	2:09	40.1	234.2	26.3
Sept. 10	4:49	73.7	261.7	26.3
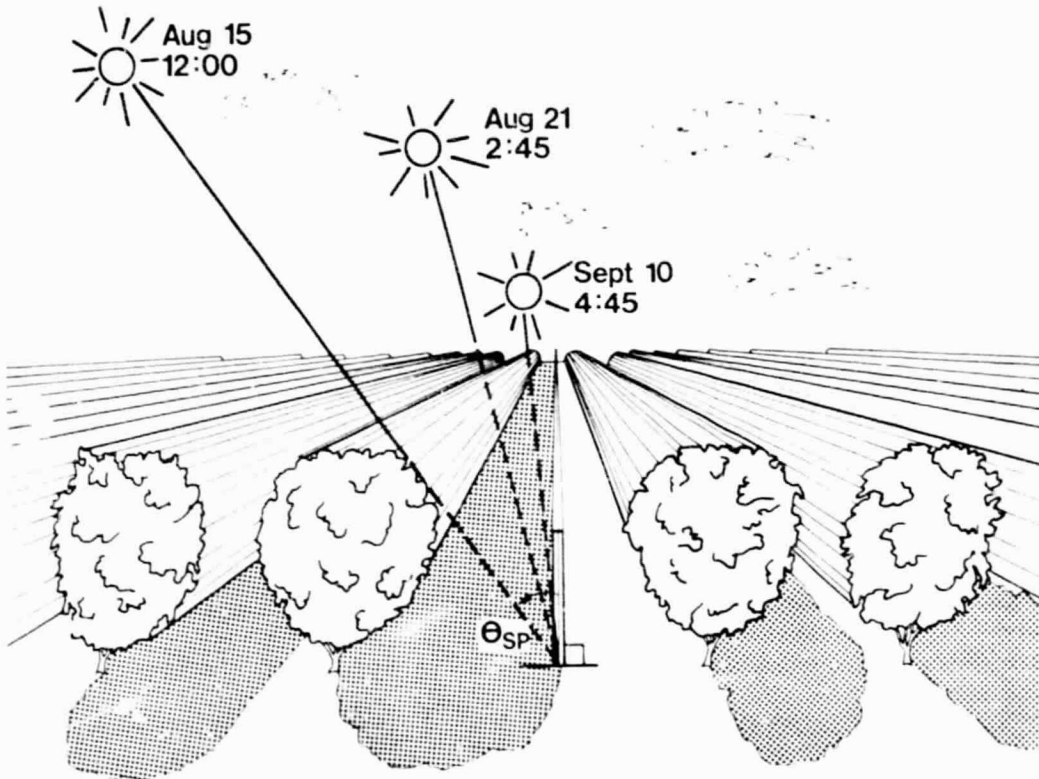
Figure A-5.6. Illustration of the solar projected angle θ_{sp} as observed when looking to the west. Three dates and the corresponding observation times result in the same shadow pattern and $\theta_{sp} \approx 26°$.

order of the row azimuth. Again the peak response was when the sun was shining down the rows, lighting the soil surface, and thus giving a higher reflectance reading.

Equations to predict the shadow cast by rectangular or spherical rows as the sun zenith and azimuth change throughout the day have been defined by many (Idso and Baker, 1972; Jackson et al., 1979; Verhoff and Bunnik, 1978). For this study, an equation was used to express the solar zenith (θ) and azimuth angle (ϕ) in relation to a projected ray onto a plane perpendicular to the row azimuth. This function, called the projected solar angle, $\theta_{sp} = \tan^{-1}(\tan\theta\sin\phi)$, is illustrated in Figure A-5.6.

The response in the red (0.6-0.7 μm) wavelength band has been plotted as a function of θ_{sp} for the three diurnal studies in 1979 (Figure A-5.7). The canopies with lower soil covers, 64 and 78 percent, showed greater changes in reflectance due to changing sun angle than the near full canopy of 94 percent soil cover. The RF of the canopies with 94 percent soil cover, changed only slightly more during the day than the RF of the full canopy. The first two dates appeared to have two functions present; the first being highly dependent on θ_{sp}, the second independent of θ_{sp}.

The dependent zone, where the RF is changing rapidly with changes in θ_{sp}, is a function of the sunlit soil reflectance and the vegetation reflectance (Figure A-5.7). The variation about the mean might be due to local variations in soil cover or even possibly instrument position about the row at low sensor altitudes. Some of this variation was thought to be due to the interaction of sun zenith angle with the surface roughness of the canopy with large zenith angles causing longer shadows and thus lower reflectance. However, no evidence of this was apparent from the analysis of the data.

In the independent region (Figure A-5.7), where the soil surface was completely shadow covered, the measured reflectance was explainable by one variable, the percent soil cover. Just as for the dependent zone, local variations in soil cover might cause the amount of variation seen about the mean. The critical angle, beyond which a change in the projected angle no longer results in a change in RF, shifts to lower θ_{sp}'s for higher soil covers or canopy heights.

5.4 Summary and Conclusions

The primary objective of this research was to explain diurnal changes in reflectance factor of a row crop canopy. This is critically important when the measured reflectance factor in the red region of a given plot may vary 100 percent or more during the day. The canopy geometry was a key factor in determining both the diurnal range of the spectral response and the critical angle. The effect of solar zenith angles between 20 and 60 degrees on the measured reflectance was found to be nonsignificant in the RF measured at nadir over all the plots including the bare soil and full canopy plots. The near infrared RF and greenness function were not sensitive to changes in solar illumination angle in the row crop canopy observed. These transformations may thus
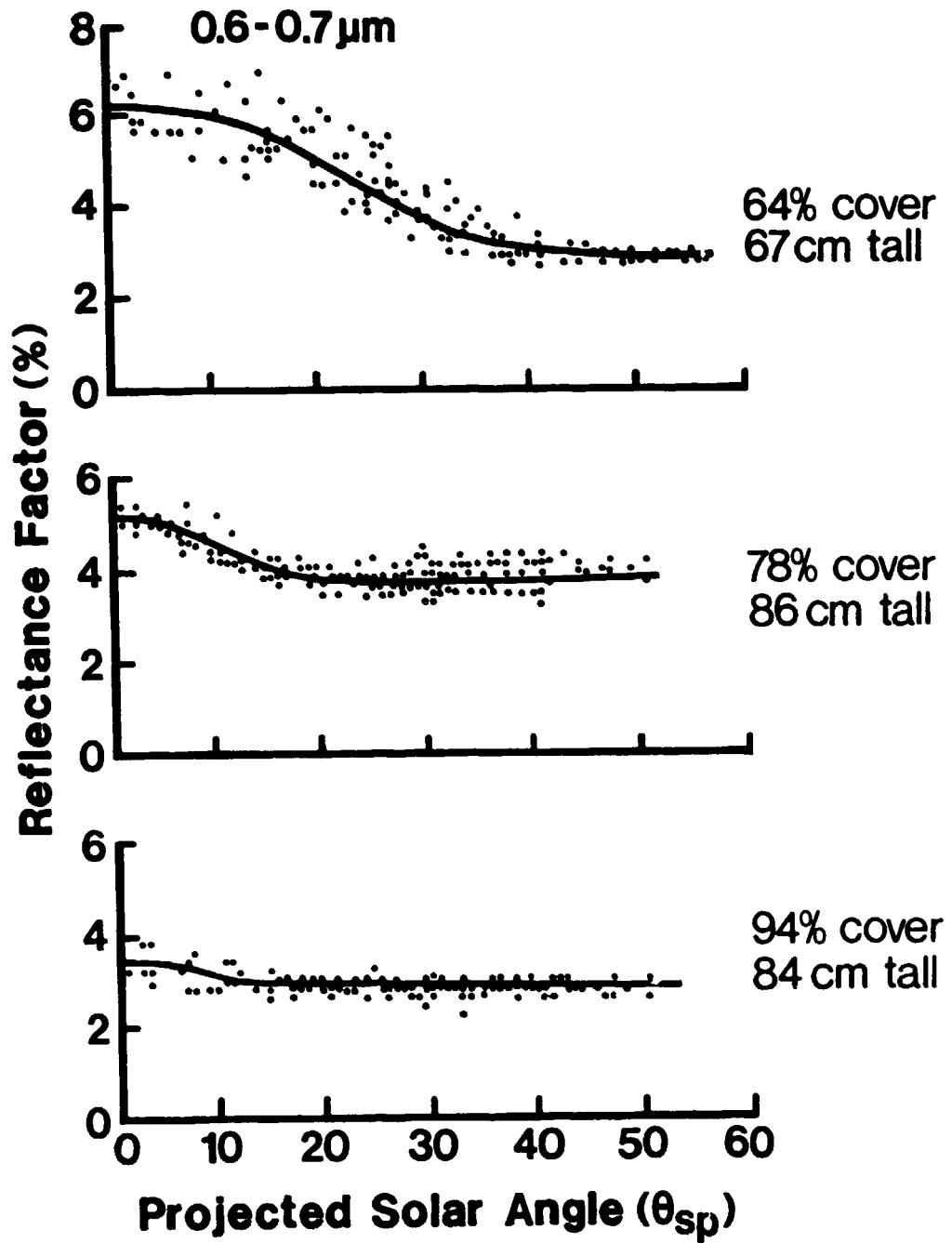
Figure A-5.7. Relationship between RF in the red wavelength band (0.6-0.7 μm) and projected solar angle θsp for three different canopies.

prove to be more useful in relating the response to such agronomic variables as percent soil cover, leaf area index, and plant biomass over a wide range of illumination angles.

Future studies should include a wider range of solar zenith and azimuth angles and more row azimuth angles. This objective, along with a decrease in plot to plot variability, could be obtained by placing the plot to be studied on a turntable. This would allow for a quick change in the row direction with a minimum of plot to plot variation. To more effectively study effects due to the solar zenith angle on soybean row crops, measurements should be taken at low latitudes where the range in zenith angles will be the greatest.

The results indicate that changes in canopy shadowing may be a significant factor, particularly in the visible wavelength regions, influencing the spectral reflectance of crop canopies. A physical model accounting for this variation was developed. It will be used in future investigations to simulate the variation which may be expected with varying row directions and amounts of canopy cover as a function of date, time of day, and latitude.

5.5 References

1. Chance, J.E. and E.W. LeMaster. 1977. Suit's reflectance models for wheat and cotton: theoretical and experimental test. Applied Optics 16: 407-412.

2. Crecelius, D.W. 1978. The time of day effect on the reflectance of spring wheat canopies in the four Landsat MSS bands. M.S. Thesis, Purdue University, W. Lafayette, IN.

3. Colwell, J.E. 1974. Vegetation canopy reflectance. Remote Sensing of Environment 3: 175-183.

4. Duggin, M.J. 1977. Likely effects of solar elevation on the quantification of changes in vegetation with maturity using sequential Landsat imagery. Applied Optics 16: 521-523.

5. Egbert, D.D. 1977. A practical method for correcting bidirectional reflectance variations. Proc. Symp. on Machine Processing of Remotely Sensed Data, Purdue University, West Lafayette, IN. pp. 178-185.

6. Idso, S.B., R.D. Jackson, and R.J. Reginato. 1977. Remote sensing of crop yields. Science 196: 19-25.

7. Jackson, R.D., R.J. Reginato, P.J. Pinter, Jr., and S.B. Idso. 1979. Plant canopy information extraction from composite scene reflectance of row crops. Applied Optics 18: 3775-3782.

8. Kauth, R.J. and G.S. Thomas. 1976. The tasselled cap - a graphic description of the spectral-temporal development of agricultural crops as seen by Landsat. Proc. Symp. on Machine Processing of Remotely Sensed Data, Purdue University, W. Lafayette, In.

9. Malila, W.A. and J.M. Gleason. 1977. Investigations of spectral separability of small grains, early season wheat detection, and multicrop inventory planning. ERIM Report 122700-34-F. Environmental Research Institute of Michigan, Ann Arbor, MI.

10. Richardson, A.J., C.L. Wiegand, H.W. Gausman, J.A. Cullar, and A.H. Gerbermann. 1975. Plant, Soil, and shadow reflectance components of row crops. Photogrammetric Engineering and Remote Sensing 41: 1401-1407.

11. Smith, J.A., J.K. Berry, and F. Heimes. 1975. Signature extension for sun angle. Vol. I. Final Report, Contract NAS9-14467. Colorado State Univ. Ft. Collins, CO.

12. Suits, G.H. 1972. The calculation of the directional reflectance of a vegetative canopy. Remote Sensing of Environment 2: 117-125.

13. Verhoef, W. and N.J.J. Bunnik. 1976. The spectral directional reflectance of row crops. Part 1: Consequences of non-lambertian behaviour for automatic classification. Part 2: Measurements on wheat and simulations by means of a reflectance model for row crops. Report No. NIWARSPUBL-35. Netherlands Interdepartmental Working Group on the Application of Remote Sensing, Delft. 144 p.

6. Simulated Response of a Multispectral Scanner Over Wheat as a Function of Wavelength and View and Illumination Directions

V.C. Vanderbilt, B.F. Robinson, L.L. Biehl, M.E. Bauer, A.S. Vanderbilt

6.1 Introduction

Oblique viewing sensors have been proposed or scheduled for launch on at least two future earth resource satellite systems, the Systeme Probatorie d'Observation de la Terre (SPOT) (1) being developed by France, Sweden, and Belgium and the Multispectral Resource Sampler (MRS) (2) being considered by the United States. As these sensors are soon to be launched, the potential information in oblique measurements needs to be anticipated and better understood.

The spectral flux sensed by these systems will be due to the absorption and bidirectional scattering of solar radiation by both the atmosphere and ground scene. Characterization and correction of the effect of the atmosphere upon remotely sensed data have been considered elsewhere (3). This paper analyzes the spectral bidirectional scattering properties of wheat with view direction, excluding atmospheric effects.

Measurements of an information class such as wheat or corn made by multispectral scanners mounted in aircraft often show large variation with scan angle. For example, during the Corn Blight Watch Experiment, the size of the variation was sufficient to require preprocessing to remove the effect (10). The response of the aircraft sensors, which typically operate over angular variations of 40 and -40 degrees about nadir, include variations due not only to bidirectional scattering by the ground scene but also due to the atmosphere. Consequently, data from the sensors cannot be interpreted as completely indicative of the ground scene. Measurements of the bidirectional scattering properties at large view angles for various plant canopies have been reported (9, 11). None of these studies involved measurements made continuously in wavelength from 0.4 to 2.4 μm and at a variety of view angles and crop growth stages. Nor have these studies extensively investigated the reflective properties of wheat, a crop of global economic importance grown worldwide.

6.2 Materials and Methods

Data were acquired on spring wheat (<u>Triticum aestivum L.</u>) on four dates during 1975 and 1976 at Williston, North Dakota, USA (Lat. 48°8', Long. 103°44') in support of the Large Area Crop Inventory Experiment

Table A-6.1. Ancillary meteorologic and agronomic data.

Variable	Date 21 Jun 76	20 Jul 75	17 Jul 76	31 Jul 76
relative humidity (%)	51	54	36	57
air temperature (C°)	19	27	28	23
barometric pressure (mm Hg)	770.9	759.4	771.4	777.2
cloud cover (%)	1		1	5
wind direction	northeast	southwest	southeast	southeast
wind speed (km/hr)	14	16	10	13
cultivar	Waldron	Wells	Ellar	Ellar
maturity stage*	3.5/boot	4.5/fully headed	5.1/milk	5.4/ripe
row direction	east-west	east-west	north-south	north-south
row width (m)	0.18	0.21	0.18	0.18
fruit count (per m²)	0.0		444.4	394.4
plant count (per m²)	477.8	310.0	455.6	405.6
plant height (m)	0.48	0.72	0.85	0.86
leaves per plant	5.0		4.0	4.0
leaf condition (%)				
green	93		27	0
yellow	3		7	0
brown	4		66	100
dry biomass-total (gr/m²)	216.9	345.1	689.8	625.9
fruit	0.0		268.1	330.2
green leaves	84.7		51	0.0
yellow leaves				
brown leaves			25.4	56.8
stems	132.3		345.3	238.9
fresh biomass-total (gr/m²)	1131.1		1466.1	840.0
plant moisture (%)	81		53	25
leaf area index**	1.85	1.48	0.81	0.0

*maturity stage according to Large[18]
**leaf area index is the green one-sided leaf area per unit ground area
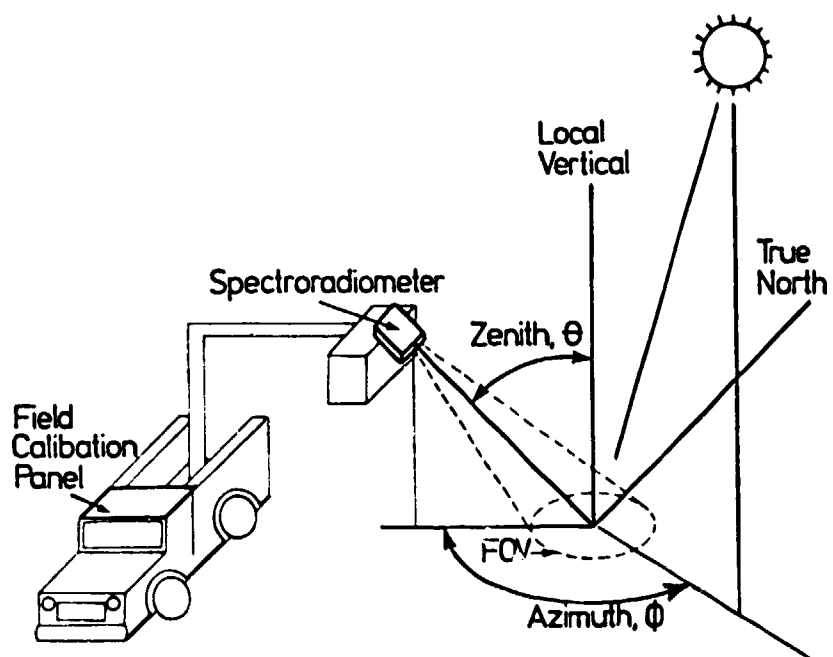
Figure A-6.1. Coordinate system used for data analysis.

(12). On each date agronomic measurements were made to characterize the condition of the wheat canopy (Table A-6.1). Meteorologic data (Table A-6.1) were acquired at the North Dakota Agricultural Experiment Station at Williston, located near the test sites.

All spectral data were acquired continuously in wavelengths 0.46 to 2.4 μm, using an Exotech model 20C spectroradiometer positioned 6 m above the soil. On each of the four dates, spectral data and a photograph of the instrument field of view were taken in each of 33 view directions, eight azimuths (the eight points of the compass) at four zenith angles (15°, 30°, 45° and 60°) plus nadir. Data were acquired approximately from three hours before solar noon to four hours after solar noon. The spectral data, acquired as radiances, were subsequently calibrated to bidirectional reflectance factors (BRF) using spectral radiance measurements taken periodically of a 1.1 m x 1.1 m barium sulfate ($BaSO_4$) painted field standard (14, 15). The reflectance of the field standard was measured with reference to pressed $BaSO_4$, a laboratory standard with known reflectance properties.

Analysis of the bidirectional response of the canopy was performed on data at 48 wavelengths selected at 0.02 μm intervals from 0.44 to 1.0 um, at 0.04 μm intervals from 1.0 to 2.0 μm, and at 0.08 μm intervals from 2.0 to 2.24 μm. A spectra was discarded for analysis purposes if the associated photograph indicated the field of view of the instrument might include the shadow cast by the spectroradiomater, boom, or truck or in some way did not properly represent the scene. At each of the 48 wavelengths, a stepwise forward regression program was used to select from a global set of possible terms the twenty which best explained the variation in the BRF data with time and view angle (Figure A-6.1). The global set included the terms of the spherical harmonic series (17) through Y_{44}, powers of time through t^6, and all the interaction terms. The coefficient of variation (R^2) of each regression varied systematically by date and wavelength, ranging between 0.86 and 0.98 in the visible spectral region, 0.93 and 0.98 in the near-infrared and 0.76 and 0.96 in the middle-infrared. The standard deviation of the quantity (100% residual/measured) varied between 3.5% and 10.7% in the visible spectral region, 2.5% and 5.2% in the near-infrared, and 3.3% and 16.4% in the middle-infrared.

6.3 Results

Figure A-6.2 shows the normalized BRF plotted as a function of wavelength for the wheat canopy measured 21 June 1976 three hours before noon looking 90 degrees to the sun azimuth. The BRF is normalized to the BRF at nadir at each wavelength. The scale on the wavelength axis changes at both 1.0 and 2.0 μm. Figure A-6.2 shows that the BRF is a pronounced function of view zenith direction and wavelength. In the green spectral region (0.56 μm) the BRF decreases for view zenith directions between 0 and about 20 degrees then increases for angles greater than 30 degrees. In the red region (0.66 μm) the BRF decreases until a view zenith direction of 40 degrees, then is constant. In the near-infrared (0.76-1.28 μm) the BRF increases with increasing view
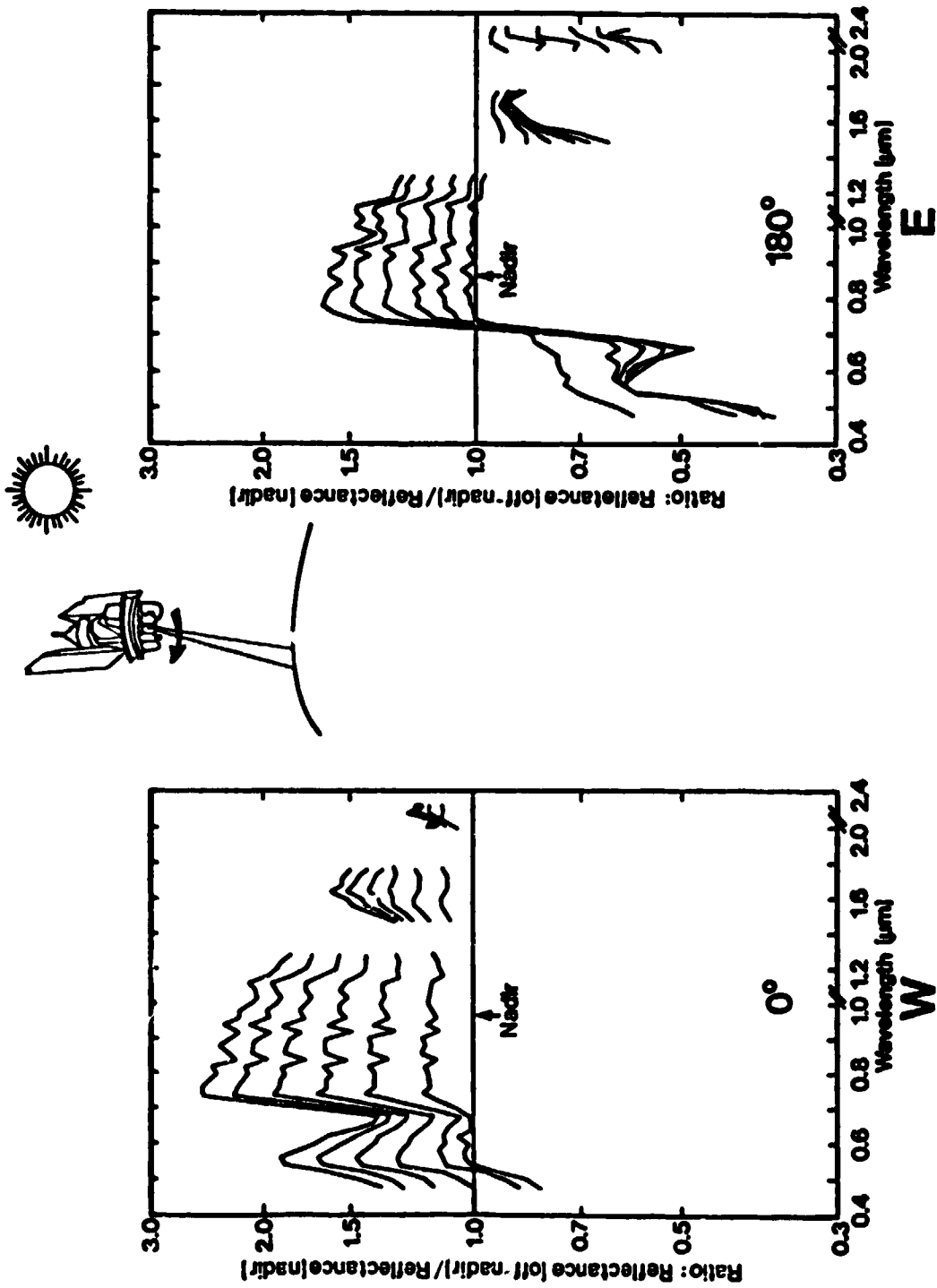
Figure A-6.2. Normalized reflectance factor of spring wheat three hours before solar noon on 21 June 1976 with view azimuths of 0° (west) and 180° (east). Solar azimuth was 43° zenith, 109° azimuth.
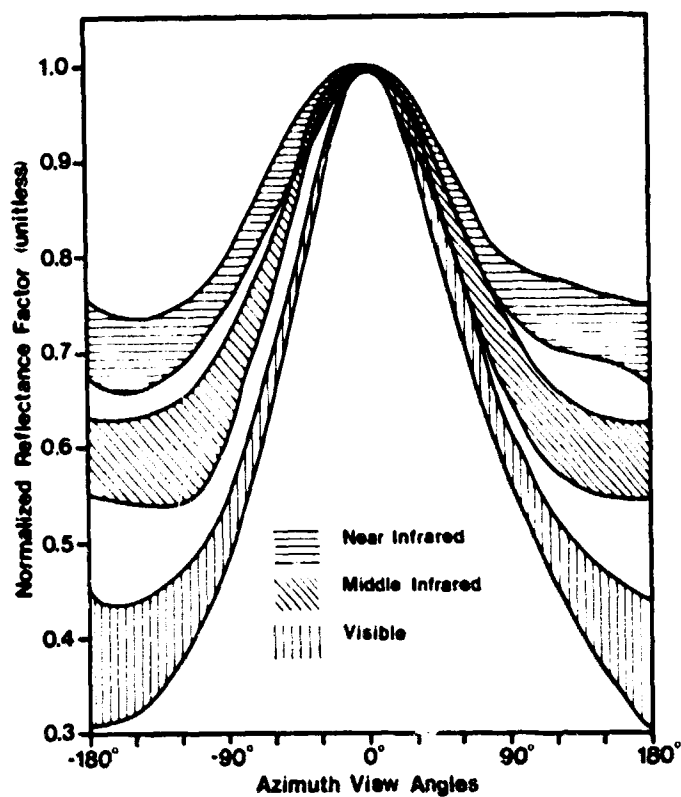
Figure A-6.3. Normalized reflectance factor of spring wheat three hours
before solar noon on 17 July 1976 illustrating differential response of
wavelength regions as a function of view azimuth angle. View azimuth is
measured from "hot spot."
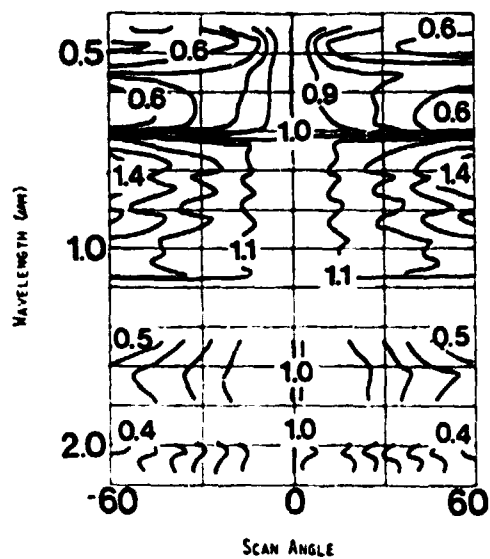
Figure A-6.4. Simulated, normalized reflectance factor for a multispectral line scanner plotted in topographic notation with contour lines at 0.1 intervals. In this example from noon on 17 July 1976 the aircraft is flying toward the sun. This same coordinate system is used in each of the 24 plots in Figures A-6.5 and A-6.6.
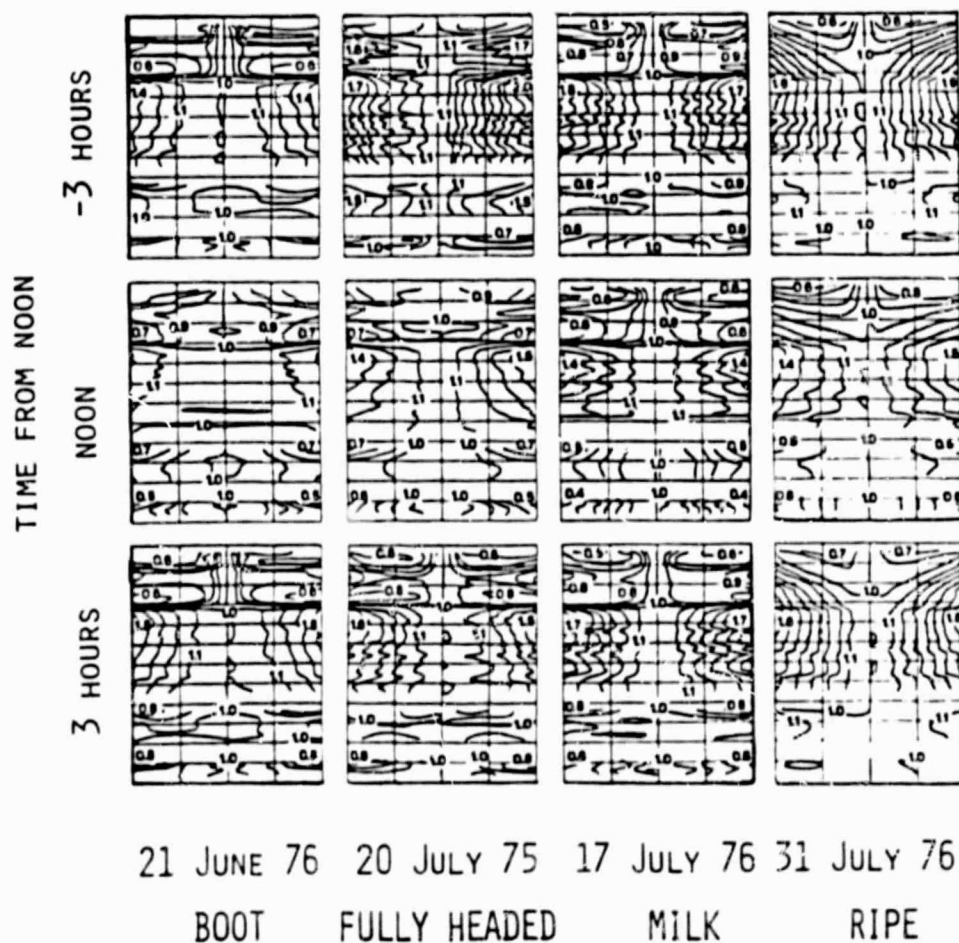
Figure A-6.5. Reflectance factor response of a multispectral line scanner (MSS) normalized to nadir and ±60° about nadir. In the case of the MSS flying toward the solar azimuth (illustrated here) the response is generally symmetrical about the nadir scan angle for all wavelengths, all times, and all growth stages.
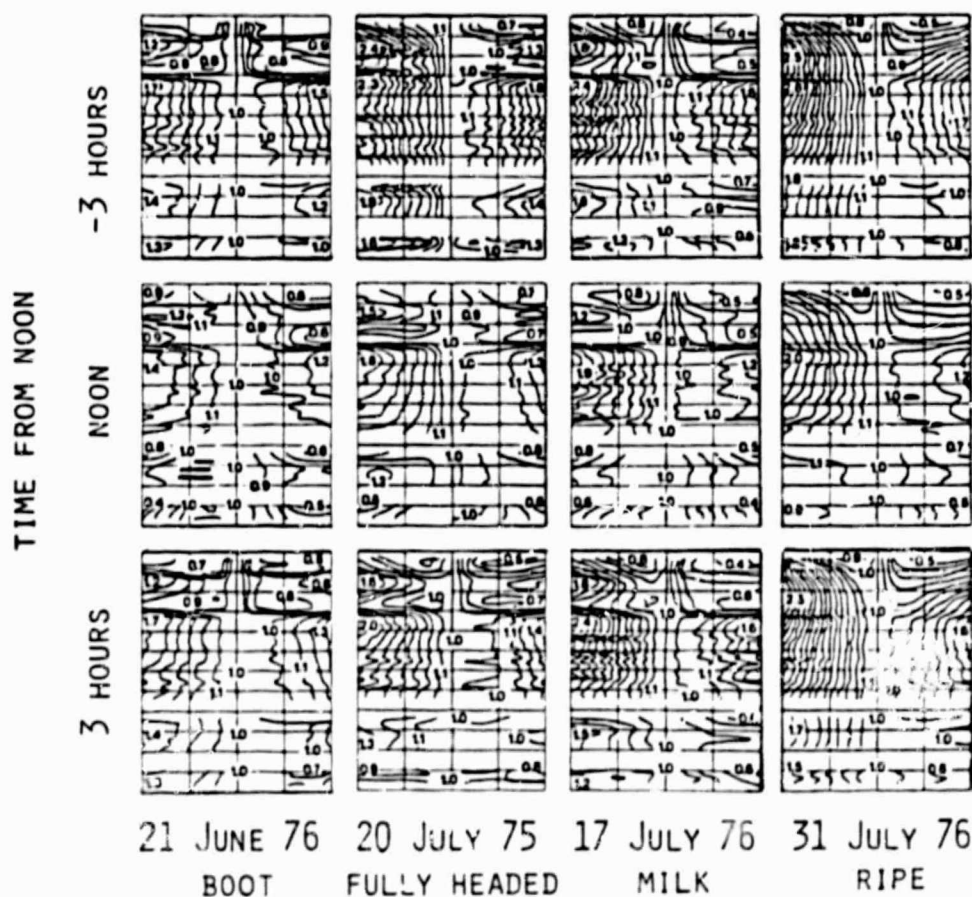
Figure A-6.6. Reflectance factor response of a multispectral line scanner
(MSS) normalized to nadir and ±60° about nadir. In the case of the MSS
flying in a direction 90° to the sun azimuth direction (illustrated here)
the response is symmetric with illumination angle from noon, but is not
symmetric with scan angle.

zenith angle. In the middle-infrared at 1.68 μm the response is similar to that in the red spectral region.

The results shown in Figure A-6.3 represent the normalized BRF of the canopy on one date 17 July 1976 three hours before noon.   The results in Figure A-6.3 are based on the simulated response of a conical scan normalized to 1.0 at the canopy hot spot, the antisolar point, and scanning in azimuth angle with the zenith view angle fixed at the angle of the canopy hot spot.   The results were obtained by dividing the wavelength axis into three wavelength regions, visible (0.44-0.68 μm), near-infrared (0.76-1.28 μm), and middle-infrared (1.48-1.76 μm and 2.08-2.24 μm).   On Figure A-6.3 the range of the canopy BRF responses in each wavelength region is signified by the appropriate stippled area. For example, at an azimuth angle of -90°, the BRF in the visible region ranged between 0.5 and 0.55 of the BRF at the hot spot.   Figure A-6.3 shows that the response as a function of azimuth angle measured from the hot spot is symmetric and decreases.   The decrease of the response is greatest in the visible region and least in the near-infrared region.

Figure A-6.4 shows the wavelength and scan angle scales which apply to each plot in the 3 x 4 array of plots in Figures A-6.5 and A-6.6. The wavelength scale changes at 1.0 and 20 μm.   The scan angle scale is organized for data from a multispectral line scanner scanning 60 degrees about nadir.   Negative scan angles are zenith angles to the left of nadir.

Figure A-6.6 shows the BRF response of a MSS normalized to the response at nadir and scanning 60 degrees about nadir.   The wavelength and zenith scan angle scales of each of the 24 plots in Figure A-6.6 are illustrated in Figure A-6.4.   Each line of plots in Figure A-6.6 represents a particular time.   Each column of plots in Figure A-6.6 represents a specific crop development stage.   In each plot the normalized BRF at a particular scan angle and wavelength is indicated by the height quantized in topographic notation by contour lines at 0.1 unit intervals.   The BRF on a contour line labeled 1.1 is 1.1 times the BRF at nadir.   The contour line immediately adjacent to the line nadir BRF, depending on the sequence of contour lines.

The results in Figure A-6.5, the case of the MSS-equipped aircraft flying toward the solar azimuth, show the normalized BRF with scan angle is generally symmetrical about the nadir scan angle for all wavelengths, all three times, and all four growth stages.   For example, the BRF for (scan angle 60 degrees, 3 hours, 21 June 1976,   0.64 μm) is 0.6 of the BRF at nadir at 0.64 μm.   In the near-infrared spectral region, the BRF generally increases with increasing scan angle for all three times and all four crop development stages. In the visible and middle-infrared regions, a simple pattern doesn't exist; the BRF may increase or decrease depending upon wavelength, illumination angle, and development stage.

Figure A-6.5 also shows the BRF with scan angle for three hours before noon is very similar to the response three hours after noon, suggesting that the BRF is fairly symmetric not only in scan angle but

C - 2

also with illumination angles from noon. Generally, for a particular wavelength, whatever changes that do occur with scan angle are enhanced at the two times away from noon as compared to noon. In each plot the transition between the visible and near-infrared spectral regions is abrupt for the green, healthy canopies (columns labeled 21 June 1976, 20 July 1975, and 17 July 1976) and markedly less so for the senescent canopy (column labled 31 July 1976) without the strong red chloropyll absorption band.

Figure A-6.6, the case of the aircraft flying in a direction 90 degrees to the sun azimuth direction, reveals a BRF similar to that of Figure A-6.5. The same transition phenomenon is evident at 0.7 µm between the visible and the near infrared regions. The curves are fairly symmetric with illumination angle from noon. In the near-infrared region, the BRF generally increases for increasing scan angles regardless of crop development stage or time. (Note the minor but systematic exception to this rule near nadir where the BRF is between 0.9 and 1.0 of nadir BRF.) However, unlike Figure A-6.5 the response curves of Figure A-6.6 are not symmetric with scan angle.

6.4 Discussion

The results, Figure A-6.3, are consistant with the concept that the effects of shadowing on BRF are modulated by the effects of light multiply scattered by canopy components. Radiation is multiply scattered when it is reflected or transmitted more than one time by foliage or soil in the canopy. Light tends to be multiply scattered in crop canopies in regions of the spectrum where the foliage absorbs little light (i.e., the near infrared band from 0.8 µm to 1.3 µm) and tends not to be multiply scattered in regions of the spectrum where foliage absorbs a significant proportion of the incident light (i.e., the red wavelength band prior to senescence). Multiply scattered light tends to reduce the contrast between two adjacent surfaces in the canopy, one surface illuminated by direct solar radiation and the other surface shadowed. The BRF of a crop canopy is the sum of the individual contributions of the shadowed and illuminated surface areas in the canopy. If the contrast between the shadowed and illuminated areas is negligible, then changes in the proportion of shadowed surface area to illuminated surface area in the canopy will not be evident in the canopy BRF. Conversely, if the contrast is significant, then changes in the proportion of shadowed to illuminated surface area in a canopy will be evident as changes in the canopy BRF. Therefore, the canopy BRF is a function of both the proportion of shadowed to illuminated surface area in the canopy and the importance to the canopy radiation environment of multiply scattered light, which reduces the contrast between the shadowed and illuminated surface areas.

The results, Figure A-6.3, are for one zenith view angle, that of the hot spot. If the canopy foliage were randomly distributed both spatially and azimuthally, then, because the zenith view angle is constant, the relative proportions of the canopy components in the field of view of a sensor would not change with azimuth scan angle. The

proportion of illuminated to shadowed foliage would be greatest at the hot spot, an azimuth scan angle of zero, and least at an azimuth scan angle of 180 degrees. If the BRF of the canopy were merely a function of the proportion of illuminated to shadowed foliage, then the stippled areas of Figure A-6.3 should coincide. The regions do not coincide indicating that other factors must be included in the analysis.

At any azimuth scan angle away from the hot spot, the stippled areas are ordered from top to bottom, near-infrared, middle-infrared, and visible. The ranking corresponds with a ranking of the importance of multiply scattered light in each spectral region. Each stippled area representing a spectral region is almost symmetric with azimuth scan angle from the hot spot; the proportion of illuminated to shadowed areas is similarly symmetric provided the canopy foliage is randomly distributed. Consequently, the results, Figure A-6.3, are consistent with the argument that the effects of multiply scattered light serve to modulate the effects of shadowing on the BRF of the canopy.

The results, Figures A-6.3 and A-6.5, are consistent with the argument that shadows cast by foliage are an important factor in the variation of BRF with view direction. Considering Figure A-6.5, the proportion of shadowed to sunlit foliage and soil should be approximately the same at equal angles left and right of nadir provided the foliage is randomly distributed. Since the BRF of a crop canopy is the sum of the individual contributions of the shadowed and illuminated surface areas in the canopy, then the BRF should be symmetrical in scan angle from nadir as it is in Figure A-6.5, regardless of wavelength. Considering Figure A-6.6, the curves are asymmetric in scan angle about nadir. At all wavelengths, the normalized sensor response is noticeably larger on the side of the flightline away from the sun, toward the canopy hot spot where shadows cast by foliage would not be seen. Shadows cast by foliage would be observable on the opposite side of the flightline, the side with the lower response indicated by Figure A-6.6. Thus, the results support the argument that shadowing is an important factor in the variation of BRF with view direction.

The results, Figure A-6.6, are consistent with the argument that shadows cast by foliage are an important factor in the variation of BRF not only with view direction but also with illumination angle. The proportion of shadowed to illuminated surface areas in a canopy changes with sun angle during the day. The proportion varies from unity (all shadow) at sunrise and sunset to a low value sometime during the day. For a particular view direction fixed relative to the illumination direction the proportionality, a function in time, will be symmetric about solar noon if the azimuthal orientation and spatial distributon of the foliage is symmetric about a north south line and if confounding factors (i.e., phototropism, plant geometry changes due to wind or moisture stress, etc.) are not important.

For a particular view direction fixed relative to the sun direction, the BRF should, in general, be symmetric in time and sun angles about solar noon, provided (1) the geometry of the canopy remains properly symmetric throughout the day and (2) the spectral properties of

the canopy components are constant or vary symmetrically in time about solar noon. (For example, if significant soil surface dry down occurred during a day, then the canopy would fail to satisfy criteria 2 when the soil reflectance changes, in any, were asymmetric about solar noon.) The results, Figures A-6.5 and A-6.6, show the BRF for a particular wavelength and scan angle is generally symmetric in time about solar noon, supporting the argument that shadowing is an important factor for explaining the variation in BRF with illumination angles.

The results, Figures A-6.5 and A-6.6, are consistent with the notion that the BRF changes in certain ways with scan angle because the probability of observing the various components of the canopy changes significantly with scan angle. For example, the probability of observing bare soil is generally greatest at nadir and decreases rapidly with increasing scan angle across the canopy. Figure A-6.5 and several plots in Figure A-6.6 reveal an abrupt change of BRF with scan angle near nadir for the visible spectral region, suggesting the effect of the soil should be considered for understanding the properties of the BRF under these conditions.

As a second example, for most canopies at large scan angles only the upper layers of the canopy are visible. The upper layers of a canopy are well illuminated --no higher foliage shadows the topmost layer. Thus, at large, incrementally increasing scan angles the proportion of shadows should decrease and the BRF should increase. Figures A-6.5 and A-6.6 reveal such a pattern in the near-infrared spectral region of all plots and in the visible portions of several plots. The pattern may exist throughout the visible spectral region where the BRF might increase at scan angles larger than the 60 degrees measured.

6.5 References

1. Chevrel, M.,M. Courtois, and G. Weill. 1980. The SPOT satellite remote sensing mission. Proc. 1980 ACSM-ASP Convention, St. Louis, Missouri.

2. Schnetzler, C.C., and L.L. Thompson. 1979. Multispectral resource sampler: an experimental satellite sensor for the mid-1980's. Proc. SPIE Technical Symp., vol. 183, Huntsville, Alabama.

3. Turner, R.E. and M.M. Spencer. 1972. Atmospheric model for correction of spacecraft data. Proc. 8th Intl. Symp. Remote Sensing of Envrionment, Ann Arbor, Michigan, pp. 895-934.

4. Suits, G.H. 1972. The calculation of the directional reflectance of a vegetative canopy. Remote Sensing of Environment 2: 117-125, 1972.

5. Smith J.A., and R.E. Oliver. 1972. Plant canopy models for simulating composite scene spectroradiance in the 0.4 to 1.05

micrometer region.   Proc. 8th Intl.   Symp. on Remote Sensing of Environment, Ann Arbor, Michigan, pp. 1333-1354.

6. Vanderbilt, V.C.   1980.   A model of plant canopy polarization response.   Proc. Symp. on Machine Processing of Remotely Sensed Data, W. Lafayette, Indiana, pp. 98-108.

7. Colwell, J.E. 1974. Vegetation canopy reflectance. Remote Sensing of Environment 3: 175-183.

8. Bunnik, N.J.J.   1978.   The multispectral reflectance of shortwave radiation by agricultural crops in relation with their morphological and optical properties. H. V. Veenamn & Zonen B.V., Wageningen.

9. Chance, J.E. and E.W. LeMaster.   1977. Suits reflectance models for wheat and cotton: theoretical and experimental tests.   Applied Optics 16:   407-412.

10. MacDonald, R.B., M.E. Bauer, R.D. Allen, J.W. Clifton, J.D. Erickson, and D.A. Landgrebe.   1972 Results of tne 1971 corn blight watch experiment.   Proc. 8th Intl. Symp. on Remote Sensing of Environment, Ann Arbor, Michigan, pp. 157-190.

11. Kriebel,   K.T.   1974.   Das spektrale reflexionsvermogen einer bewachsenen oberflache teil 1:   methode und anwendung.   Beitrate zur Physik der Atmosphare 47:   14-44.

12. Bauer, M.E. M.C. McEwen, W.A. Malila, and J.C. Harlan.   1978. Design, implementation, and results of LACIE field research. Proc. LACIE Symp., National Aeronautics and Space Administration, Johnson Space Center, JSC-16015, pp. 1037-1066.

13. Leamer, R.W. V.I.   Myers, and L.F. Silva.   1973.   A spectroradiometer for field use. Rev. Sci Instrum. 44: 611-614.

14. Nicodemus, F.E. J.C. Richmon, J.J. Hsia, I.W. Ginsberg, and T. Limperis.   1977. Geometrical considerations and nomenclature for reflectance.   National Bureau of Standards, U.S.   Department of Commerce, NBS MN-160.

15. Robinson, B.F. and L.L. Biehl.   1979.   Calibration procedures for measurement of reflectance factor in remote sensing field research. In Measurements of Optical Radiation, SPIE 196: 16-26.

16. Gram, F. and G.W. Luckey.   1978.   Optical sphere paint and a working standard of reflectance. Applied Optics 7: 2289-2294.

17. Morse, P.M. and H. Feshbach.   1953.   Methods of Theoretical Physics, McGraw-Hill Book Co., New York.

18. Large, E.C. 1954.   Growth stages in cereals.   Plant Pathology 3: 128-129.

7. A Model of Plant Canopy Polarization Response

V.C. Vanderbilt

7.1 Introduction

Sensors to remotely measure the linear polarization of ground scenes have been proposed for the Multispectral Resource Sampler (MRS) (17), a satellite sensor system proposed to complement the Thematic Mapper. At present justification for a sensor on MRS to measure scene polarization is limited (2-7). This report discusses a model for the amount of linearly polarized light reflected by the shiny leaves of such crops as wheat, corn, and sorghum. The theory demonstrates that, potentially, measurements of the linearly polarized light from a crop canopy may be used as an additional feature to discriminate between crops. Examination of the model suggests that, potentially, satellite polarization measurements may be used to monitor crop development stage, leaf water content, leaf area index, hail damage and certain plant diseases. The model adds to our understanding of the potential information content of scene polarization measurements acquired by future satellite sensor systems such as MRS.

7.2 Development of the Model

Development of the mathematical model for polarization of light from a wheat canopy requires four assumptions:

1. There exist on the wax surface of each shiny leaf small flat areas, Δa, which specularly reflect light.

2. The wax layer is essentially clear and absorbs little light. This means that for the wax layer the complex index of refraction can be adequately approximated by its real component, a reasonable supposition for the visible spectral region where any light energy absorbed by the wax layer is then unavailable to the chloroplasts to promote photosynthesis. Limited evidence supports this assumption (19).

3. Specular light reflection occurs principally at the air-wax boundary. Comparatively negligible amounts of light are reflected specularly to an observer and from the boundaries between epidermal cell walls, cell membranes, and the various cutible layers. These boundaries have comparable indices of refraction and often appear rough in electron micrographs.
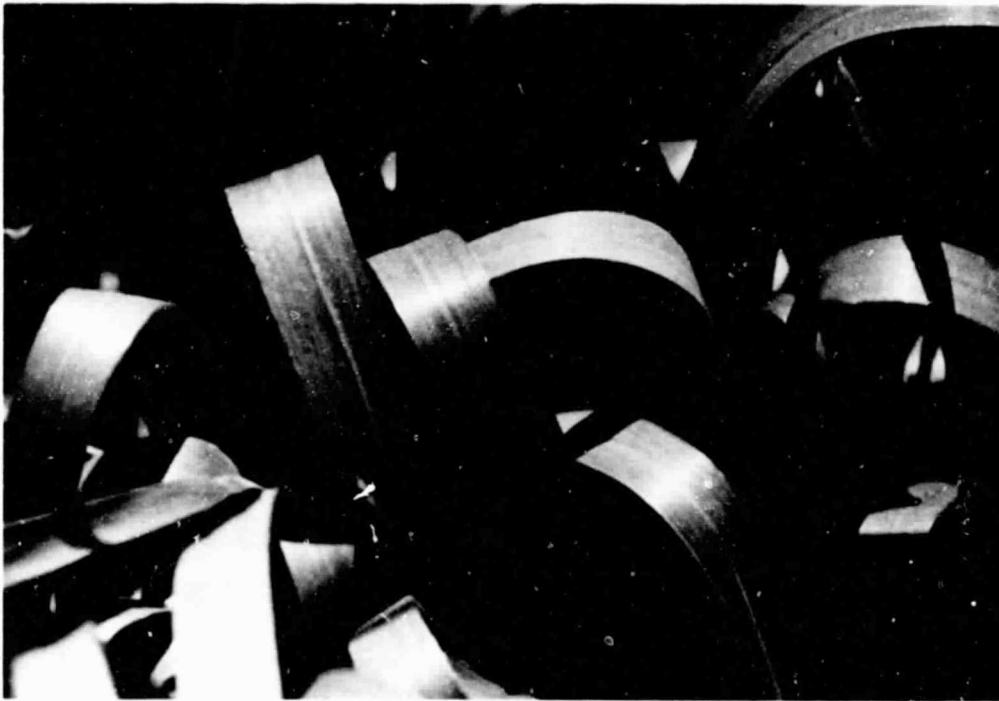
Figure A-7.1. Specular Reflection. The camera received specularly reflected sunlight from the bright areas of these wheat flag leaves.
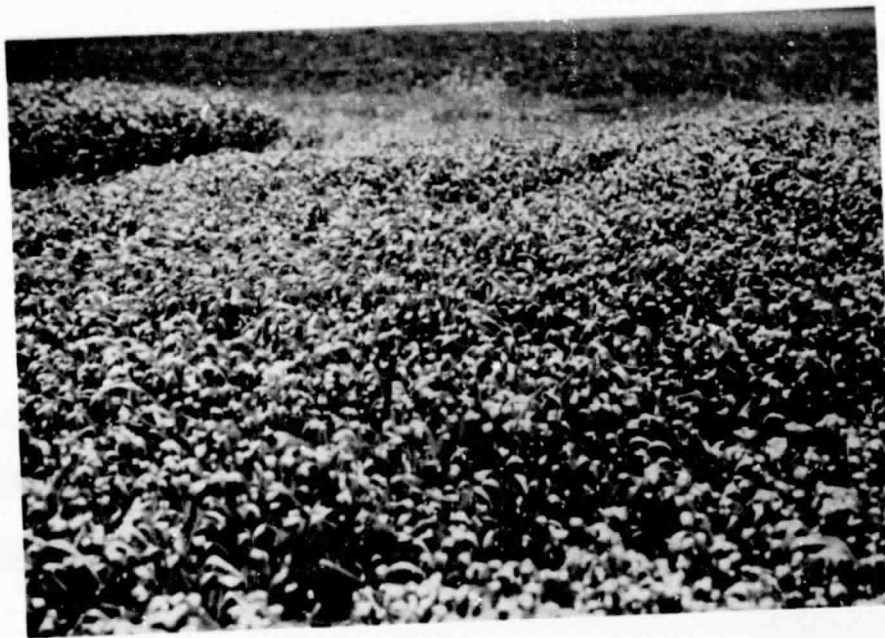
Figure A-7.2. Polarized Light from Canopy. These photos, taken with a polarizer oriented for transmission of maximum specularly reflected light (top) and minimum specularly reflected light (bottom), demonstrate that the specularly reflected light is polarized.

4. The magnitude of polarized light from sources (moist soil, for example) other than sunlit leaves is insignificant.

On the micro scale level, Figure A-7.3, sunlight is specularly reflected by one of the small leaf areas to an observer only if the area is properly oriented. The area Δa must be oriented such that the angle of incidence, γ, equals the angle of reflectance and such that the vectors $\vec{E}$, $\vec{n}$ (the unit vector normal to Δa), and $\vec{V}$ are coplanar. If the area Δa specularly reflects light to an observer, then the radiant flux incident on Δa is $P_s|\vec{E}|\cos\gamma$ where $\gamma = \gamma(\theta_s, \theta_v, \phi_v)$ and P_s is the probability of finding in a small volume an area Δa illuminated directly by the sun as opposed to being shaded by intervening foliage. The probability of finding in a small volume an observable area Δa is symbolized by P_v.

The probabilities, P_s and P_v, are functions both of the (x,y,z) location of the leaf in the canopy and of directions of illumination and observations, respectively. For example, P_s and P_v will approach unity for the topmost leaves of a dense, preheaded wheat canopy if the aggregation of these leaves forms a layer one leaf thick at the extreme top of the canopy essentially impenetrable to direct illumination. The probabilities will be less than unity for more typical canopies with some soil and/or non-leaf foliage illuminated and observed and some leaves not illuminated and/or not observed.

Even though the incident sunlight is not polarized, each small area, Δa, polarizes the specular portion of the reflected sunlight provided the angle of incidence is neither 0 or 90 degrees (8). If Δa is smooth, the magnitude of the light that is specularly reflected and polarized by Δa is described mathematically by the Fresnel equations and Stokes vector and depends only upon the angle of incidence, γ, and index of refraction of both the epicuticle wax layer and air (18).

Most often Δa is not a perfectly smooth surface but instead supports small acicular structures which diffusely scatter light that would otherwise be specularly reflected (11,12). To account for this the Fresnel equations are modified by a factor, K (dimensionless). It is assumed here that $k(\theta_s, \theta_v, \phi_v, \lambda)$ is identical for all leaves and is not a function of lateral position and direction on the leaf surface. The value of K varies between zero and one.

Define a probability density function $f_a(\theta, \phi)$ for leaves such that the probability that any one of the leaf areas Δa is oriented within a solid angle $\Delta\omega_a$ about (θ_a, ϕ_a) is $\Delta\omega_a f_a(\theta_a, \phi_a)$ (dimensionless). The units of $f_a = f_a(x,y,z,\theta,\phi)$ are $[sr^{-1}]$. Because the area Δa must be correctly oriented to reflect light to an observer, the Jacobian (15) provides

$$\Delta\omega_a = \Delta\omega_v/4\cos\gamma = A_v\cos^2\theta_v/4h^2\cos\gamma \qquad (1)$$
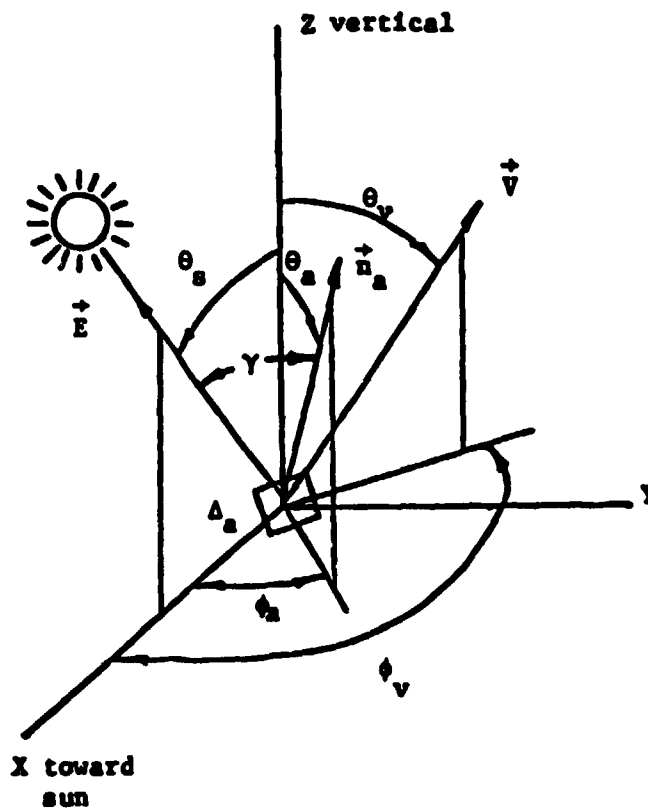
Figure A-7.3. Coordinate System. A small leaf area Δa specularly
reflects sunlight toward an observer, $\vec{V}$, if and only if the vectors $\vec{E}$,
$\vec{n}_a$ and $\vec{V}$ are coplanar and the angles of incidence (γ) and reflectance
are equal.
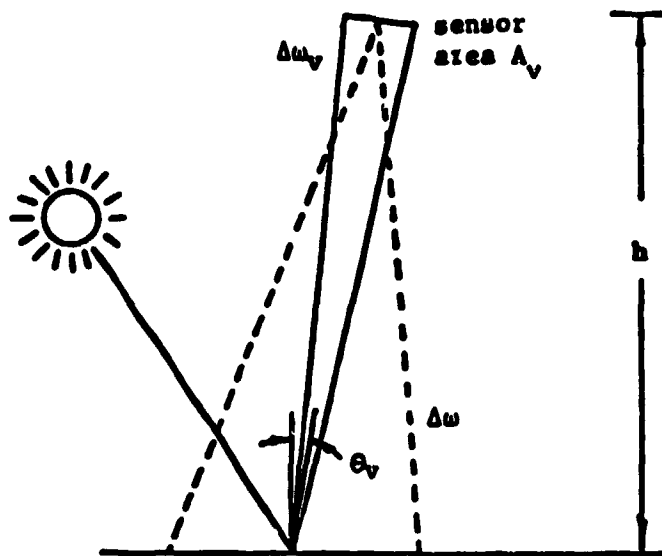
Figure A-7.4. Canopy Response. A sensor measures the canopy response over a solid angle $\Delta\omega$.

On the macro scale level, Figure A-7.4, the radiant flux due to specularly reflected sunlight received from leaves in the field of view of a sensor is found by summing the flux contributed by each leaf area Δa in each volume j in the field of view. For a Δa the radiant flux specularly reflected into a solid angle $\Delta\omega_v$ by a randomly selected area is the quadruple product of (1) the radiant flux incident on the area Δa, (2) the specular reflectance of Δa, (3) the probability that Δa is correctly oriented to specularly reflect light in a solid angle $\Delta\omega_v$ about direction (θ_v, ϕ_v) and (4) the probability that Δa is observed.

$$\Phi_S = |\vec{E}| \; KS_S \overset{\text{all } V_j \text{ in}}{\underset{j=1}{\sum}} f_{aj} P_{sj} P_{vj} A_j A_v \cos^2\theta_v / 4h^2 \qquad (2)$$

source dependent term   canopy dependent terms   sensor dependent terms

$$\Phi_Q = |\vec{E}| \; KS_Q \overset{\text{all } V_j \text{ in}}{\underset{j=1}{\sum}} f_{aj} P_{sj} P_{vj} A_j A_v \cos^2\theta_v / 4h^2 \qquad (3)$$

The percent linear polarization is proportional to the linearly polarized flux divided by the total flux, the sum of the diffuse and specular fluxes.

$$100\% \Phi_Q / (\Phi_D + \Phi_S) \qquad (4)$$

To illustrate the properties of the polarization model, the response of two hypothetical canopies will be examined.

Example A: Sparse Wheat Canopy.   If the properties of the canopy are constants for those layers containing leaves, that is, if $P_{sj} = P_{si} = P_s$, $P_{vj} = P_{vi} = P_v$, $A_j = A_i = A$, and $f_{aj} = f_{ai} = f_a$, for all (V_j, V_i) in the field of view such that $A \neq 0$, then

$$\overset{\text{all } V_j \text{ in}}{\underset{j=1}{\sum}} P_{sj} P_{vj} A_j \qquad (5)$$

and

$$\phi_S = |\vec{E}| P_s(LAI) KS_S f_a P_v A_v \Delta\omega / 2\cos^3\theta_v \qquad (6)$$

source   canopy   sensor

$$\phi_Q = |\vec{E}| P_s(LAI) KS_Q f_a P_v \Delta\omega A_v / 2\cos\theta_v \qquad (7)$$

where LAI is leaf area index. The linearly polarized portion of the total scene radiance is (14)

$$L_Q = \phi_Q / A_v \Delta\omega = |\vec{E}| P_s(LAI) KS_Q f_a P_v / 2\cos\theta_v \qquad (8)$$

Example B: Preheaded, Dense Wheat Canopy. If the probability $P_{sj} P_{vj} = 1$ for V_j in the topmost layer of the canopy and $P_{sj} P_{vj} = 1$ for V_j in all lower layers, then the ϕ_S and ϕ_Q are proportional to the leaf area index only of the topmost layer. A winter wheat canopy measured just prior to heading might have the following characteristics: LAI = 2.0 for top layer containing flag leaves with a wax layer index of refraction = 1.5, f_a = uniform = 0.0796 sr^{-1}, K = 0.9, and $P_s = P_v = 0.9$ for top layer and $P_s = P_v = 0.0$ for all lower layers. The linearly polarized portion of the canopy radiance (eq. 8) and the linearly polarized flux measured by a sensor over such a canopy are shown in Figure A-7.5. The calculations are for a sensor with a field of view of 15 degrees or = 0.216sr, entrance optics of area 0.002m^2, and spectral band of 0.6-0.7 μm (red wavelengths).
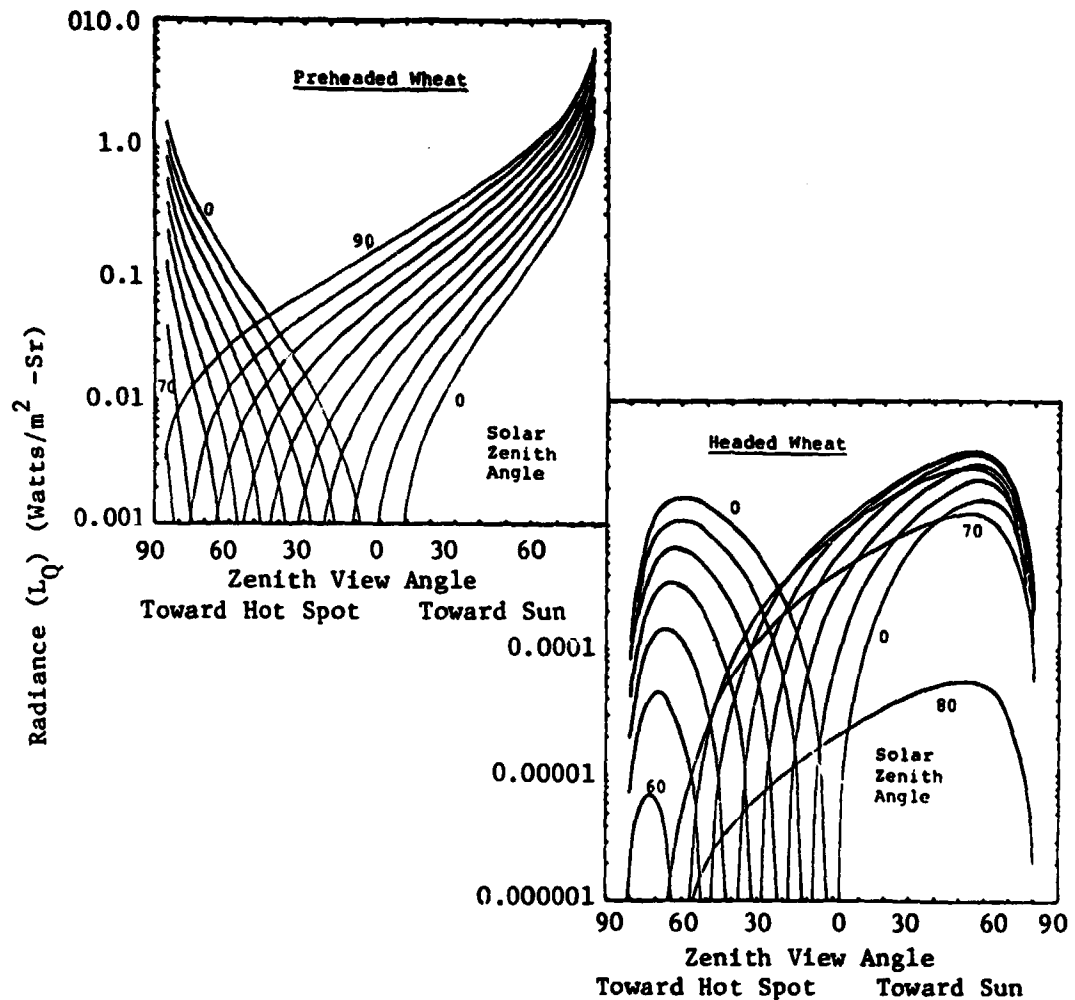
Figure A-7.5. Polarization Response of Preheaded and Headed Wheat
Canopies. Prior to heading the response is zero at the anti-solar
point, the "hot spot," and increases with increasing zenith view
angle. After heading the response remains zero at the anti-solar
point, is maximum at intermediate zenith view angles, and approaches
zero for near-horizontal view directions where heads and stems obstruct
view of polarizing flag leaves.

Example C: Headed, Dense Wheat Canopy. The polarization response
of a wheat canopy is expected to change significantly during the heading
growth stage (Figure A-7.2). This is because the probabilities P_s and
P_v of a headed wheat canopy, unlike those of a preheaded canopy are
pronounced functions of sun angle and view angle.   The product P_sP_v may
be estimated for a hypothetical headed canopy with LAI = 2.0 by applying
linear regression techniques to data for a canopy with LAI = 1.0 and
scaling by a factor of 2.0 (21).

$$P_sP_v = .232 \exp (-1.17((1/\cos\theta_v) + (1/\cos\theta_s))) \qquad (9)$$

Equation 9, derived assuming P_s and P_v to be independent, provides
erroneous estimates of P_sP_v at angles near the canopy hot spot direction
where the probability P(leaf observation leaf illumination) approaches
unity.   Figure A-7.6 shows the linear polarization response for a
source-canopy-sensor with the parameters of Example B except P_sP_v given
by equation (9).

7.3 Discussion

The model shows the magnitude of the polarization response of a
plant stand is related to the solar insolation and the characteristics
of the canopy and the sensor.   The response depends on the optical and
geometric properties of the portion of the canopy in the instrument
field of view.

The calculations show that a sensor would measure zero linearly
polarized light at the anti-solar, the canopy "hot-spot," where the
angle of incidence of the sunlight is zero.   The sensor would measure
the maximum amount of polarized light in the solar azimuth direction
(Figure A-7.5), provided the small areas a are randomly oriented in
azimuth and zenith directions.   Otherwise the direction of maximum
polarization may be shifted, as might occur when a strong wind
preferentially orients the flag leaves of wheat downwind.

The theory shows that when the specular flux is much, much greater
than the diffuse flux the percent linear polarization is not directly
related to the canopy agronomic properties.   This might occur in the
chlorophyll absorption region in the red portion of the spectrum viewing
at large zenith angles toward the sun azimuth angle.   However, even
though the percent linear polarization in certain circumstances may
contain limited information related to canopy agronomic factors, the
magnitude of the linearly polarized flux is always directly related to
the canopy agronomic properties.   Under these conditions, the magnitude
of the linearly polarized flux provides more information concerning
these canopy properties than does the percent linear polarization. This
is because the magnitude of the linearly polarized flux is always
directly related to the canopy agronomic properties while the percent
linear polarization is not.   This magnitude is directly computed from
measurements of linearly polarized flux.   Thus, the model provides a
theoretical basis for the same, but empirically based result noticed by
Egan (5).

The information in canopy polarization data, when obtained from satellite sensors, probably will be used in conjunction with other remotely sensed data and will be extracted by analysis of frequent, synoptic data sets, by using the temporal and spatial information to make relative comparisons between the fields in the data for one date and between the dates for one field. One polarization measurment of one field for one date probably will have little value unless it is compared to polarization data for that field and other fields for that date and other dates. This is because it is unrealistic from the model to expect that canopy polarization data will be calibrated in an absolute sense to discriminate a particular crop or to correlate uniquely to a particular agronomic variable. Frequent, synoptic polarization data from a satellite sensor potentially aid in assessing crop vigor and growth stage and in determining areas of hail damage and pestilence, all potentially possible from comparisons between field and across dates. Perhaps daily satellite coverage is feasible using a low spatial and spectral resolution sensor in a geosynchronous orbit.

The canopy polarization response described by the model is a function of wavelength only because the index of refraction of the cuticle wax layer is a function of wavelength. From the physics of the optical properties of materials (8), it is expected that the index of refraction of the wax layer will gradually and monotonically increase with decreasing visible wavelength, displaying no perturbations or "fine structure" with wavelength. However, the model indicates the percent linear polarization of a healthy green canopy will be large in the blue and red spectral regions, small in the green, and even smaller in the near infrared region away from any absorption bands. This is because the total canopy flux, the normalization factor used when computing percent polarization, exhibits a green vegetation response.

From the model there appears little need to measure the canopy spectral polarization response with high wavelength resolution in the visible spectral region; a polarization sensor covering the entire visible region or a large portion of it might suffice. Conversely, in the infrared spectral region the cuticle wax layer may absorb in narrow spectral regions defined by the structural properties of the constituent waxes of the layer, by the resonant frequencies of the translational and rotational vibration modes of molecules of the layer. If absorption bands do exist in the infrared opectral region, high resolution spectral polarization data from these wavelength regions may possibly provide information concerning the properties relatable to crop species and light regime.

The connection between leaf polarization measurements and leaf moisture content, noted by Egan, is supported by a morphological model for the structural changes which occur in a leaf undergoing dehydration. When the leaf water content and leaf thickness decrease and the leaf cells dehydrate and collapse, the surface appears rough in thin sections of senescent leaves and of leaves under moisture stress. As the surface roughness increases, the specular portion of the light reflected by the leaf decreases because there are fewer areas Δa which are similarly

oriented. The amount of linearly polarized light reflected by the canopy decreases in company with the decrease of specularly reflected light. These arguments suggest that the canopy polarization response should decrease with decreasing leaf water content in the canopy and therefore serve as an indicator of canopy moisture stress. Visual evidence supports this hypothesis. Leaves under moisture stress often appear less shiny than fully turgid leaves. Dry, senescent leaves often have a matte surface finish.

Detection of the date of heading of a wheat canopy (Figure A-7.2), information which is needed for use with phenologically based models to predict the ultimate grain yield of the crop, might be feasible using satellite polarization measurements (Figure A-7.6). The eventual weight of grain produced by each wheat plant is largely determined by the condition of the flag leaf, its size and vigor, and by the weather regime endured by the plant following heading when the grain head begins to fill. Knowledge of the date of heading permits a better estimate of the post-heading weather for the crop.

Prior to heading the topmost foliage on the wheat plant is the flag leaf, easily the most visible and illuminated canopy component (Figure A-7.2). Following heading, wheat heads are the topmost foliage and partially obscure the flag leaves to both sunlight and observation, changing the values of both P_S and P_V. Figure A-7.5 shows that the magnitude of the polarized light, which depends directly upon the specular reflections from flag leaves, will decrease by a factor of 60 for $\theta_S=30$ and $\theta_V=0$ for the two hypothetical canopies during heading as the leaves are increasingly obscured to both illumination and observation. The obscuration of the flag leaves is enhanced at off nadir observation angles directed toward the solar azimuth (Figure A-7.5). Potentially both the condition of the flag leaves and the date of heading of a crop might be monitored using polarization measurements obtained from a satellite sensor with both on and off nadir viewing capability.

Applicability of the polarization model should extend to many species because shiny leaves which specularly reflect sunlight are ubiguitous, not stratified according to geography or climate. Other plants besides wheat, sorghum, and corn with specularly reflecting leaves include coffee, sudan grass, banana, orange, sugarcane, and many forest species. Schieferstein and Loomis (16) found epicuticular wax deposits on about half of the plant species they tested. However, the mere presence of a cuticle wax layer does not guarantee that a leaf will specularly reflect and polarize a significant portion of the incident light; the leaf must also appear shiny. Fibrillar light scattering significantly diminishes the polarization response of pubescent soybean leaves. And the surface of the wax layer of some species is insufficiently smooth to specularly reflect light.

7.4 Conclusions

This report discusses a model for the amount of linearly polarized light reflected by the shiny leaves of such crops as wheat, corn, and

sorghum, each a grain of major economic importance to the world. The model is based upon the morphological and phenological characteristics of the canopy and upon the Fresnel equations which describe the light reflection process at the smooth boundary separating two dielectrics.

The theory demonstrates that, potentially, measurements of the linearly polarized light from a crop canopy may be used as an additional feature to discriminate between crops such as wheat and barley, two crops so spectrally similar that they are misclassified with unacceptable frequency. Examination of the model suggests that, potentially, satellite polarization measurements may be used to monitor crop development stage, leaf water content, leaf area index, hail damage, and certain plant diseases. Such information is needed for use with models which predict crop grain yield.

The model adds to our understanding of the potential information content of scene polarization measurements. The information content of these measurements has not been extensively investigated and needs to be understood to evaluate the potential usefulness of the proposed polarization sensor for the satellite borne Multispectral Resource Sampler. The efficacy of a satellite sensor measuring the linear polarization of a scene through the atmosphere remains to be determined.

7.5 References

1. Breece, H.T. and R.A. Holmes. 1971. Bidirectional scattering characteristics of healthy green soybean and corn leaves in vivo. Applied Optics 10: 119-127.

2. Curran, P.J. 1979. A photographic method for the recording of polarized visible light for soil surface moisture indications. Remote Sensing of Envir. 8: 249-266.

3. Curran, P.J. 1979. The use of polarized panchromatic and falsecolor infrared film in the monitoring of soil surface mositure. Remote Sensing of Envir., 8: 249-266.

4. Egan, W.G. 1968. Aircraft polarimetric and photometric observations. Proc. 5th Intl. Symp. Remote Sensing of Envir., Univ. of Michigan, Ann Arbor, MI, pp. 169-189.

5. Egan, W.G. 1970. Optical Stokes parameters for farm crop indentification Remote Sensing of Environment. 1: 165-180.

6. Egan, W.G. and H.B. Hallock. 1969. Coherence polarization phenomena in remote sensing. Proc. IEEE 57: 621-628.

7. Egan, W.G., J. Grusauskas, and H.B. Hallock. 1968. Optical depolarization properties of surfaces illuminated by coherent light. Applied Optics 7: 1529-1534.

8. Fowles, G.R. 1968. Introduction to Modern Optics. Holt, Rinehart and Winston, Inc., New York.

9. Evans, L.T. and H.M. Ranson. 1970. Photosynthesis and respiration by the flag leaf and components of the ear during grain development in wheat. Aust. J. Biol. Sci. 23: 245-254.

10. Gausman, H.W. 1974. Leaf reflectance of near infrared, Photogrammetric Engineering 40: 183-191.

11. Greulach, V.A. 1973. Plant Function and Structure. Macmillan, New York.

12. Martin, J.T. and B.E. Juniper. 1970. The Cuticles of Plants. New York: St. Martin's Press.

13. Miller, E.E. and J.M. Norman. 1971. A sunfleck theory for plant canopies 1. lengths of sunlit segments along a transect. Agron J. 63: 735-738.

14. Nicodemus, F.E., J.C. Richmond, J.J. Hsia, I.W. Ginsberg, and T. Limperis. 1977. Geometrical considerations and nomenclature for reflectance. National Bureau of Standards, U.S. Department of Commerce, NBS mn-160.

15. Roberts, A.W. 1972. Introductory Calculus. Academic Press, New York.

16. Schieferstein, R.H. and W.E. Loomis. 1956. Wax deposits on leaf surfaces. Plant. Physiol. 31: 240-247.

17. Schnetzler, C.C. and L.L. Thompson. 1979. Multispectral Resources Sampler: an experimental satellite sensor for the mid-1980's. Proc. SPIE Technical Symp., vol. 183, Huntsville, Al, May 1979.

18. Shurcliff, W.A. and S.S. Ballard. 1964. Polarized Light. D. Van Nostrand Co., New York.

19. Sinclair, T.R. 1969. Pathway of solar radiation through leaves. Master's Thesis, Purdue University.

20. Smith, J.A. and R.E. Oliver. 1972. Plant canopy models for simulating composite scene spectroradiance in the 0.4 to 1.05 micrometer region. Proc. 8th Intl. Symp. on Remote Sensing of Environment, Ann Arbor, MI., pp. 1333-1354.

21. Vanderbilt, V.C. 1976. An experimental geometrical characterization of two vegetative canopies. Ph.D. thesis, Purdue University.

B. FIELD RESEARCH DATA ACQUISITION, PREPROCESSING, AND DISTRIBUTION

Larry L. Biehl

This section describes the results of work conducted under Task 1B, Field Research Data Acquisition and Preprocesing, and Task 3B, Field Research Data Base Management and Distribution. The objectives of these tasks were to acquire, preprocess, and distribute the data required to accomplish the objectives of the AgRISTARS Supporting Field Research project (described in reference 1 and Section A of this report).

The test locations are three-five by six nautical mile segments in Cass County, North Dakota, Webster County, Iowa, and Wharton County, Texas and three agricultural experiment stations, the Purdue University Agronomy Farm at West Lafayette, Indiana, the University of Nebraska, Sandhills Agricultural Laboratory near North Platte, Nebraska, and the University of Nebraska Field Laboratory, Mead-Wahoo, Nebraska. The major crops in the test sites are: Cass County, spring wheat, barley and sunflowers; Wharton County, cotton and rice; Webster County, corn and soybeans; Sandhills, irrigated corn; and Purdue, corn, soybeans, and winter wheat. Institutions that were involved in data acquisition were: NASA/Johnson Space Center, Purdue University, North Dakota State University, and University of Nebraska.

1. Experiments

Based on the previous, proven experience since 1974, there were two kinds of tests sites for 1980 - controlled experimental plot sites and commercial field sites. The data from experiments in commercial field test sites provide a measure of the natural variation in the temporal-spectral characteristics of the cover type. The data from experiments in controlled plot test sites enable more complete understanding and interpretation of the spectra collected from commercial fields.

The experiments for 1980 include some that have been continued from previous years to sample the different yearly weather patterns and new experiments to obtain measurements over additional crops (spring wheat, barley, sunflowers, cotton, and rice) and measurement/canopy variables (canopy geometry and non-vertical reflectance view angles).

1.1 Objectives

The following overall objectives were selected for the experiments at each test site:

Purdue University Agronomy Farm

- To determine effects of fertilization and disease on the growth, development and spectral characteristics of winter wheat.

- To determine the relationship of crop canopy variables (development stage, LAI, biomass, soil background etc.) to reflectance and radiant temperature of corn, soybeans, and winter wheat.

- To determine effects of varying agronomic practices (planting date, row spacing, plant population, cultivar, soil type) on spectral response of corn and soybeans.

- To support the development of corn and soybean yield models which use spectral response as a function of crop development stage as an input.

- To determine the relationships of percent soil cover, row direction, solar illumination angle, view angle, and canopy geometry to reflectance of soybean canopies.

Sandhills Agricultural Laboratory

- To determine relationship of moisture stress on reflectance and radiant temperature characteristics of corn.

Webster Co., Iowa

- To determine spectral characteristics and separability of corn, soybeans and other crops as a function of growth stage and cultural practices.

- To verify spectral-agronomic relationships.

Cass Co., North Dakota

- To determine spectral characteristics and separability of spring wheat, barley, sunflowers and soybeans as a function of growth stage and cultural practices.

<u>Wharton Co., Texas</u>

- To determine spectral characteristics and separability of cotton, rice, and soybeans as a function of growth stage and cultural practices.

1.2 Experiment Descriptions

<u>Purdue Agronomy Farm.</u> Six experiments were conducted at the Purdue Agronomy Farm to accomplish the objectives stated above. The experiments include studies of crop stress, cultural practices, and canopy geometry characteristics. The experiments, treatments, and spectral instrument systems are summarized in Table B-1.

1. <u>Winter Wheat Fertilization and Disease Experiment.</u> This experiment was a continuation of the 1979 Winter Wheat Experiment. The purpose was to investigate the effects of disease and nitrogen fertilization on the spectral and agronomic characteristics of winter wheat. There were three nitrogen fertilizer rates (0, 60, and 120 kg/hectare), and three disease treatments (resistant cultivar, susceptible cultivar, and susceptible cultivar treated with fungicide) with two replications in a randomized complete block design, Figure B-1. Measurements of reflectance and radiant temperature of the wheat canopies were made with the Exotech 20C field spectroradiometer system and the Exotech 100 field radiometer system at approximately weekly intervals from tillering through ripe stages of development. Agronomic characterizations of the canopies included: leaf area index, biomass, percent soil cover, height, lodging, disease severity, leaf nitrogen concentration, and grain yield.

2. <u>Winter Wheat Disease Experiment.</u> The purpose of this experiment was to investigate the effects of disease (rust) on the spectral response of winter wheat. There were two disease treatment levels with three replications. Each plot was 6 meters square. Measurements of the reflectance and radiant temperatures of two replications of the wheat canopies were made at approximately weekly intervals from the time the wheat was inoculated with rust until the wheat was ripe. Several observations were made of each plot to study the effects of varying severity levels as the disease spread throughout the plot.

3. <u>Corn Cultural Practices Experiment.</u> 1980 was the second year for this experiment. The specific objectives of this experiment were to determine (1) the threshold of early season spectral detection of corn, (2) the spectral response of corn as a function of development stage and amount of vegetation, (3) the effect soil background differences, particularly soil color, on the spectral response and early detection of corn. The treatments were as follows:

Table B-1. Summary of the 1980 Supporting Field Research
Experiments at the Purdue Agronomy Farm

Experiment, Treatments, and Primary Sensor System

Winter Wheat: Nitrogen Fertilization and Disease
            (Exotech 20C and Exotech 100)

    3 Cultivars/Disease Levels
    3 Nitrogen Fertilizer Rates (0, 60, and 120 kg/ha)
    2 Replications

Winter Wheat: Disease (Exotech 20C)

    2 Disease levels
    2 Replications

Corn: Cultural Practices (Exotech 100)

    7 Planting Dates (May 7, 16, 22, 29, June 11, 18, July 3)
    3 Populations (25, 50, 75 thousand plants/ha)
    2 Soil Types (Chalmers - darker, Fincastle - lighter)
    2 Replications

Soybeans: Cultural Practices (Exotech 100)

    7 Planting Dates (May 16, 27, June 12, 18, July 7, 16, 30)
    2 Row Widths (25, 76 cm)
    2 Cultivars (Amsoy 71, Williams)
    2 Soil Types (Chalmers - darker, Toronto - lighter)
    2 Replications

Soybeans: Sun-view angle (Exotech 100)

    8 View Azimuth Angles (0, 45, 90, 135, 180, 225, 270, 315 degrees)
    7 View Zenith Angles (0, 7, 15, 22, 30, 45, 60 degrees)
    5-12 Solar Azimuth-Zenith Angle Periods
    3 Maturity Stages

Soybeans: Row direction - Solar Azimuth and Zenith Angles (Exotech 100)

    37 Row directions (90, 95, 100, ..., 270)
    3 Backgrounds (3M black, 3M white, Russell soil)
    3 Soil Covers
    4-5 Solar Azimuth-Zenith Angle Ranges (time periods)
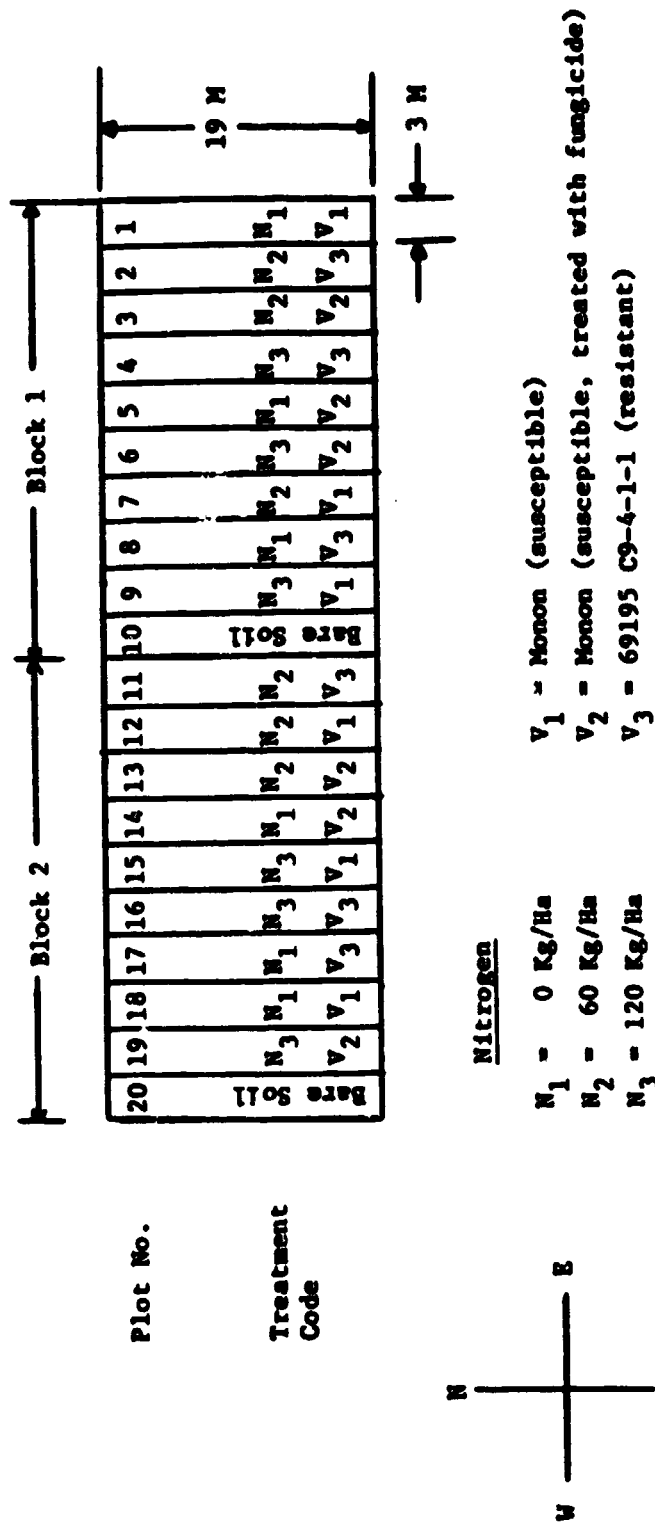
Figure B-1. Design and treatment descriptions of the 1980 Purdue Agronomy Farm Winter Wheat Experiment.

Soil Type

S_1 = Chalmers (dark-colored)

S_2 = Fincastle (light-colored)

Plant Population

P_1 = 25,000 Plants/ha

P_2 = 50,000 Plants/ha

P_3 = 75,000 Plants/ha

Planting Date

D_1 = May 7, 1980

D_2 = May 16, 1980

D_3 = May 22, 1980

D_4 = May 29, 1980

D_5 = June 11, 1980

D_6 = June 18, 1980

D_7 = July 2, 1980

CHALMERS

FINCASTLE

15 m

N

4.6 m
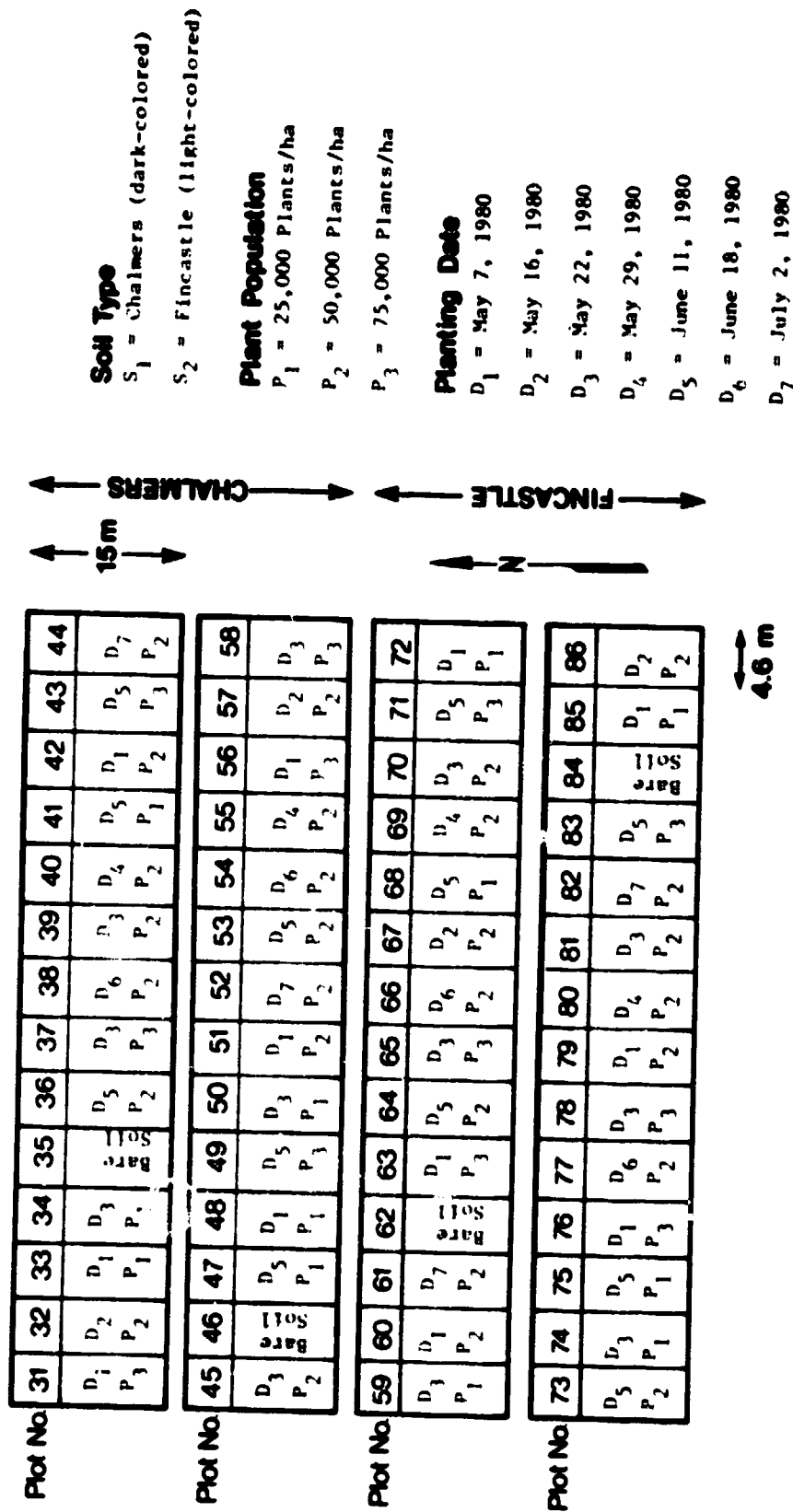
Figure B-2. Design and treatment descriptions of the 1980 Purdue Agronomy Farm Corn Cultural Practices Experiment.

FIELD 31-3B

CHALMERS

9.4 m

9.4 m

4.6 m

FIELD 31-1B

TORONTO ——— CHALMERS

N

Plot No. 101 102 103 104 105 106 107 108 109 110 111 112 113 114 115 116 117 118 119 120 121 122 123 124 125 126

Plot No. 127 128 129 130 131 132 133 134 135 136 137 138 139 140 141 142 143 144 145 146 147 148 149 150 151 152

153 154 155 156 157 158 159 160

165 166 167 168 169 170 171 172

Planting Dates

D_1 = May 16, 1980
D_2 = May 27, 1980
D_3 = June 12, 1980
D_4 = June 18, 1980
D_5 = July 7, 1980
D_6 = July 16, 1980
D_7 = July 30, 1980

Soil Type

S_1 = Chalmers (dark-colored)

S_2 = Toronto (light-colored)

Cultivar

C_1 = Amsoy 71 (Maturity group II)

C_2 = Williams (Maturity group III)

Row Width

R_1 = 25 cm

R_2 = 75 cm

Figure B-3. Design and treatment descriptions of the 1980 Purdue Agronomy Farm Soybean Cultural Practices Experiment.

Figure B-3. Design and treatment descriptions of the 1980 Purdue Agronomy Farm Soybean Cultural Practices Experiment.
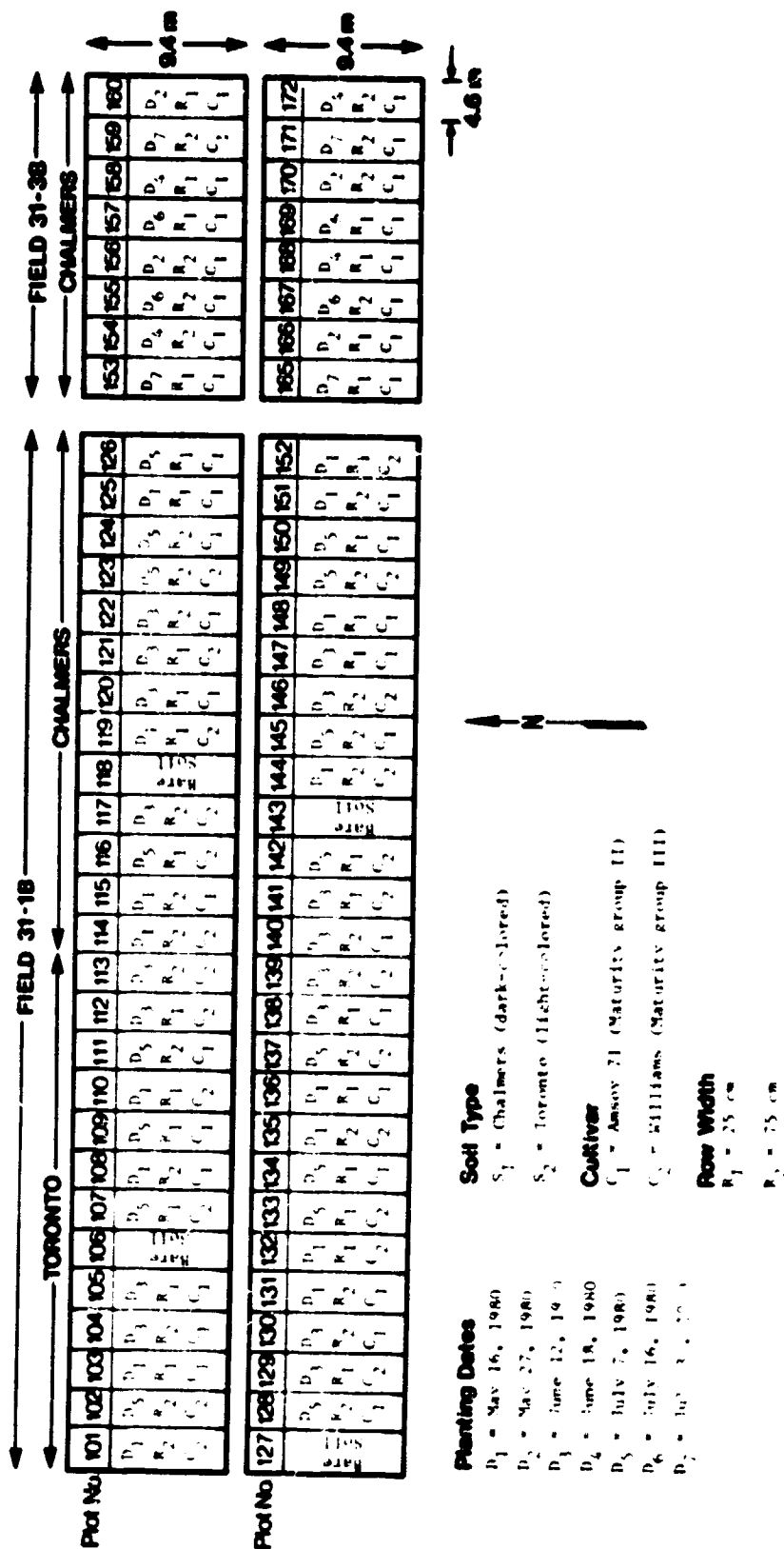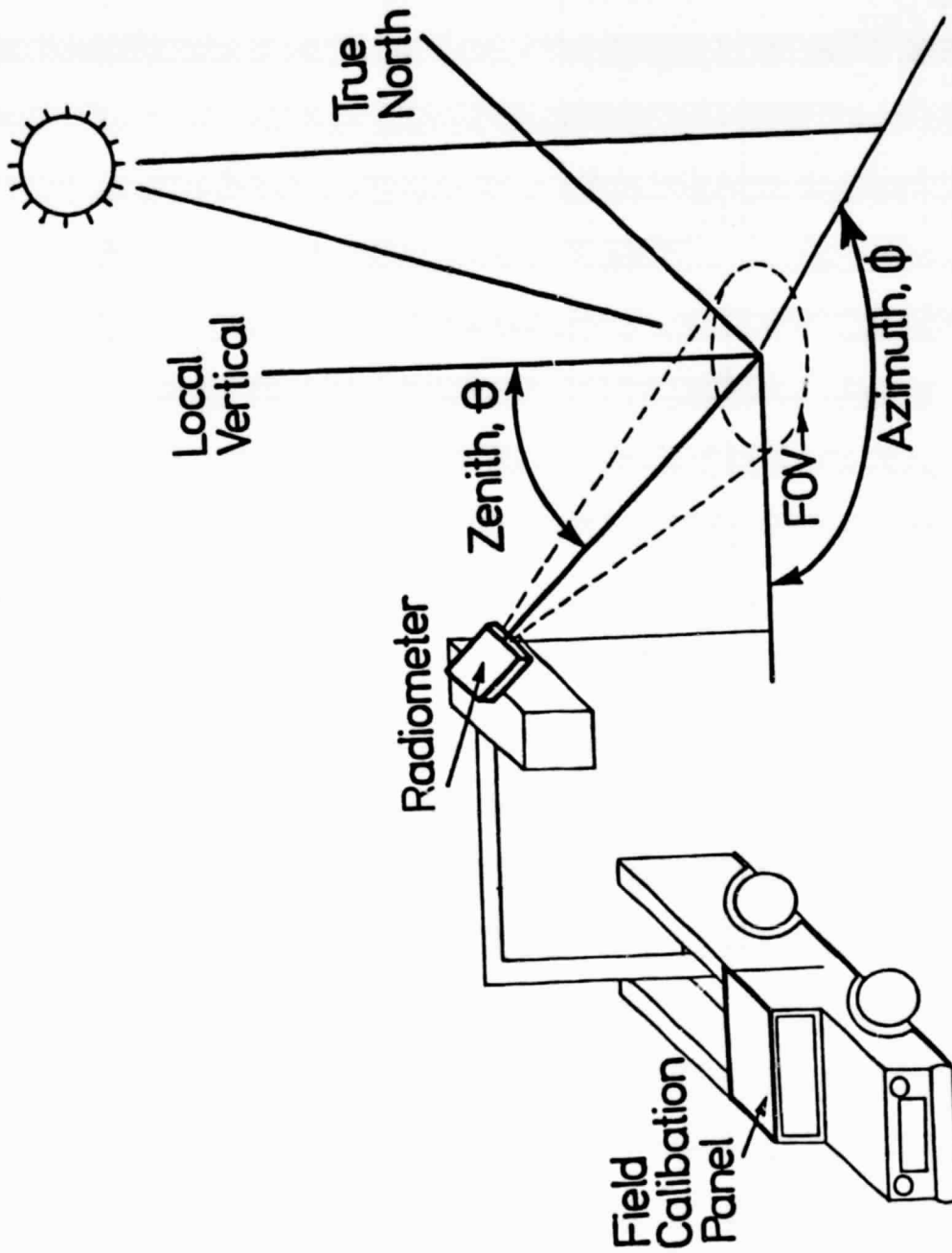
Figure B-4. Illustration of data collection for soybean sun-view angle experiment. Data for seven view zenith and eight view azimuth angles were obtained for several different solar zenith and azimuth angles.

Instrument positioned over calibration panel.
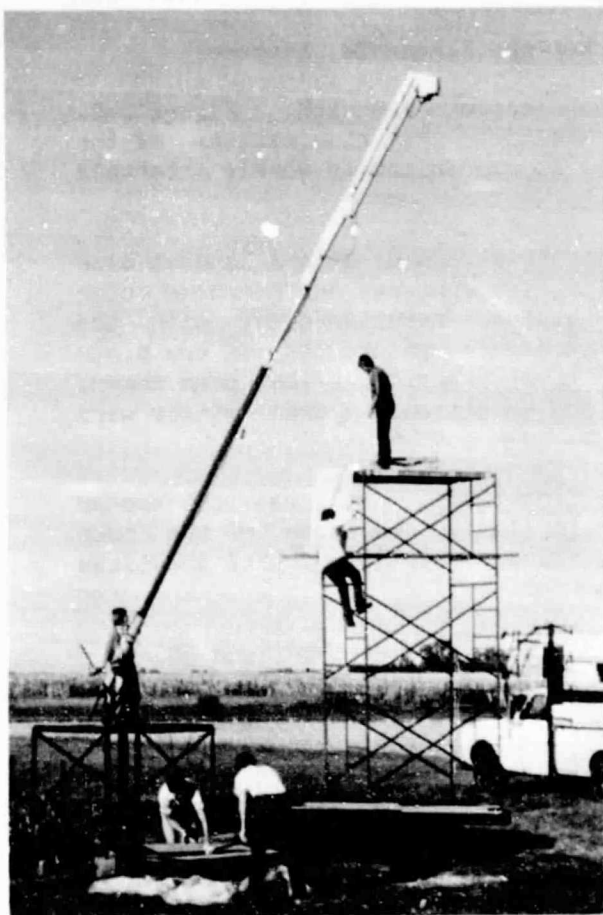
Instrument boom, turntable, and calibration tower.

Instrument positioned over soil trays.
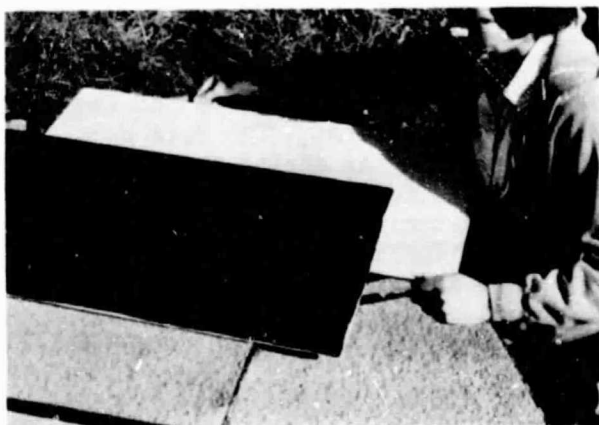
Three backgrounds used for experiment.
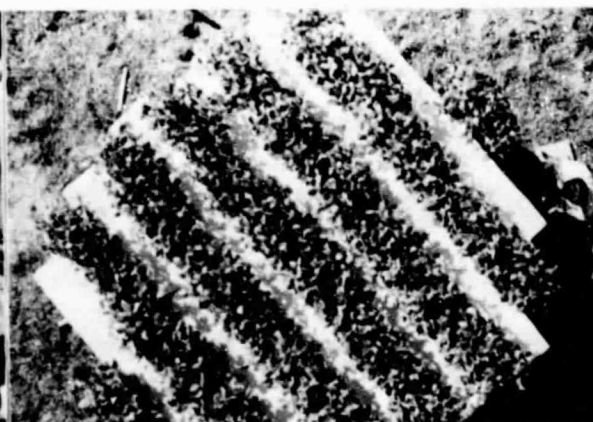
Soybeans on turntable with white background.

Figure B-5. Illustration of apparatus used for soybean row direction experiment including turntable, boom for Landsat band radiometer, and reflectance calibration tower. Boxes of soybeans used on turntable are shown in upper right photos.

7 planting dates (May 7, 16, 22, 29, June 11, 18, and July 13)
3 Plant Populations (25,000, 50,000 and 75,000 plants per hectare)
2 Soil Types (Chalmers, darker and Fincastle, lighter)

A split plot design with two replications was used, Figure B-2. Spectral measurements, along with agronomic characterizations of the canopies and surface soil, were made at approximately weekly intervals throughout the growing season.

The spectral reflectance measurements were made with a Landsat band radiometer (Exotech Model 100). Radiant temperatures and overhead color photographs of the canopies were obtained simultaneously with the reflectance measurements. The major agronomic measurements of the plots included growth stage, percent soil cover, height, leaf area index, biomass, and surface soil moisture and condition. Grain yields were measured at harvest time.

4. **Soybean Cultural Practices Experiment.** 1980 was the second year for this experiment. Treatments similar to those of the corn experiment, but representing major different soybean cultural practices were selected. The treatments were as follows:

7 Planting Dates (May 16, 27, June 12, 18, July 7, 16, and 30)
2 row spacings (25 and 76 cm)
2 Cultivars (Amsoy, narrow canopy type and Williams, bushy type)
2 Soil Types (Chalmers, dark and Toronto, light)

A split plot design with two replications was used, Figure B-3. Spectral and agronomic measurements were made as for the corn experiment.

5. **Soybean Sun-View Angle Experiment.** The purpose of this experiment was to characterize a soybean field by its reflectance at various view and illumination angles and by its physical and agronomic attributes. Reflectance measurements were acquired in the four Landsat wavelength bands through view zenith angles of 0, 7.5, 15, 22, 30, 45 and 60 degrees and view azimuth angles of 0, 45, 90, 135, 180, 225, 230, and 315 degrees as illustrated in Figure B-4. The field of view of the Landsat band radiometer above the ground was ten meters. The data were collected for various solar zenith and azimuth angles during three days each representing a different development stage for the soybean canopy. Measurements were also made of leaf transmittance. An ancillary data set was collected in conjunction with reflectance measurements to describe the soybean field by its canopy geometry, ground cover, biomass, leaf area index, and development stage. These data sets satisfy the input requirements for testing the validity of most mathematical models of canopy reflectance.

6. **Soybean Row Direction Experiment.** The overall objective of this experiment was to determine and model the effects of rows and row direction (shadowing) on the reflectance of soybean canopies as a function of solar azimuth and zenith angles. A secondary objective was

to determine how reflectance may vary with changes in percent soil cover and soil background conditions. Different row directions were used to introduce varying amounts of shadow in the composite of foliage, soil, and shadow viewed by a sensor.

A four meter diameter turntable (Figure B-5) was constructed for this experiment. Boxes with soybean canopies were placed on the turntable in rows. The turntable was rotated beneath a Landsat band radiometer mounted 8.8 meters above the canopies. The backgrounds were trays of Russell soil or boards painted with 3M flat black and 3M flat white, providing a wide range in reflectance backgrounds. The turntable is easily rotated to obtain any desired row direction.

Data were obtained for three levels of soil cover, three backgrounds, and 37 row directions for several ranges of solar azimuth and zenith angles.

Webster County, Iowa. The crops of interest in the Webster County, Iowa test site are corn and soybeans. Spectral data were acquired by the helicopter mounted FSS at two or three week intervals, coinciding with Landsat overpasses of the site throughout the growing season. Aircraft NS001 scanner data were acquired on four missions during the growing season. Identifications of cover types in all fields were recorded on site maps. Detailed agronomic observations were made on 10 fields each of corn and soybeans. The observations included: development stage, leaf area index, percent soil cover, plant population, development stage, biomass (for spring wheat and barley canopies only). Less detailed agronomic observations were also collected on 80 fields in the test site. Grain yields were obtained for each of the observed fields.

Wharton County, Texas. The crops of interest in the Wharton County test site are rice and cotton. Spectral data were acquired by the aircraft scanner on three missions during the growing season. Identification of cover types in all fields were recorded on site maps. Periodic observations were made on 10 fields of each rice and cotton. The observations include: leaf area index, percent soil cover, plant population, and development stage. Yields were obtained for each of the observed fields.

2. Data Acquisition

2.1 Purdue Agronomy Farm

The spectral measurements of the experiments were made by either the Exotech 20C spectroradiometer field system or the Exotech 100 Landsat band radiometer field system. Both systems also include Barnes PRT-5 sensors and 35 mm cameras, sighted to view the same area as the spectral sensors. The spectral measurements for the experiments are summarized in Table B-2.

Table B-2. Summary of spectral, meteorological, and canopy
geometry measurements collected at the Purdue Agronomy Farm
for the 1980 field research experiments.

Measurements Type and Description

Spectral Measurements

  Bidirectional reflectance factor

    Exotech 20C (0.45 - 2.32 μm)
    Exotech 100 (Landsat MSS spectral bands)

  Radiant temperature (cultural practices and disease experiments only)

  Color photographs

  Leaf Transmittance (sun-view angle experiment only)

    Exotech 100 (Landsat MSS spectral bands)

Meteorological Measurements

  Air temperature
  Barometric pressure
  Relative humidity
  Wind speed and direction
  Total solar incidence

Canopy Geometry Measurements (sun-view angle experiment only)
25 cm of row at 2 locations in field for each date.

  XYZ location of each leaf
  θ, ϕ orientation of each leaf
  Area of each leaf

Table B-3. Summary of agronomic measurements collected at the Purdue
Agronomy Farm for the 1980 field research experiments.

Agronomic Measurements

Amount of Vegetation

      Plant Height
      Percent Soil cover
      Number of plants per square meter
      Number of leaves per plant
      Leaf area index
      Total fresh and dry biomass (g/m^2)
      Dry biomass of leaves, stems, and heads, ears or pods (g/m^2)

Crop Condition

      Percent leaves green, yellow, and brown
      Plant water content (g/m^2)
      Presence and severity of stress

Soil Background Condition

      Percent moisture
      Munsell color
      Roughness

Additional Data for Specific Experiments

      Leaf nitrogen concentrations (wheat fertilizer experiment)

Grain Yield

Table B-4. Summary of 1980 data acquisition by the Purdue/LARS Exotech 20C spectroradiometer field system at the Purdue Agronomy Farm.

Measurement Date	Experiment		
	Winter Wheat	Wheat Disease	Panel Calibration
Week of	———— Number of Observations ————		
April 27	--	--	5
May 4	27	--	16
11	--	--	--
18	--	--	25
25	73	--	--
June 1	--	--	--
8	50	53	--
15	75	70	--
22	--	--	--
29	25	--	--
Aug. 3	--	--	12

Table B-5. Summary of 1980 data acquisition by the Purdue/LARS Exotech 100
field radiometer systems at the Purdue Agronomy Farm.

Measurement Date	Winter Wheat	Soybean Cultural Practices	Corn Cultural Practices	Soybean Variety	Sun-View Angle	Row Direction	Other Crops
				Experiment			
week of			number of observations				
May 25	79	--	186	--	--	--	--
June 1	--	--	--	--	--	--	--
8	80	308	281	120	--	--	--
15	100	336	224	120	--	--	--
22	--	--	--	--	--	--	--
29	80	--	30	--	--	--	--
July 6	--	--	--	--	--	--	--
13	40	174	112	120	347	--	6
20	--	308	224	--	430	--	14
27	--	--	--	--	--	--	--
Aug. 3	--	--	--	--	--	--	--
10	--	--	--	--	--	--	--
17	--	204	224	--	--	--	6
24	--	--	--	--	827	--	--
31	--	120	56	--	--	--	6
Sep. 7	--	--	--	--	--	--	--
14	--	172	112	--	--	--	6
21	--	136	112	--	--	601	--
28	--	68	112	--	--	1525	--
Oct. 5	--	68	112	--	--	--	--

To obtain data which can be readily compared, the two instrument systems are operated following similar procedures. The instruments are operated from aerial towers at six to ten meters above the target at heights which minimize any row effect and shadowing of skylight, yet ensure that the field of view of the instrument includes only the desired subject. Care is taken to avoid scene shadowing and reflective interaction due to personnel or vehicles.

The routine data taking mode of the instruments is straight down for determination of bidirectional reflectance factor, except for the soybean sun-view angle experiment. Measurements of the painted barium sulfate reference panel are made at 15-20 minute intervals. Two measurements of each plot were typically made by moving the sensor so that a new scene within the plot filled the field of view. The data also include vertical and oblique color photographs of each plot.

Detailed agronomic measurements of the crop canopies included crop development stage, measurements of amount of vegetation, crop condition (stress), soil background condition, grain yield, and additional measurements for specific experiments. The specific agronomic measurements and observations are listed in Table B-3. The canopy geometry measurements collected for the soybean sun-view angle experiment are summarized in Table B-2.

Augmenting the spectral and agronomic measurements are meteorological data, Table B-2. A record of the irradiance was collected by a total incidence pyranometer on strip charts. Additional environmental data including precipitation, pan evaporation, dew point, solar radiation, and net radiation were acquired hourly by a computerized agricultural weather station located on the Agronomy Farm.

Spectral measurements, along with agronomic and meteorological data, were acquired on each day that weather conditions permitted. A general summary of the data collection by experiment for the Exotech 20C and Exotech 100 is given in Tables B-4 and B-5, respectively. Crop development stages from seedling to senescence for 1980 are represented in these data.

2.2 Iowa, North Dakota, Nebraska, and Texas Test Sites

The spectral measurements of the experiments at the other test sites (Webster County, Iowa; Cass County, North Dakota; Wharton County, Texas; and Sandhills Agricultural Laboratory, MacPherson County, Nebraska) were made by the NASA/JSC helicopter-mounted field spectrometer system (FSS), the aircraft thematic mapper simulator scanner (NS001), the aircraft scatterometer-radiometers and/or the aircraft side-looking radar systems. The spectral measurements are summarized in Table B-6. The helicopter and aircraft systems also include 70 mm and 9 inch cameras, respectively, sighted to view the same areas as the spectral systems. The data collection by the helicopter and aircraft sensors are summarized in Tables B-7 and B-8, respectively.

Table B-6. Summary of spectral measurements collected at
Webster County, Cass County, Wharton County, and the University
of Nebraska Agricultural Laboratories.

Sensor System	Spectral Range	
Helicopter-mounted FSS	0.4 – 2.4	μm
	8.0 –14.0	μm
NS001 Thematic Mapper Simulator	0.47– 0.52	μm
	0.53– 0.60	μm
	0.63– 0.69	μm
	0.76– 0.90	μm
	1.00– 1.31	μm
	1.54– 1.70	μm
	2.10– 2.30	μm
	10.40–12.40	μm
Multifrequency Microwave Radiometer	C Band	
Scatterometers	0.40 GHz	
	1.60 GHz	
	4.75 GHz	
	13.30 GHz	
APQ-102 (Side-Looking Radar)	X Band	

Table B-7. Summary of 1980 crop year data acquisition by the NASA/JSC helicopter-mounted field spectrometer system (FSS).

Measurement Date	Test Site	
	Webster Co. Iowa	Cass Co. N. Dakota
week of	data acquisition date	
April 13	4/18	--
20	--	4/23
27	--	--
May 4	5/8	--
11	--	5/15
18	5/22	--
25	--	--*
June 1	--	--
8	--*+	--
15	--	6/17+
22	--	--
29	7/1+	--
July 6	--	7/9+
13	7/17+	--
20	--	7/22+
27	--	--
Aug. 3	8/6+	--
10	--	8/14+
17	8/19+	--
24	--	--
31	--	9/4+
Sep. 7	9/10	--*
14	--	--*
21	9/26	--
28	--	--*+
Oct. 5	--	--
12	10/18	--
19	--	--*
26	10/30	--
Nov. 2	--	11/6

* Mission planned, but no data collected because of inclement weather conditions.

+ Detailed agronomic measurements collected.

Table B-8. Summary of 1980 crop year data acquisition by the NASA/JSC aircraft multispectral scanner system. (NS001, radiometer-scatterometers, side looking radar.)

Measurement Date	Iowa Webster Co.	Nebraska McPherson Co.	Nebraska Saunders Co.	N. Dakota Cass Co.	Texas Wharton Co.
week of			data acquisition date		
April 13	--	--	--	--	
20	--	--	--	--	4/14[1]
27	--	--	--	--	--
May 4	--	--	--	--	--
11	--	--	--	--	--
18	--	--	--	5/12[2] 5/15[1]	--
25	--	--	--	--	--
June 1	--	--	--	--	--
8	--	--	--	--	--
15	--	6/17[1]	--	--	--
22	--	--	--	6/17[1,4]	--
29	7/1[1]	--	--	--	6/24[1]
July 6	--	--	--	--	--
13	--	7/15[1]	--	--	--
20	--	--	--	--	7/16[1]
27	--	--	--	--[5]	--
Aug. 3	8/6[1]	--	--	--	--
10	--	--	--	--	--
17	8/19[1,2,3]	--	--	8/13[1,2]	--
24	--	--	8/21[1]	--	--
31	--	--	....	--	--
Sep. 7	9/10[1,2,3]	--	--	--	--
14	--	--	--	--	--
21	--	--	--	--	--
28	--	--	--	--	--
Oct. 5	--	--	--	--	--
12	--[5]	--	--	--	--

1. NS001 data
2. Radiometer-scatterometer data
3. Side looking radar data
4. Marginal weather conditions
5. Mission planned, but no data collected because of equipment malfunction

Table B-9. Summary of Agronomic Measurements collected
at Webster County, Cass County, and Wharton County.

Agronomic Measurements

Initial Interview (of 80 fields in site)

      Crop species
      Acres planted
      Planting date
      Emergence date
      Seeding rate
      Previous year field use
      Irrigated
      Row direction
      Row width
      Pesticides applied

Periodic Observations (every nine days of 80 fields in site)

      Canopy height
      Ground cover
      Canopy color
      Growth stage
      Surface moisture
      Weediness
      Disease damage
      Insect damage
      Hail damage
      Lodging damage
      Pesticide applied

Final Interview (of 80 fields in site)

      Acres harvested
      Harvest date
      Production
      Percent moisture at harvest
      Harvest method
      Fertilizer applied
      Second crop planted

Detailed Measurements (of 10 fields for each major crop in site)

      Leaf area index
      Percent soil cover
      Plant population
      Development stage

Procedures for operating the FSS system are similar to those for the truck-mounted systems operated at the Purdue Agronomy Farm so that data from the different test sites can be readily compared. The FSS is operated at an altitude of 61 meters above the ground over the commercial fields. Measurements of a 6 x 12 meter canvas reflectance reference panel are made before each flightline from an altitude of 6 meters. The reflectance of the canvas reference panel is measured periodically at Purdue/LARS with the Exotech 20C field spectroradiometer system. The NS001 aircraft scanner system, also collected data over five canvas panels representing five different reflectance levels.

Agronomic data include initial field inventories, nine-day periodic observations, detailed agronomic measurements made approximately every two or three weeks, and end of season surveys, Table B-9.

The ground surveys and periodic observations were collected by USDA/ESCS personnel. The detailed agronomic measurements were collected by North Dakota State University in Cass County and Purdue University in Webster County. The data acquisition for the detailed agronomic measurements is summarized in Table B-7.

Augmenting the spectral and agronomic measurements are meteorological data. The meteorological measurements include air temperature, relative humidity, barometric pressure, wind speed and direction, rainfall observation and optical depth. A record of the irradiance is collected by a total incidence pyranometer on strip charts during the spectral data collection as a record for general sky (cloud) conditions.

3. Data Preprocessing

The spectral, agronomic, and meteorological data are calibrated and preprocessed into comparable formats for easy access and analysis by researchers. The spectrometer/radiometer data are preprocessed into LARSPEC format. The aircraft scanner data are preprocessed into LARSYS format.

Preprocessing of the 1979 Exotech 20C spectroradiometer data, the Exotech 100 Landsat band radiometer data, the 197. MS and NS001 aircraft scanner data and all but four dates of the 1979 FSS data were completed early this year. The 1977 Exotech 100 Landsat band radiometer data collected in Williston, North Dakota were also processed into LARSPEC format as requested by researchers.

A major portion of the preprocessing of the 1980 Exotech 20C and Exotech 100 data collected at the Purdue Agronomy farm has been completed. The preprocessing accomplishments for 1980 and the present status are summarized in Table B-10.

Table B-10. Summary of Field Research data preprocessing
accomplishments for 1980.

Instrument/Data Type	1979-1980 Crop Years Status	
	Completed	In Processing
Aircraft Multispectral Scanner (Dates/Flightlines)	8/34	7/
Helicopter Mounted Field Spectrometer (Dates/Observations)		
Field averages	13/787	20/
Individual scans	13/14,426	20/
Truck Mounted Field Spectrometer (Dates/Observations)		
Purdue/LARS Exotech 20C	7/207	16/
Truck Mounted Field Multiband Radiometer (Dates/Observations)		
Purdue/LARS Exotech 100	20/7841	28/

4. Data Library and Distribution

The development of the field research data library at Purdue/LARS was initiated in the fall of 1974 by the NASA/Johnson Space Center with the cooperation of the United States Department of Agriculture (USDA) as a part of the Large Area Crop Inventory Experiment. The purpose of the data base is to provide fully annotated and calibrated multitemporal sets of spectral, agronomic, and meteorological data for agricultural remote sensing research. Spectral, agronomic, and meteorological measurments were made over primarily wheat on three LACIE test sites in Kansas, North Dakota, and South Dakota for the first three years. In 1978 and 1979 the data library was expanded to include data collected for corn and soybean experiments in Indiana, Iowa, and Nebraska, as well as from a major U.S. soils experiment. In 1980 the library was expanded again to include data collected for spring wheat, barley, sunflowers, and soybeans in North Dakota and cotton, rice, and soybeans in Texas.

Milestones achieved during the past year have been:

- Inclusion of nearly all 1979 crop year data,
- Distribution of data to researchers, and
- Determination of cause of anomaly in FSS data at 0.70 μm.

The general organization of the field research data library is illustrated in Figure B-6. The data in the library includes spectral measurements, agronomic measurements, meteorological measurements, photography, mission logs, and data verification reports. The data formats available to researchers are digital tape, film, and data listings.

The data have been collected over several test sites and for different crops as illustrated in Table B-11. The test sites are of two types, controlled experimental plots and commercial fields (Table B-12). The instruments used to collect the spectral data are listed in Table B-13. The spectrometer data are processed into comparable units, bidirectional reflectance factor, in order to make meaningful comparisons of the data acquired by the different sensors at different times and locations (2).

The reflectance factor measurements, along with most of the corresponding agronomic and meteorological measurements, are stored in Purdue/LARS spectrometer/radiometer data storage tape format. The multispectral scanner data are approximately linearly related to scene radiance. Information is available for the researcher to calibrate the scanner data to in-band bidirectional reflectance factor if desired. Most of the scanner data are stored in LARSYS Version 3 format; some data are available in Universal format. A summary of the spectral data in the data library is given in Table B-14.

In the past twelve months, 29 aircraft scanner runs and 23,000 spectrometer/ radiometer observations have been made available to researchers. Three institutions have received field research data during the past year. In addition all the data are routinely available
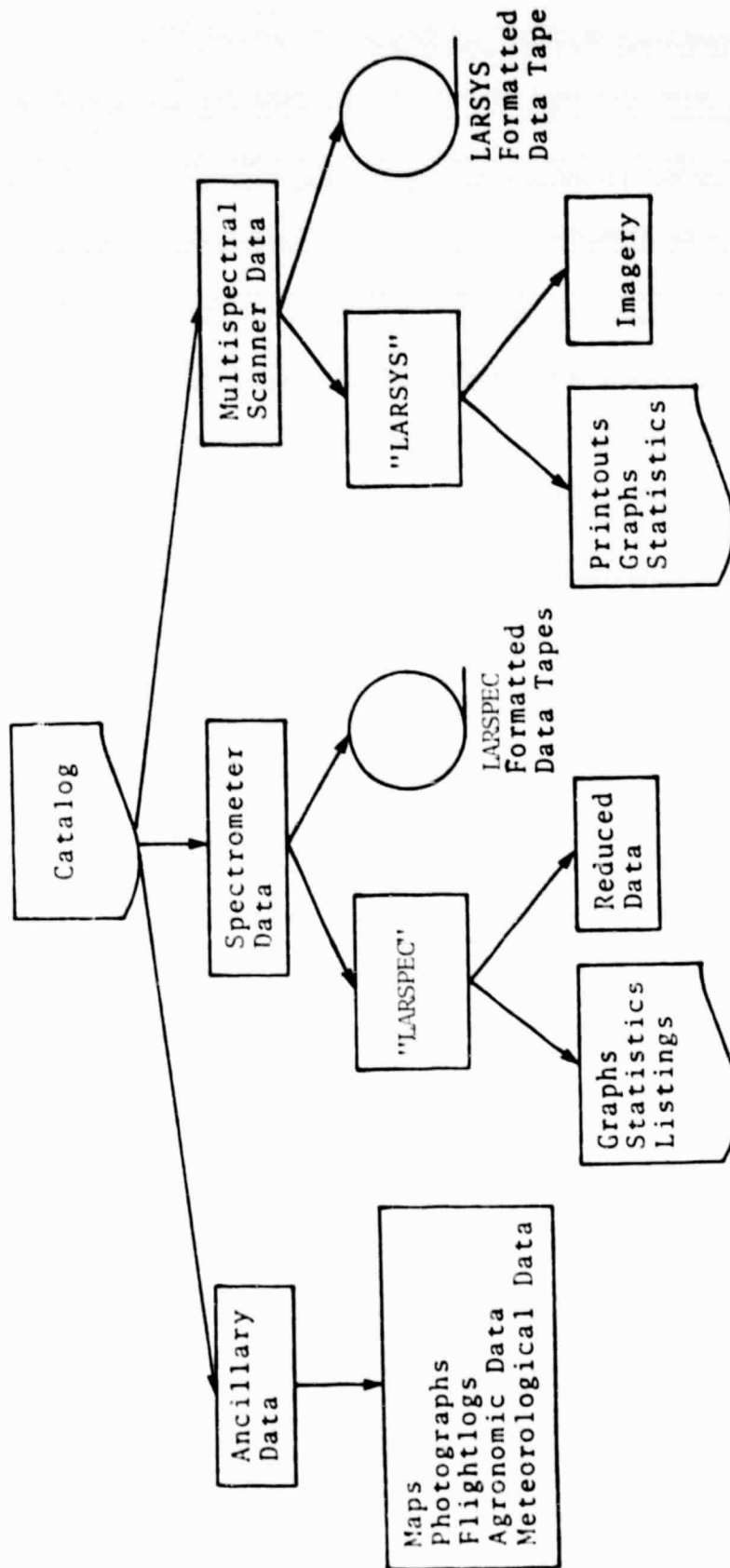
Figure B-6. Organization of field research data library. LARSPEC and LARSYS are Purdue/LARS software systems to access and analyze spectrometer/radiometer and multispectral scanner data.

Table B-11. Summary of field research test site locations and major crops.

Test Sites State County	Major Crops	Crop Years
Indiana, Tippecanoe	Corn & Soybeans Winter Wheat	1978-1980 1979-1980
Iowa, Webster	Corn & Soybeans	1979-1980
Kansas, Finney	Winter Wheat	1975-1977
Nebraska, McPherson	Corn	1979-1980
North Dakota, Cass	Spring Wheat Barley Sunflowers Soybeans	1980
North Dakota, Williams	Spring Wheat	1975-1977
South Dakota, Hand	Spring Wheat Winter Wheat	1976-1979
Texas, Wharton	Cotton Rice Soybeans	1980
'U.S. & Brazil'	250 Soil Types	1978

Table B-12. Summary of field research controlled experimental plot test sites and commercial field test sites.

Location	Crop Years
Controlled Experimental Plot Test Sites	
Indiana, West Lafayette. Purdue University Agronomy Farm.	1978-80
Kansas, Garden City. Kansas State University Agriculture Experiment Station.	1975-77
Nebraska, Sandhills. University of Nebraska Agriculture Experiment Station.	1979-80
North Dakota, Williston. North Dakota State University Agriculture Experiment Station.	1975-77
Commercial Field Test Sites	
Iowa, Webster County	1979-80
Kansas, Finney County	1975-77
North Dakota, Cass County	1980
North Dakota, Williams County	1975-77
South Dakota, Hand County	1976-79
Texas, Wharton County	1980

Table B-13.   Summary of major sensor systems used for field research.

Platform and Sensor	Crop Years
Spacecraft Multispectral Scanners	
Landsat 1	1975-77
Landsat 2	1975-79
Landsat 3	1978-80
Aircraft Multispectral Scanners	
24-channel Scanner (MSS)	1975-76
11-channel Modular Multispectral Scanner (MSS)	1975-79
8-channel Thematic Mapper Simulator (NS001)	1979-80
Helicopter-mounted Spectrometer	
NASA/JSC Field Spectrometer System (FSS)	1975-80
Truck-mounted Spectrometers	
NASA/ERL Exotech 20D Field System	1975
NASA/JSC Field Signature Acquisition System (FSAS)	1975-77
Purdue/LARS Exotech 20C Field System	1975-80
Truck-mounted Multiband Radiometers	
Purdue/LARS Exotech 100 Landsat Band Radiometer Field System	1977-80

Table B-14. Summary of spectral data in the field research data
library by instrument and data type.

Instrument/Data Type	1975-1979 Crop Years
Landsat MSS	
Whole Frame CCT (Frames)	124
Aircraft Multispectral Scanner	
(Dates/Flightlines)	54/335
Helicopter Mounted Field Spectrometer	
(Dates/Observations	
Field Averages	87/7657
Individual Scans	87/129,255
Truck Mounted Field Spectrometer	
(Dates/Observations	
NASA/JSC FSAS	45/813
Purdue/LARS Exotech 20C	124/7978
NASA/ERL Exotech 20D	45/645
Truck Mounted Field Multiband Radiometer	
(Dates/Observations)	
Purdue/LARS Exotech 100	68/17,038

Table B-15. Summary of recipients of field research data.

Organization	Number of Requests
Ecosystem, Inc. Gambrills, Maryland	1
Environmental Research Institute of Michigan Ann Arbor, Michigan	*√
General Electric Corporation Philadelphia, Pennsylvania	2
Godddard Institute for Space Studies New York, New York	4√
IBM Corporation Palo Alto, California	1√
NASA/Goddard Space Flight Center Greenbelt, Maryland	>5
NASA/Johnson Space Center Houston, Texas	*√
Purdue University West Lafayette, Indiana	*√
University of South Florida Tampa, Florida	1
USDA, SEA Temple, Texas	1√
USDA, SEA Weslaco, Texas	1

* Access to data through Purdue/LARS computer system

√ Recipients of field research data during 1980

to researchers at Purdue/LARS. Investigators at the NASA/Johnson Space Center and the Environmental Research Institute of Michigan have direct access to the digital data via remote terminals to the LARS' computer. Table B-15 summarizes the institutions that have received data during the past four years and indicates which institutions received data during this past year.

There has been an offset in the FSS data around 0.70 μm since November 1974, Figure B-7. Several possible causes for the offset have been examined including offband radiation, software processing error, and wavelength calibration. After examination of the wavelength calibration, staff at NASA/JSC concluded in April 1980 that the major cause of the offset is an inaccurate wavelength calibration in the 1974-79 FSS data. The procedure consists of first modifying LARSPEC to correct the wavelength calibration and later of correcting the FSS data tapes.

5. Software Development and Documentation

The achievements during the past year in software and hardware development to preprocess, verify and analyze the 160,000 observations of spectrometer data and 340 flightlines of aircraft scanner data include:

- Development of new FSS preprocessing system,
- Development of new laboratory spectrometer preprocessing system,
- Expansion and documentation of LARSPEC,
- Implementation of users graphics software (SAS/GRAPH), and
- Addition of Tektronix 4054 graphics terminal.

5.1 Preprocessing Software

Two major preprocessing software capabilities were developed this year. The first is a new software system to process the FSS data more efficiently and the second is a software system to process the laboratory (Clevenger) spectrometer system data. The new FSS software system places the ESCS observations, meteorological data and calibrated FSS spectral data onto a LARSPEC formatted tape. The system can create a LARSPEC tape of individual FSS observations or averages of FSS observations for each field. The system also includes the capability to plot the FSS calibration panel data for data verification, Figure B-8.

5.2 Analysis Software

Statistics-Graphics. During this past year a Tektronix 4054 graphics terminal was installed on the Purdue/LARS computer to provide high resolution graphic output along with a COMTAL color digital display terminal. A user software system called SAS/GRAPH was installed on the computer to allow researchers easy access to the capabilities of the graphics terminal to display their data and statistical output.
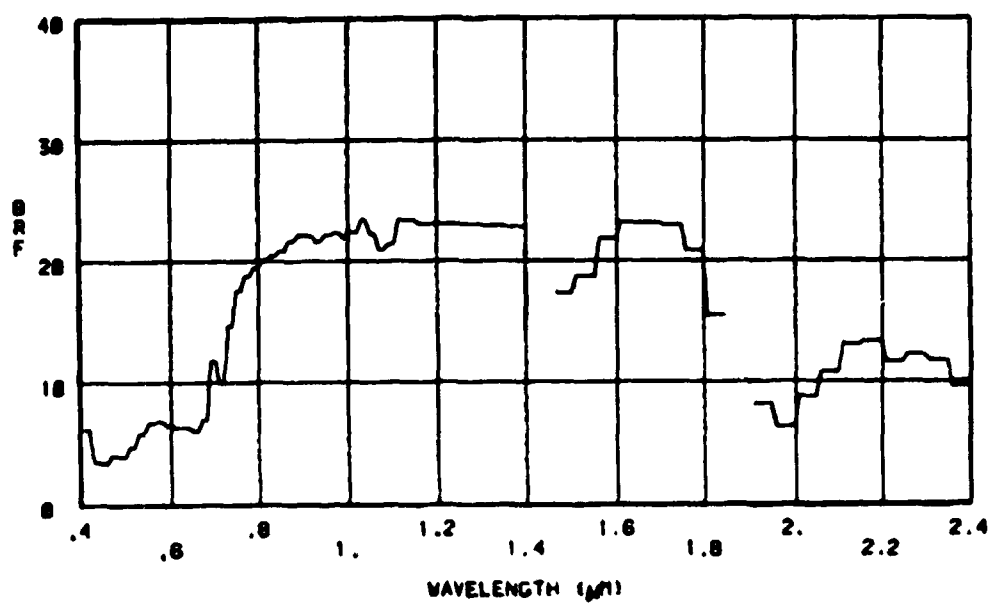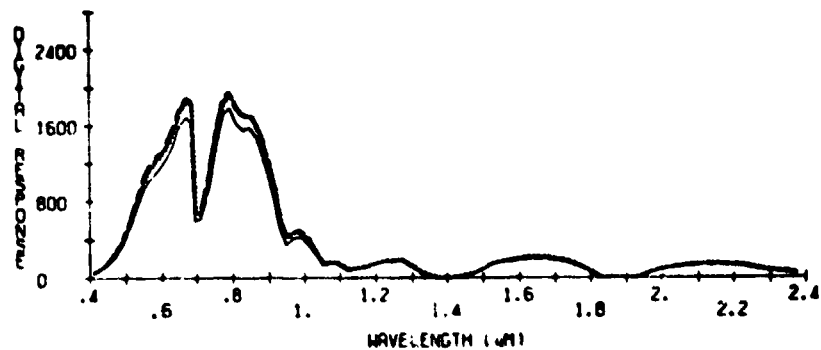
Figure B-7. Illustration of anomoly in FSS data around 0.7 μm.
This example is for winter wheat collected on November 5, 1974.

DATE 8/30/79   SITE 893   LATITUDE 0422300N   LONGITUDE 0941000W
SUN ANGLE CORRECTED CALIBRATION VALUES

LINE TYPE	FLIGHT LINE	CAL TIME	IFOV	SOLAR ZENITH
—————————	1	150937	1.25	52.77
··········	2	163545	1.25	39.98
·—··—··—··—··	3	185606	1.25	37.8
------------	4	171717	1.25	36.65
·—·—·—·—·	5	173501	1.25	34.37

COEFFICIENTS OF VARIATION OF SUN ANGLE CORRECTED VALUES.

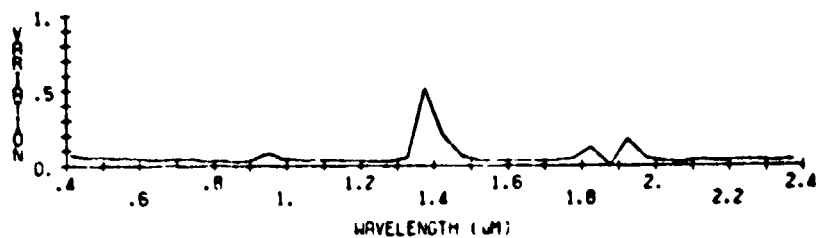AVERAGE COEFFICIENTS OF VARIATION - .04

Figure B-8. Plot of FSS reflectance calibration panel data
from the new FSS software system for data verification.
The panel data have been corrected for changes in sun
angle. Under ideal data collection conditions there will
be very little difference in the curves.

In addition, programmer software called GCS was interfaced with the Tektronix 4054 to allow easy development of custom graphics capabilities in research software systems.

LARSPEC is the software system on the Purdue/LARS computer which accesses the spectrometer/multiband radiometer data and associated agronomic and meteorological measurements. During this past year the LARSPEC User's Manual (3) was completed and distributed. Major capabilities that were added to LARSPEC are: (1) expanded punch capability for identification record data, (2) addition of Decwriter (with graphics board) as medium resolution graphics output device, (3) and addition of Tektronix 4054 terminal as high resolution graphics device. The interface of the LARSPEC system with the Tektronix 4054 graphics terminal provides the capability to conveniently review the spectrometer data. For example, Figure B-7 was obtained from the Tektronix 4054 graphics terminal, using LARSPEC.

6. Acknowledgements

The experiment design was led by Marvin Bauer, Craig Daughtry, Vern Vanderbilt, Larry Biehl and Barrett Robinson. The plot preparation and field measurements of wheat, corn, and soybeans were directed by Larry Hinzman. Barrett Robinson and Larry Biehl were responsible for the spectral measurements.

Jon Ranson, Lou Nash, Jeff Kollenkark, Vic Pollara, Chris Brooks, Judith Ward, Tom Bonsett, Sue Roth, Rick Noller, Vic Fletcher, Jim York, Chuck Rhykerd, Lynn Kirschner, E.B. Rawles, Wade Rudyanski, Donna Parker, Carol McFadyen, and Diana Braddick assisted in plot preparation and data collection.

Cathy Kozlowski assisted by Don McLaughlin, Mike Guba, Sheryl Skifstad, Mike Sepp, Cathy Axtell, Selma Al-Abbas, Ching Lue, and Gay Benson were responsible for data preprocessing. Nancy Fuhs, Jerry Majkowski, Jill Heinrich, and Todd Plantenga assisted with the data base management and distribution and software development.

7. References

1. Bauer, M.E., L.L. Biehl, C.S.T. Daughtry, M.M. Hixson, B.F. Robinson, and V.C. Vanderbilt. 1980. Supporting Field Research Project Plan, 1980-82. NASA, Johnson Space Center, Houston, Texas.

2. Robinson, B.F. and L.L. Biehl. 1979. Calibration Procedures for Measurement of Reflectance Factor in Remote Sensing Field Research. SPIE Vol. 196, pp. 16-26, Measurements of Optical Radiation. SPIE, Box 10, Bellingham, WA.

3. Fuhs, N.C. and L.L. Biehl. 1979. LARSPEC User's Manual. Publication 121279, LARS/Purdue University, W. Lafayette, IN.

C. DEVELOPMENT OF MULTIBAND RADIOMETER SYSTEM[*]

Barrett F. Robinson

1. Introduction

To develop the full potential of multispectral data acquired from satellites, increased knowledge and understanding of the spectral characteristics of specific earth features is required. Knowledge of the relationships between the spectral characteristics and important parameters of earth surface features can best be obtained by carefully controlled studies over areas, fields, or plots where complete data describing the condition of targets is attainable and where frequent, timely spectral measurements can be obtained. Available instrumentation systems have been either inadequate or too costly to obtain these data. Additionally, there is a critical need for standardized acquisition and calibration procedures to ensure the validity and comparability of data.

The objective of this task is to develop a multiband radiometer system for agricultural remote sensing field research. The radiometric instrument is a multiband radiometer with 8 bands between 0.4 and 12.5 micrometers; the data acquisition system records data from the multiband radiometer and ancillary sources. The radiometer and data handling systems are adaptable to helicopter, truck, or tripod platforms. The system is also suitable for portable hand held operation. The general characteristics of the system are that it is: (i) comparatively inexpensive to acquire, maintain, and operate; (ii) simple to operate and calibrate; (iii) complete with the data handling software and (iv) well documented for use by researchers.

The instrument system developed during this contract is a prototype of an economical system which can be utilized by many researchers to obtain large numbers of accurate, calibrated spectral measurements. As such, it is a key element in improving and advancing the capability for field research in remote sensing.

This report describes the design specifications and performance evaluation of the multiband radiometer and data recording modules, preparation of system and user's manuals, construction of a truck-mounted boom, and development of data handling software.
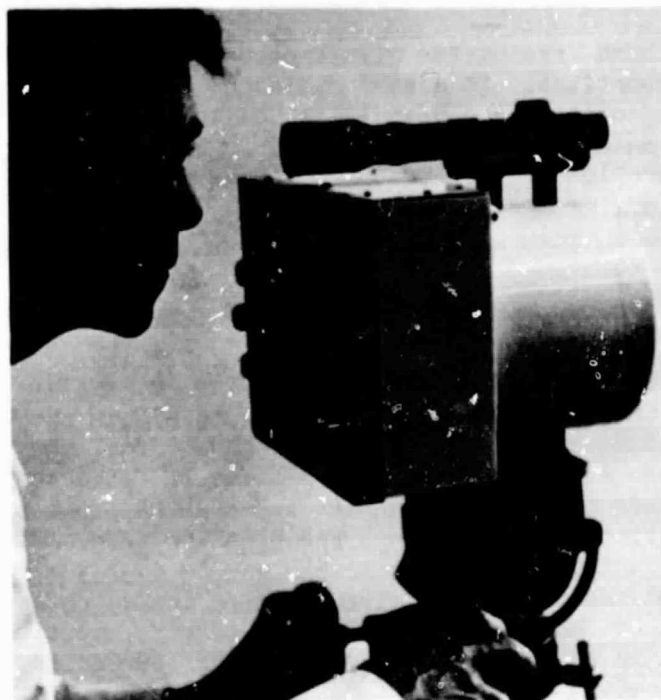
Figure C-1. Photograph of multiband radiometer. (Courtesy of Barnes Engineering Co.)

WAVELENGTH (μm)
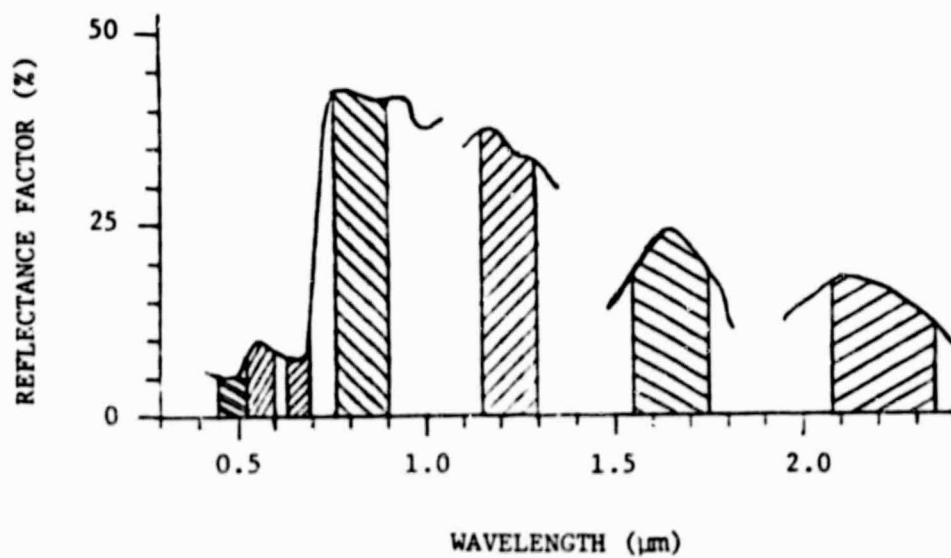
Figure C-2. Spectral distribution of passbands superimposed on a typical vegetation spectrum.

2. Description and Features of the Prototype Multiband Radiometer

The multiband radiometer simultaneously produces analog voltages which are proportional to scene radiance in each of eight spectral bands. The radiometer is a stand-alone device capable of operation with a variety of data acquisition systems. The prototype radiometer is capable of operation from $0°$ to $60°C$, when mounted on a tripod, truck boom, helicopter, or small plane.

2.1 Calibration

To achieve reliability in reflectance measurement, a field calibration procedure is to be employed for reflective spectral bands (1). For the thermal channel direct comparison with two reference black bodies at known temperatures will be used for the most accurate measurement of thermal radiance. As well, the stability of the instrument allows the measurement of spectral radiance temperature with $0.4°C$ (1 s.e.e.) accuracy without field calibration. In-band radiance calibration of the reflectance channels may be easily accomplished using a 1000 watt standard of spectral irradiance and a reflectance standard for accuracies of about 10% (see Dynamic Range, section 3.4); better accuracies may be obtained with more accurate sources and correction for detector temperature using the signal provided.

2.2 Features

Spectral Bands. The prototype unit has eight spectral bands--seven which match the spectral bands of the Thematic Mapper multispectral scanner and an additional band from 1.15 to 1.30 μm. A summary of the spectral bands is shown in Table C-2 and Figure C-2.

Chopping Arrangement. The multiband radiometer has eight modular optical-electronics units centered on a 10.6 cm circle. The front-mounted chopper modulates the flux to the optical modules (see Figure C-3).

Modularity. The prototype instrument is equipped with co-aligned fields of view ($1°$, $15°$ and diffuser) which may be exchanged under clean field conditions. Additionally, the entire optical/electronic module (detector, preamplifier and all optics) is a self-aligning capsule which may be easily replaced under clean field conditions.

Controls and Display. The gain of each reflective channel is selectable by a panel mounted switch. The panel mounted analog meter indicates the channel output voltage of the selected channel or the chopper temperature signal. An indication of battery status is provided on the analog meter when the on-off switch is switched to the battery voltage position. A red LED indicates when the on-off switch is on and the unit is energized. An amber LED indicates when the battery is low.
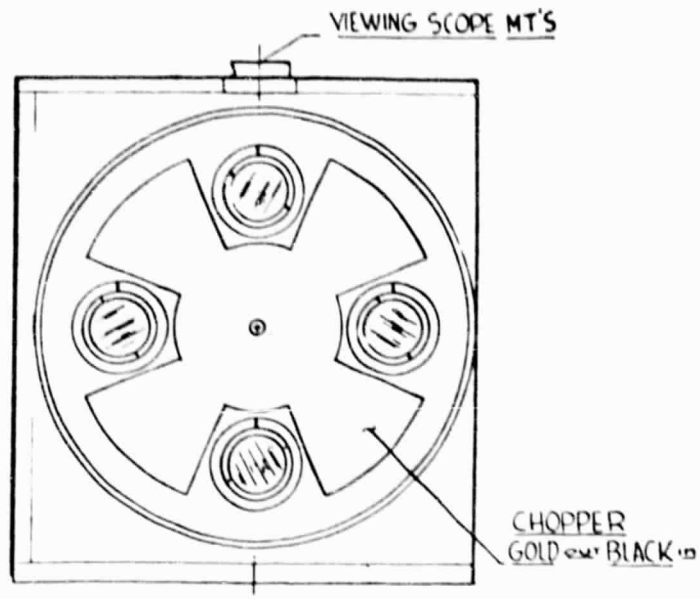
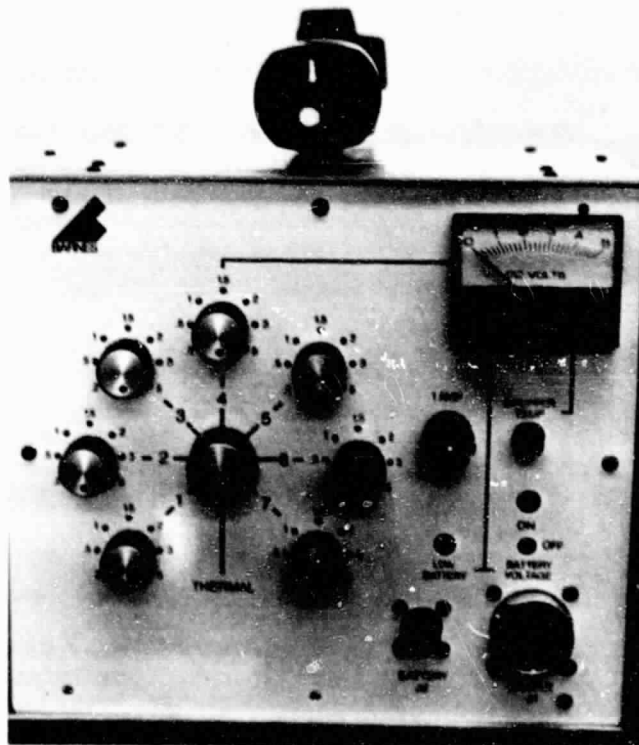Figure C-3.   Chopping arrangement for the multiband radiometer.

Figure C-4.   Controls and displays on rear panel of the multiband
    radiometer.

Gain Status Signals. On command from an external source (TTL zero) the output from each reflective channel is switched from data signal to an analog voltage indicating the gain setting of the channel. This feature is useful for reading the gain of the channel into a data logging device when the radiometer is mounted on the end of a long boom.

Camera Boresight. The instrument is equipped with a mount suitable for boresighting a 35-mm camera to 0.2^{o} of the optical axis.

Camera Control. A camera control signal may be fed, through the input cable, to a jack on the exterior of the electronics case to enable remote camera operation.

Low Battery Warning Signal. The multiband radiometer provides a TTL zero signal when the battery is judged to be too low for accurate operation.

System Temperature Signals. Signals indicating the temperature of the chopper, detector, and frame are imbedded in the prototype radiometer. These signals are in the 0 to 5 volt range and all are continuously available to the data logger.

Dimensions. 26.4 x 20.5 x 22.2 cm
10.3 x 8.07 x 8.74 in
7.25 Kg (prototype)
5.4 Kg (production).

Power. The instrument may be powered by any 12 volt battery and is protected for vehicular operation. Two sealed lead acid battery sets (12 volt, 5 amp hour) were supplied with the prototype. These batteries (5 lb/set) may be easily carried in a "fanny-pack" and each set will operate the radiometer more than 10 hours.

Cables. Connecting cables of 1.2m and 15m were provided with the prototype for handheld and boom operation, respectively.

3. Performance of Prototype Radiometer

Table C-1 summarizes the results of laboratory tests performed for acceptance of the prototype instrument. Test results and design or construction modifications are discussed in indicated sections.

3.1 Accuracy

Channel linearity for the reflective channels was determined by a "sums of sources" technique using four sources irradiating a painted Barium Sulfate surface which was viewed with 15° field of view (see Figure C-5). Stated linearity is the standard error of estimate of the least squares line relating the eleven sums to the instrument response over the ranges indicated in Table C-1 (0-100% refers to normal range).

Table C-1. Summary of test results for multiband radiometer.

Test		Detector Type			Notes
		Silicon	PbS	$L_1Ta\,O_3$	
Channel Linearity	0-100%	0.1%	0.1%	0.4°C	See Section 2.1
	0-300%	0.2%	2.0%		
Induced Instability	(100%)	None	None	None	See Section 2.1
Limit of Relative Noise	4 Hz	0.08%	0.08%	0.6°C @ .15 Hz	Peak variation to Mean See Section 2.1
	20 Hz	0.23%	0.25%		
Limit of Relative Error	25°C	0.08%	0.08%	0.6°C @ .15 Hz	3σ Limits, 20 Hz
-5° Step +20min	20°C	1.7%	1.7%	1.0° @ .15 Hz	Blown Air
+5° Step +20min	35°C	-1.7%	-2.8%	1.0° @ .15 Hz	See Section 2.1
Field of View		See Section 2.2			
Spectral Response		See Section 2.3			
Frequency Response	Low	4 Hz	4 Hz	0.15 Hz	See Section 2.4
	High	20 Hz	20 Hz	T.B.D.	

Actual linearity may be better than the stated value of 0.1% and is probably the best obtainable using the technique. During the tests of the prototype unit, it was discovered that small systematic non-linearity (typically 0.1% reflectance units) was present in the reflective channels. Breadboard tests cf the precision rectifier circuit indicated that the non-linearity could be removed by adding an offset control to an op-amp. Barnes had made provisions for this addition and will modify the prototype and production models.

Channel linearity for the thermal channel was determined for chopper temperatures from 15°C to 30°C and target temperatures from 15°C to 40°C by assuming an equation of the form

$$V = a + bT_{CH} + cT_{BB} \qquad (C-1)$$

where V is the thermal channel voltage response

T_{CH} is the chopper temperature (C)
T_{BB} is the black body temperature (C)
a, b, and c are regression coefficients.

The standard error of estimate for computing black body temperature from V and T was $0.36°C$. Investigation using a more appropriate form for the Equation C-1 has been attempted with mixed results. Investigation will continue until the channel is described over a wider range of chopper and target temperatures.

Figure C-6 shows the thermal reference source and the test chamber used for environmental performance tests of the multiband radiometer. To ensure repeatability of positioning the field of view, the radiometer was mounted securely to the optical table which supports the chamber.

Radiance Induced Instability. No change in channel gain or offset due to viewing bright or dark targets was noted. Dark level, 17% reflector, 100% reflector, 17% reflector, dark level,... were viewed in sequence with full solar irradiance. No "settling" or "hysteresis" phenomena were noted.

The limit of relative noise. The peak variation from the mean divided by the mean is reported in Table C-1 for the reflective channels. Since almost all the noise in the reflective channels is demodulation residuals, the relative noise is constant except at very low signal strengths. The NEΔT (3σ) value given in Table C-1 is typical of the performance of the channel for the range of instrument temperatures. The thermal channel performance is limited by detector and amplifier noise. Since the channel gain remains nearly constant, the absolute noise remains nearly constant.

The limit of relative uncertainty for measurement of reflectance factor is given in Equation C-2 for the case where no correction is made for changes in detector temperature.
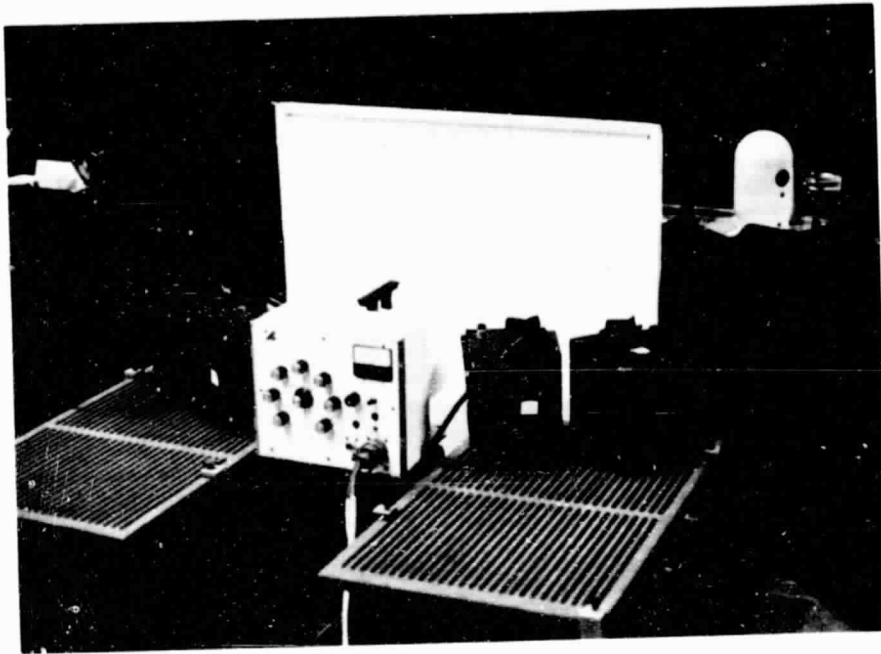
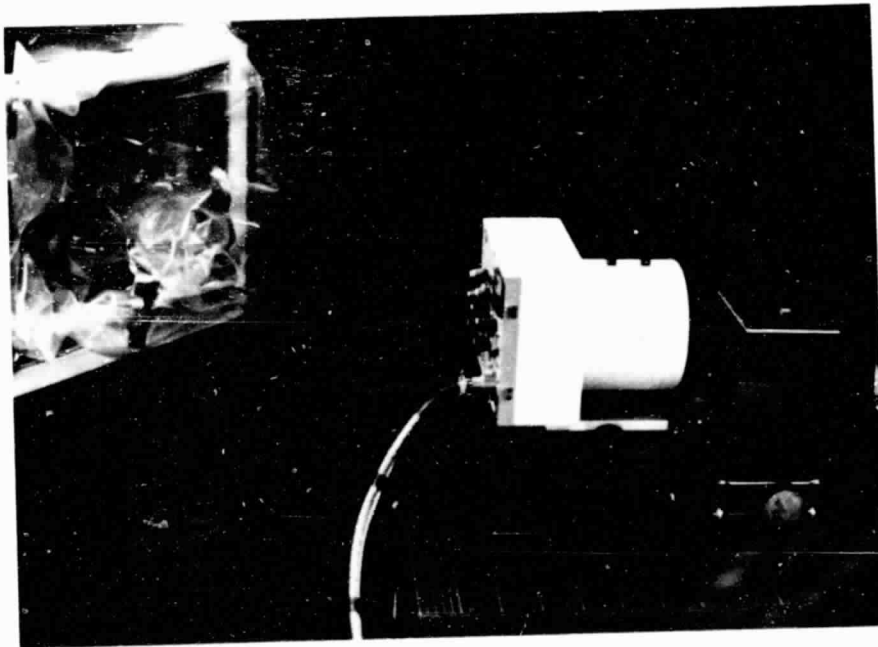Figure C-5.   Laboratory set-up for linearity tests.

Figure C-6.   Chamber and source used for environmental performance
tests of the thermal channel.

$$\frac{\Delta R}{R} = \frac{3\sigma \ (volts)}{3 \ (volts)} + \frac{1}{A} \frac{dA}{dT} \Delta T \qquad\qquad (C-2)$$

where R is the measured reflectance, σ is the r.m.s. noise for the "full scale" response of 3 volts, A is the channel responsivity and T is the temperature of the detector. It can be recognized that $3\sigma/3$ is the limit of relative noise from Table C-1.

The desired performance criterion was $\Delta R/R$ less than 1% for silicon channels (2% for lead sulfide channels) for a time period of 20 minutes following immersion of the radiometer in an air bath of 5°C higher or lower in temperature. To obtain the data for the -5 step given in Table C-1, the instrument was brought to equilibrium at 20°C using a rapidly circulating bath of blown air (40 c.f.m.). Then the blown air was cooled to much less than 15°C initially then the chamber and its contents were allowed to reach equilibrium at 15°C using only slightly cooler blown air--warming to 15°C. The effect was a -5°C temperature step. The instrument response was measured before the change in air bath temperature and as the instrument cooled toward the new equilibrium temperature of 15°C.

Data given in Table C-1 are for the maximum changes in responsivity for the temperature steps for 20 Hz bandwidth. Thus the limit of error for the 5° step condition (35 -40°C) would be an apparent -2.8% of value change in a reflectance measured before the step and 20 minutes after the step.

For the thermal channel, chopper temperature is included in the determination of the measured radiance or temperature and the uncertainty is determined by the standard error of estimate for the predicting algorithm and the channel noise. Data given for the limits of error for the dynamic conditions in Table C-1 include only one standard error of estimate for the prediction equation because all measurement errors @ 0.15 Hz were well within that sum (0.4 + 0.6).

3.2 Field of View

Initial testing of the fields of view was accomplished by the radiometer manufacturer (Barnes Engineering Co.). A large collimated source was used to obtain the angular response characteristics of the 1 degree and 15 degree fields of view. The results of these tests were verified by Purdue using a point source transect technique. In addition, the off axis response was investigated by Purdue using an intense point source. Figure C-7 shows the centroids of the 1 degree fie's of view superimposed on the half response for Channel 6. Typical point source transect measurements for the prototype instrument are presented in Figures C-8 and C-9. The prototype was found to have unacceptable off-axis response. The source of the off-axis response was traced to lack of blacking of chopper-cover and optical capsule surfaces. Barnes will correct the prototype and production models. The measured half responses of the fields of view were nominally circular patterns of 1.2 degrees and 14 degrees diameter.
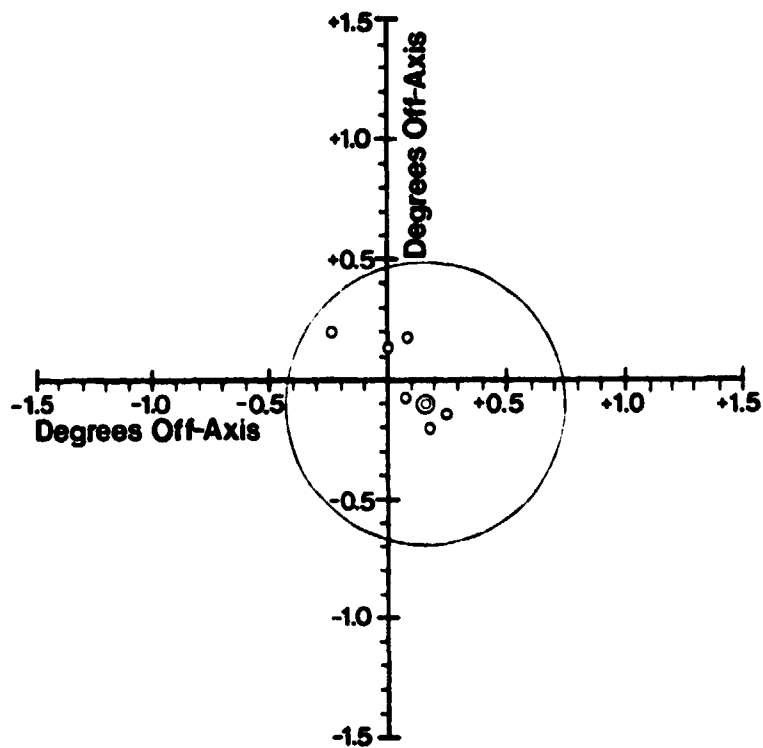
Figure C-7. Centroids of 1° fields of view superimposed on half-
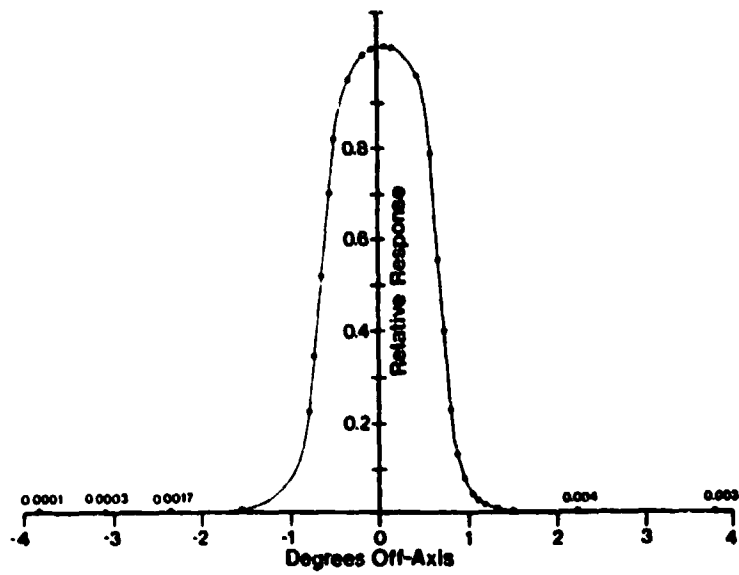response for channel 6.

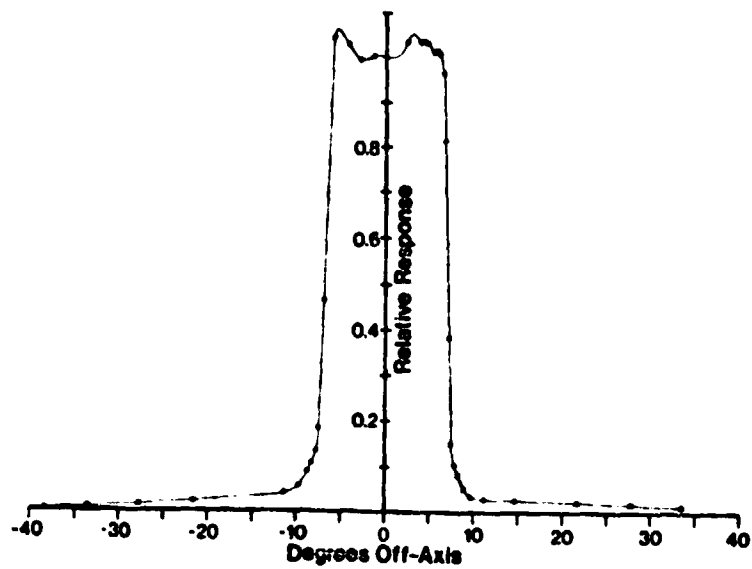Figure C-8. Relative response vs. degrees off-axis, channel 4, 1° field of view.

Figure C-9. Relative response vs. degrees off-axis, Channel 6, 15° field of view.

3.3 Filters and Spectral Response

Filter performance was provided by the vendor (OCLI) and was tested by Barnes. The major performance characteristics of the spectral filters are given in Table C-2. The 50% response wavelengths were as specified except for Channel 6 (1.55-1.75 μm) which was 28 nm and 33 nanometers high for the lower and upper 50% response points. This was judged to be acceptable due to the steep slopes and low out of band response. Figure C-10 shows the transmittance versus wavelength curve for the channel 3 filter (0.63-.69 μm). The in-band transmittance, flatness, and steep slopes are characteristic of the filter set. However, for this filter only, the integrated out-of-band transmittance (including the responsivity of the silicon detector) was unacceptable. The effect of the out-of-band component would be a 50% of value error for measuring vegatation in sunlight. The vendor (OCLI) will provide a replacement filter and insure that production units meet the out-of-band performance specifications.

Spectral Response. The relative and (approximate) absolute spectral response of the completed radiometer were measured by the manufacturer. This test indicated that the system performed as predicted and revealed no abnormal behavior.

3.4 Dynamic Range

The dynamic range behavior was established by the linearity tests in Section 2.1. In addition, a 1000 watt standard of spectral irradiance and a calibrated barium sulfate reflectance standard were used to adjust the gain of the reflective channels so that the radiance of a barium sulfate panel normal to the solar irradiance (clear day-near noon) will produce a response of 3 volts when the gain setting is 1. The manufacturer reported that a field test indicated results within 10% except for Channel 3 which had considerable out-of-band response. Calculation of the in-band radiance was performed prior to evaluation of the filters and it is felt that this procedure can be improved slightly for production instruments and that it will provide a suitable means for performance evaluation of in-service units as well as establishing a radiance scale of reasonable accuracy.
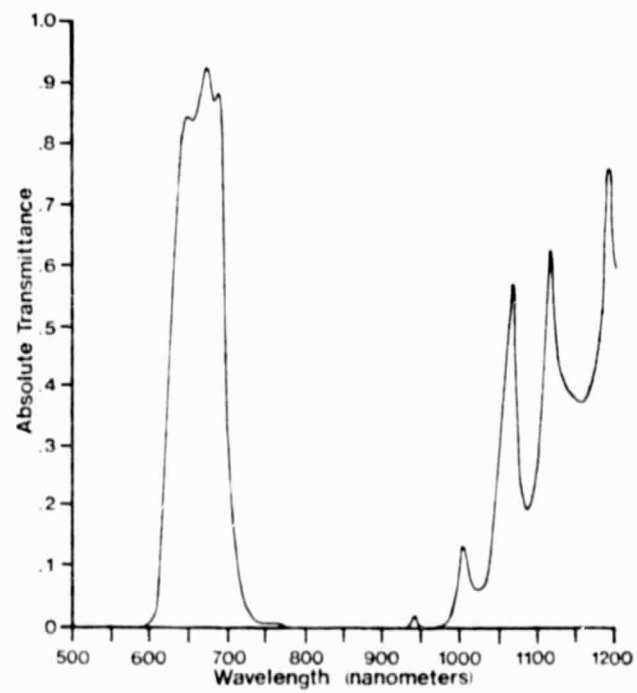
Figure C-10. Spectral transmittance of channel 3 (0.63-.69 μm) filter.

Table C-2. Major performance characteristics of optical filters.

|	Specified			Measured			
	50% Response Wavelengths		Slopes	50% Response Wavelengths		Slopes	
Channel	Nanometers		%	Nanometers		%	
1	450 ± 10	520 ± 10	4.5	453	505	2.9	2.6
2	520 ± 10	600 ± 10	4.5	515	595	4.5	2.2
3	630 ± 20	690 ± 10	4.5	623	695	3.5	4.2
4	760 ± 20	900 ± 20	4.5	775	890	4.0	2.2
5	1150 ± 20	1300 ± 20	4.5	1155	1306	2.3	1.1
6	1550 ± 20	1750 ± 20	4.5	1578	1783	2.6	1.7
7	2080 ± 20	2350 ± 20	4.5	2094	2358	2.9	1.5
8	10.4 ± 0.1 μm	12.5 ± 0.1 μm	4.5	10.5 μm	12.6 μm	2.9	3.1

150
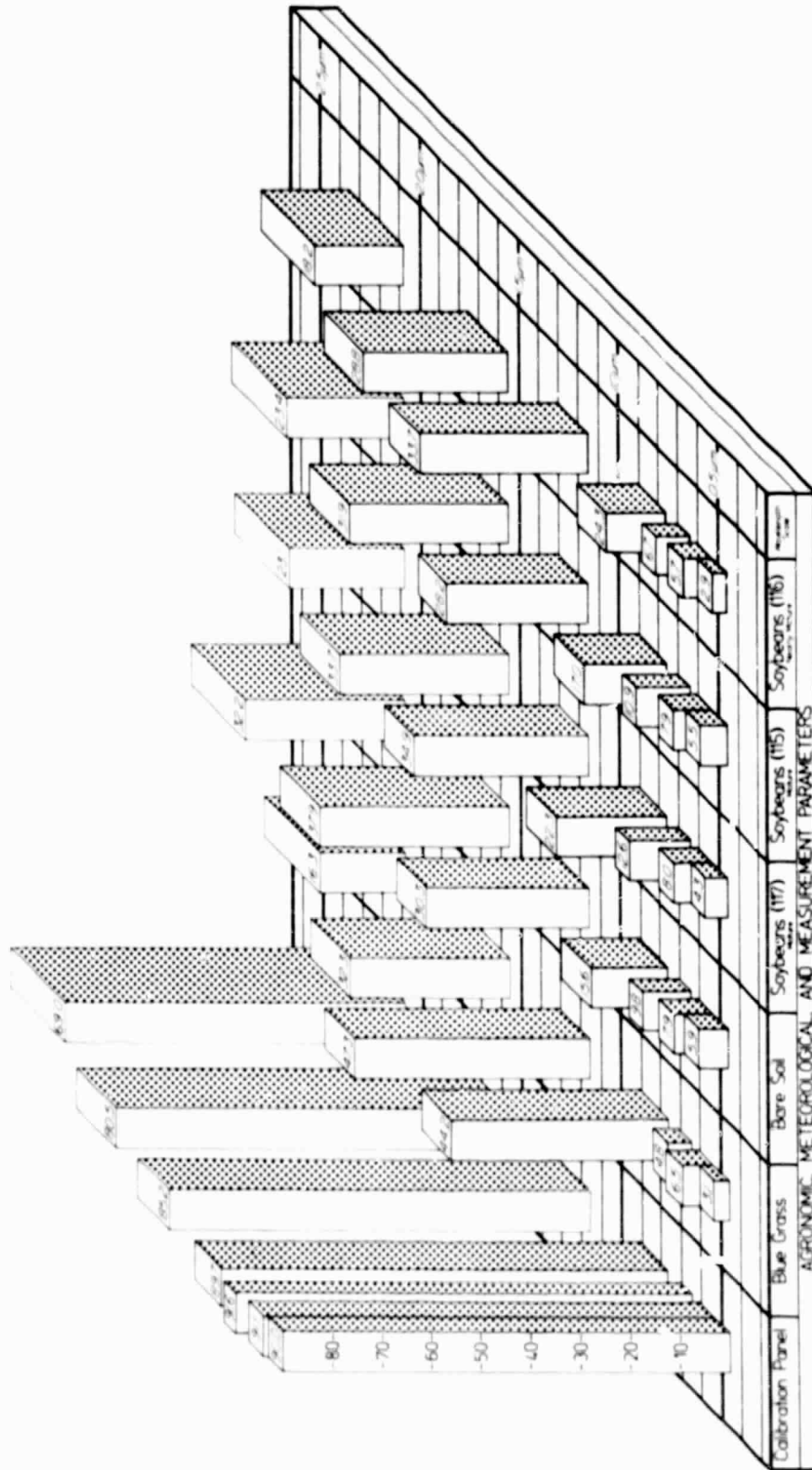
Figure C-11. Reflectance factor data acquired by the multiband radiometer for several cover types.

3.5 Field Test

The radiometer was mounted on the pick-up truck boom (see Section 6, below) and used to measure the reflectance of five subjects of varying spectral reflectance at the Purdue Agronomy farm. A data logger having 40,000 count precision was used to evaluate system performance. The results of these measurements are summarized in Figure C-11. Standard deviations for the computed reflectances were less than 1% of value. The standard deviations for measurement of the calibration panel were less than 0.4%. Ambient conditions were nearly constant and the instrument was in equilibrium with the slowly moving air (about 25 C) and the solar irradiance conditions were typical for a reasonably clear day near noon. Since extensive instrumentation would be required to establish the temperature of a surface of suitable size, the thermal channel was not used; however, all laboratory environmental performance tests used the 13 meter cable in a configuration identical to the field condition.
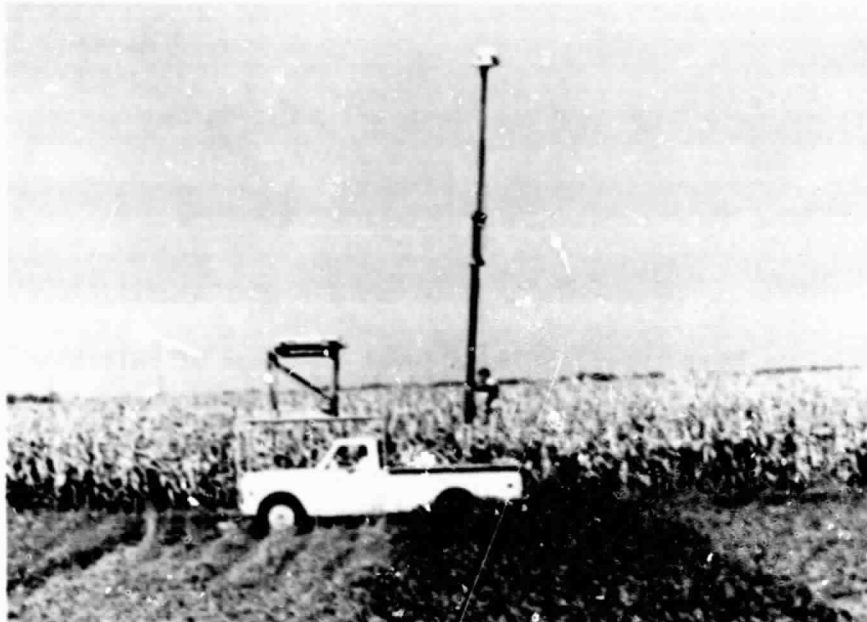
Figure C-13. Measurement of dark level response of multiband radiometer.

4. General Features of the Data Recording Module

The data recording module (a stand-alone device capable of operating with many types of sensors) operates under the same environmental conditions as the multiband radiometer. An entire data observation is measured and recorded within 0.8 milliseconds. The unit provides an interface to be used with a HP-97S printing calculator as well as a 16 bit parallel interface with a handshake system suitable for many microprocessors and minicomputers.
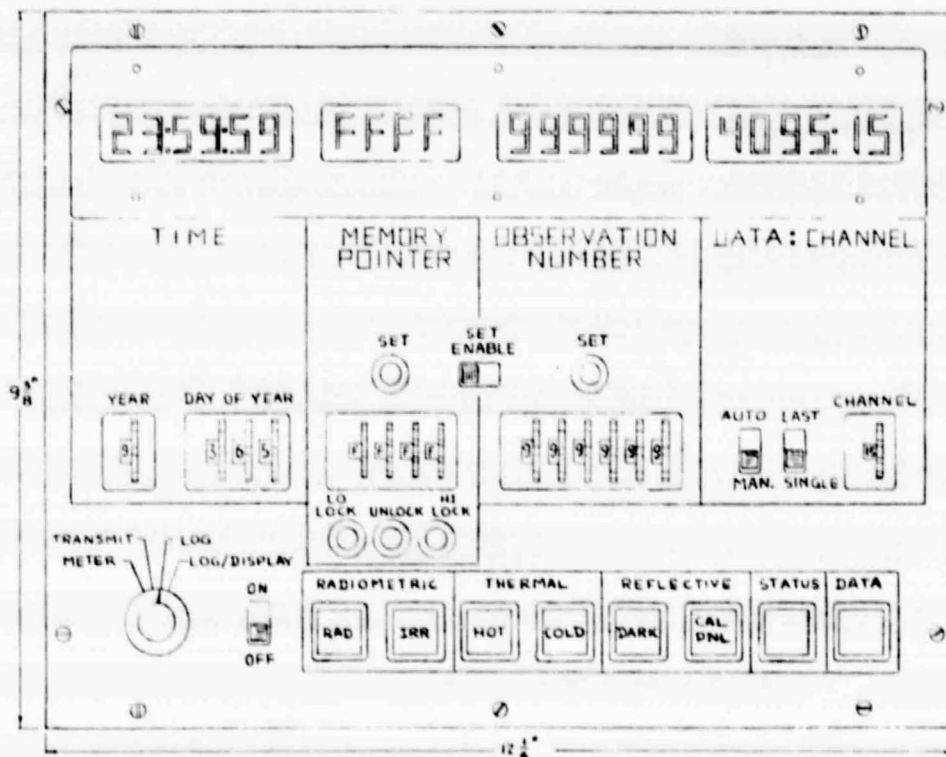

Figure C-14. Front panel controls and displays of prototype data logger.

4.1 Specifications for Developed Prototype Data Recording Module

Data Acquisition:

Inputs: 15 single ended channels with 100MΩ input impedance

Resolution: 12 bits = 5 volts

Accuracy: ±0.05 bits/°C or ±1 bit, whichever is greater

Stored Data: 1K increments to 64K
16 bit static RAM with data retention battery

Year, Data Code, Day of Year, Time, Observation Number (automatically advanced), up to 15 channels of data, or radiometer channel gain will be recorded for each observation

Data Retention: Data will be held in memory for at least 30 days before battery must be replaced.

Data Output:

Displays: Memory Address, Memory Data, Time, Observation Number

Transfer: Memory contents directly to parallel input port on a digital computer

Memory contents display to a HP-97S for on-site computation of reflectances, radiances, and temperatures

Control Functions: Intervalometer - a 2 second data acquisition rate is available by a front panel switch

Data/Gain - Status control for radiometer gain interrogation

Low battery warning - visual

Remote activation of acquisition - closure of external contact switch

Observation number (6 BCD characters) is available for use by an external device such as a data back camera.

Dimensions: (prototype)

Overall - 25 x 32 x 48 cm
9.8 x 12.6 x 189 m
9 kg

Plug-in Memory - 21 x 17 x 30.5 cm
8.3 x 6.7 x 12.0 m
2.7 kg

4.2 Results of Laboratory and Chamber Tests of the Data Logger

The linearity of the data logger was checked and all 15 channels were found to have a standard error of estimate less than 1 bit; approximately 80 data points were used.

A crosstalk test was performed using a 1 KHz full scale sine wave for the interfering signal. In no case did the interfering channel cause more than 1 bit error in any other channel.

The thermal stability was tested using high, middle, and low scale constant voltage stimuli on all channels for equilibrium temperatures of 50°, 25°, and 0°C. All stored values (20 measurements of each voltage at each temperature) were within 1 bit for all channels.

Input offset drift over a 2 month period was measured to be within ± 1 bit for all 15 channels.

The time clock performance is within 2 seconds/day (measured - 10 seconds over a 30 day period at room temperature). Internal batteries will provide up to 30 days of operation for the clock.

Common laboratory and field vibrations were simulated using one inch vertical drops and lateral impulses resulting in displacements of two to six inches while sampling a constant midscale voltage on all channels at 100 samples/second. No error was produced.

5. Development of Prototype Intervalometer and Databack Camera

A Nikon F2AS (35mm, 250 exposure) motorized databack camera was modified to imprint a 6 digit number on the left hand edge of selected exposed frames. The digits are approximately 3.2 millimeters high on a 3" x 5" print.

A prototype intervalometer was developed to initiate the action of the databack unit (trigger the transfer of the observation number from the data logger to the databack and imprinting the number onto the film) and to initiate data acquisition simultaneously with film exposure. The intervalometer/databack camera system is a stand alone system with thumbwheel switches which can be used to specify the 6 digit number to be imprinted on the film or can accept a 6 digit number from a variety of sources.

5.1 Specifications for Intervalometer/Databack Camera System

Photo Rate: 1 per second

Data Acquisition Interval: single shot or
                             0.1 sec to 9999.9 seconds

Acquisitions per photo: 1 to 10

Interface: CMOS - protected

Temperature: 0° C to 70° C (operation)

Dimensions:
    Data Back Unit: 11 x 18.4 x 4.2 cm , 0.5 kg (prototype)
    Intervalometer: 33 x 23 x 19 cm , 2.3 kg (prototype)

Power:
    Data Back Unit: 4 AA cells - 50 hours
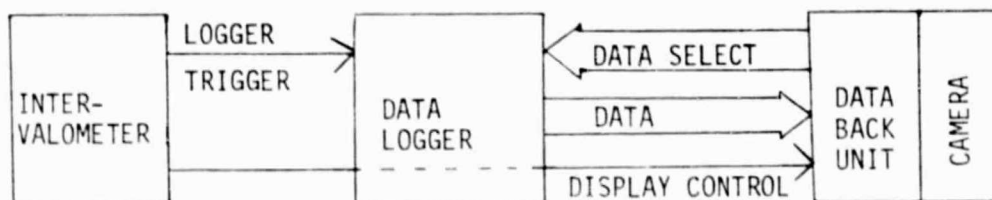   Intervalometer: 4 D cells - 200 hours

Figure C-15. Block diagram showing use of the intervalometer and databack camera.

6. Testing of the Truck-Mounted Boom

The truck mounted boom (developed last year) was used routinely throughout the growing season at the Purdue Agronomy Farm to rapidly position the Exotech Model 100 Landsat-band radiometer over experimental plots. With this boom, the instrument was positioned 7.6 meters above the ground at a distance of 3.7 meters from the edge of the truck. Figures C-12 and C-16 show the boom in operation with the prototype multiband radiometer.

6.1 Operation Characteristics

Pointing errors due to boom deflection were computed and measured to be less than $1°$ for normal operation (lower boom at about $52°$ elevation). The break-away torque required to rotate the boom from the calibration to the target position was determined to be about 90 pound-foot; this torque and the normal turning torque were found to be convenient for field operations with the normally used two foot lever. The upper boom required approximately 20 seconds for extension from and retraction to the calibration position and the ratchet operation was deemed to be safe. The lower boom required 60 seconds to raise to the operation position and 20 seconds to lower to the stowage position. Angular adjustment about the operation position was judged to be quite satisfactory and all operations were judged to be safe, provided operators and nearby personnel are alert and prudent. Stowage of the unit for daily transport of 10 miles on U.S. Highway 52 was easy, convenient, and
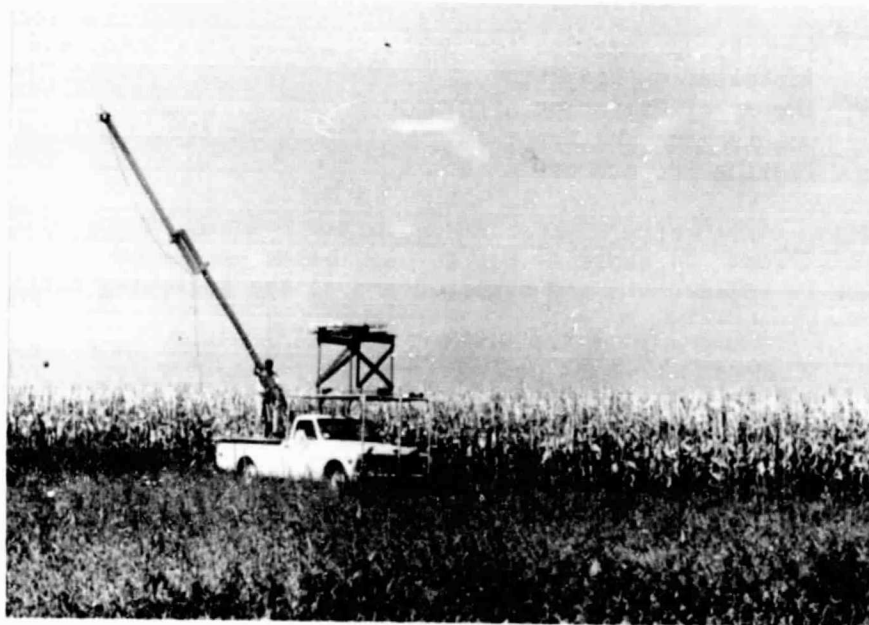

Figure C-16. Truck-mounted boom positioning the multiband radiometer.

6.2 Modifications

The braking device used in the prototype design will be replaced with a larger unit of the same type. The new brake will be adjusted to provide a bit more braking action to prevent boom rotation during strong wind gusts while protecting the mounting structures from severe rotational torques due to road bumps and quick stops. The guide roller brackets on the upper boom have been redesigned to improve the accuracy of positioning of the upper boom.

6.3 Fatigue Test

Following the growing season, the region where the mounting pin connects to the base plate was dye-penetrant tested for fatigue. No evidence of fatigue was found.

7. Interface Hardware and Software

Testing of the DEC DR-11C 16 bit parallel I/O interface to the Purdue/LARS 11/34A minicomputer was completed. Data from the prototype data logger is entered to core memory (16K data points in 5 seconds) and then stored on disk awaiting transfer from the PDP 11/34A to the IBM 3031 for calibration and reformating to LARSPEC compatible format.

8. System and User Manuals

System manuals for the multiband radiometer and data recording modules are in preparation. Each manual includes the following topics:

General Information (description, specifications, etc.)
Installation Operation
Theory of Operation
Maintenance and Repair
Testing Procedures

In addition, a user's manual is being prepared to provide information to researchers and system users on the following topics:

Fundamentals of measurement and calibration
Field measurement and calibration procedures
Performance evaluation tests
Experimental design (including a sample experiment).

9. References

1. Robinson, B.F. , and L.L Biehl. 1979. Calibration Procedures for Measurement of Reflectance Factor in Remote Sensing Field Research. SPIE Vol. 196, pp. 16-26, Measurements of Optical Radiation. SPIE, Box 10, Bellingham, WA.